Synthesis and Characterization of Ruthenium(II) Complexes with 2,6-(Diphenylazo)pyridine Ligand and 4,4′-Dicarboxy-2,2′-bipyridine Ligand

Sukanpirom Siritam

A Thesis Submitted in Partial Fulfillment of the Requirements for the Degree of

Master of Science in Inorganic Chemistry

Prince of Songkla University

2013

Thesis Title	Synthesis and Characterization of Ruthenium(II) Complexes with 2,6-(Diphenylazo)pyridine Ligand and 4,4′-Dicarboxy-2,2′- bipyridine Ligand
Author	Miss Sukanpirom Siritam
Major Program	Inorganic Chemistry

Major Advisor

……
(Asst. Prof. Dr. Kanidtha Hansongnern)

Co-advisor

……
(Dr. Walailak Puetpaiboon)

……
(Dr. Nararak Leesakul)

Examining Committee

…….Chairperson
(Dr. Cheewita Suwanchawalit)

……
(Asst. Prof. Dr. Kanidtha Hansongnern)

……
(Dr. Walailak Puetpaiboon)

……
(Dr. Nararak Leesakul)

……
(Asst. Prof. Dr. Chaveng Pakawatchai)

The Graduate School, Prince of Songkla University, has approved this thesis as partial fulfillment of the requirements for the Master of Science Degree in Inorganic Chemistry.

……
(Assoc. Prof. Dr. Teerapol Srichana)
Dean of Graduate School

This is to certify that the work here submitted in the result of the candidate's own investigations. Due acknowledgement has been made of any assistance received.

…….Signature
(Asst. Prof. Dr. Kanidtha Hansongnern)
Major Advisor

…….Signature
(Miss Sukanpirom Siritam)
Candidate

I hereby certify that this work has no already been accepted in substance for any degree, and is not being currently submitted in candidature for any degree.

…….Signature
(Miss Sukanpirom Siritam)
Candidate

ชื่อวิทยานิพนธ์ การสังเคราะห์และศึกษาคุณสมบัติของสารประกอบเชิงซ้อนของโลหะรูทิเนียมกับลิแกนด์ 2,6-(diphenylazo)pyridine และลิแกนด์ 4,4′-dicarboxy-2,2′-bipyridine

ผู้เขียน นางสาวสุกานต์ภิรมย์ ศิริธรรม

สาขาวิชา เคมีอนินทรีย์

ปีการศึกษา 2555

บทคัดย่อ

ทำการสังเคราะห์สารประกอบเชิงซ้อน $Ru(diazpy)(H_2dcbpy)Cl]Cl\cdot H_2O$ และ $[Ru(H_2dcbpy)_2(diazpy)]Cl_2\cdot 6H_2O$ (diazpy = 2,6-(diphenylazo)pyridine, H_2dcbpy = 4,4′-dicarboxy-2,2′-bipyridine) นำสารประกอบเชิงซ้อนที่สังเคราะห์ได้มาศึกษาคุณสมบัติทางเคมีโดยเทคนิคทางสเปกโทรสโกปี และทางไฟฟ้าเคมี จากข้อมูลนิวเคลียร์แมกเนติกเรโซแนนซ์สเปกโทรสโกปี (NMR) และอินฟราเรดสเปกโทรสโกปี (IR) สนับสนุนโครงสร้างของสารประกอบเชิงซ้อนดังกล่าว ซึ่งสารประกอบเชิงซ้อนทั้งสองมีแถบการดูดกลืนแสงที่เกิดจากการถ่ายโอนประจุจากโลหะไปยังลิแกนด์แบบ $t_{2g}\rightarrow\pi^*$(diazpy) ในช่วงแสงมองเห็น (visible region) นอกจากนี้ผลจากอินฟราเรด-สเปกโทรสโกปีแสดงแถบการสั่นของพันธะ N=N(azo) ที่ปรากฏทางด้านความถี่ต่ำกว่าในลิแกนด์ diazpy อิสระ ซึ่งเป็นผลมาจากการเกิด π-back bonding ได้ดีของพันธะระหว่างโลหะ Ru^{2+} กับเอโซลิแกนด์ (N=N)

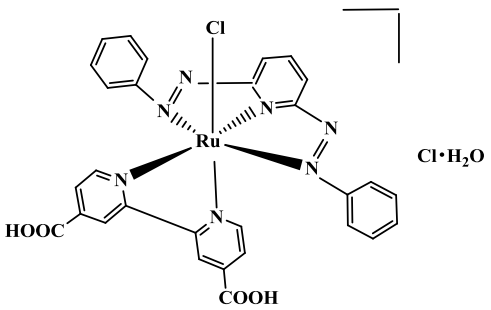

$[Ru(diazpy)(H_2dcbpy)Cl]Cl\cdot H_2O$

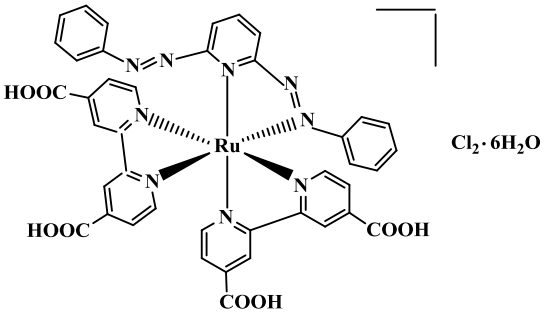

$[Ru(H_2dcbpy)_2(diazpy)]Cl_2\cdot 6H_2O$

Thesis Title	Synthesis and Characterization of Ruthenium(II) Complexes with 2,6-(Diphenylazo)pyridine Ligand and 4,4′-Dicarboxy-2,2′-bipyridine Ligand
Author	Miss Sukanpirom Siritam
Major Program	Inorganic Chemistry
Academic Year	2012

ABSTRACT

The $[Ru(diazpy)(H_2dcbpy)Cl]Cl\cdot H_2O$ and $[Ru(H_2dcbpy)_2(diazpy)]Cl_2\cdot 6H_2O$ complexes (diazpy = 2,6-(diphenylazo)pyridine, H_2dcbpy = 4,4′-dicarboxy-2,2′-bipyridine) were synthesized. The complexes were characterized by spectroscopic and electrochemical techniques. The NMR and IR data supported the structures of the complexes. Both types of complexes have absorption intense band of $t_{2g}\rightarrow\pi^*$(diazpy) metal-to-ligand charge transfer transitions (MLCT) in the visible region. In addition, results from infrared spectroscopy showed that the N=N stretching mode in the complexes appeared at a lower frequency than that in the free diazpy ligand supporting the strong π-back bonding among Ru^{2+} and azo (N=N) bond.

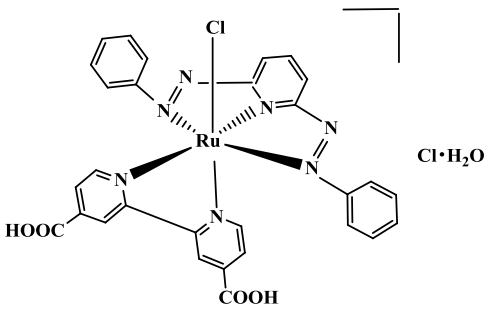

$[Ru(diazpy)(H_2dcbpy)Cl]Cl\cdot H_2O$

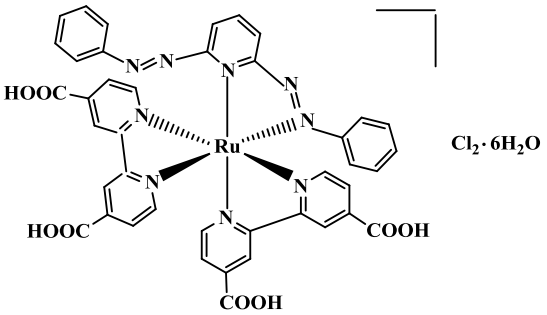

$[Ru(H_2dcbpy)_2(diazpy)]Cl_2\cdot 6H_2O$

ACKNOWLEDGEMENTS

I wish to express my deepest and sincere gratitude to my supervisor, Asst. Prof. Dr. Kanidtha Hansongnern, for her valuable instruction, expert guidance and excellent suggestion. I would like to express my appreciation to her for correction of my thesis. Everything will be always kept in my mind.

My sincere thanks are expressed to Dr. Walailak Puetpaiboon and Dr. Nararak Leesakul, my co-advisors, for their kindness, valuable advice and suggested the improvement of the report.

I would like to thank examination committees, Dr. Cheewita Suwanchawalit, and Asst. Prof. Dr. Chaveng Pakawatchai for their valuable time. I am grateful to Department of Chemistry, Faculty of Science, Prince of Songkla University for all necessary laboratory apparatus and chemicals supplies used throughout this research.

I am very grateful to the Center of Excellence for Innovation in Chemistry (PERCH-CIC): Commision on Higher Education, Ministry of Education and Graduate School, Prince of Songkla University for financial support.

Finally, none of this would have been possible without love, care and encouragement of my family and all members of CH 439. Their friendship, kindness and help have been valuable to me.

Sukanpirom Siritam

THE RELEVANCE OF THE RESEARCH WORK TO THAILAND

In this research, ruthenium(II) complexes with the 2,6-(diphenylazo)pyridine (diazpy) and 4-4′-dicarboxy-2,2′-bipyridine (H_2dcbpy) were synthesized and characterized by spectroscopic and electrochemical techniques.

Results from this work help us to understand a variety of techniques used for the synthesis and characterization of compounds. In addition, these compounds may be developed into producing, especially, an effective dye in a dye sensitized solar cell, more effective catalysts, medicinal drug, and other applications.

CONTENTS

CONTENTS (Continued)

LIST OF TABLES

LIST OF ILLUSTRATIONS

LIST OF ILLUSTRATIONS (Continued)

LIST OF ILLUSTRATIONS (Continued)

LIST OF ABBREVIATIONS AND SYMBOLS

A.R. grade	= Analytical reagent grade
brs	= Broad singlet
CH_3CN	= Acetonitrile
$CHCl_3$	= Chloroform
cm^{-1}	= Wave number
COSY	= Correlation spectroscopy
d	= Doublet
dd	= Doublet of doublet
DEPT	= Distortionless Enhancement by Polarization Transfer
Diazpy	= 2,6-(Diphenylazo)pyridine
DMF	= *N, N*-Dimethylformamide
DMSO	= Dimethyl sulfoxide
E_{pa}	= Anodic peak potential
E_{pc}	= Cathodic peak potential
EtOH	= Ethanol
g	= Gram
h	= Hour
H_2dcbpy	= 4,4′-dicarboxy-2,2′-bipyridine
HMQC	= Heteronuclear Multiple Quantum Correlation experiment
H_2O	= Water
Hz	= Hertz
J	= Coupling constant
KBr	= Potassium bromide
LiCl	= Lithium chloride anhydrous
m	= Medium
m	= Multiplet
MeOH	= Methanol

LIST OF ABBREVIATIONS AND SYMBOLS (Continued)

mg	= Milligram
MHz	= Megahertz
mL	= Milliliter
MLCT	= Metal-to-ligand charge transfer
mmol	= Millimole
mV/s	= Millivolt per second
nm	= Nanometer
NMR	= Nuclear Magnetic Resonance
NaOH	= Sodium hydroxide
ppm	= Part per million
s	= strong
t	= Triplet
tt	= Triplet of triplet
TBAH	= Tetrabutylammonium hexafluorophosphate
TMS	= Tetramethylsilane
V	= Volt
w	= Weak
°C	= Degree Celsius
λ_{max}	= Maximum wavelength
ε	= Molar extinction coefficient
δ	= Chemical shift relative to TMS
%	= Percentage

CHAPTER 1
INTRODUCTION

1.1 Introduction

Ruthenium(II) is well recognized as a metal ion capable of entering into dπ-pπ back bonding with π-acceptor ligands. The π-back bonding, in addition to the conventional σ bonding, gives rise to a number of interesting properties (Krause, *et al*., 1980). This interaction results in the more stability of ruthenium(II) center. There has been considerable interest in ruthenium complexes that contain azoimine (-N=N-C=N-) and polypyridyl (=N-C-C=N-) functional unit ligands, such as ruthenium(II) contain 2,2′-bipyridine (bpy) and 2-(phenylazo)pyridine, (azpy) (Goswami, *et al*., 1981).

The ruthenium(II) azoimine complexes are investigated due to their potential applications in many chemical reactions, i.e., the complexes of $[Ru(azpy)_2Cl_2]$ (azpy = 2-(phenylazo)pyridine) are used as catalysts in epoxidation reactions (Barf, *et al*., 1995). Besides, the α-$[Ru(azpy)_2(NO_3)_2]$ complexes are shown binding to the DNA model (Hotze, *et al*., 2000). Moreover, the *cis*-isomeric complex of $[Ru(azpy)_2Cl_2]$ is shown remarkably high cytotoxicity against a series of tumor-cell lines (Velders, *et al*., 2000) The structure of azpy is shown in Figure 1.

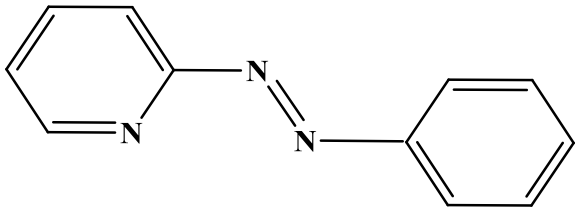

Figure 1 The structure of 2-(phenylazo)pyridine, (azpy).

The polypyridyl ligands are symmetric bidentate ligands which have σ-donor and π-acceptor properties such as 2,2′-bipyridine (bpy) and 1,10-phenanthroline (phen). The ruthenium(II) complexes with bpy and phen ligands had a lot of applications such as $[Ru(bpy)_3]^{2+}$ and $[Ru(H_2dcbpy)_2X_2]$ (H_2dcbpy = 4,4′-(dicarboxy)-2,2′-bipyridine and X = Cl^-, Br^-, I^-, SCN^-, H_2O) used as the most efficient and stable redox sensitizers on nanocrystalline TiO_2 solar cell for conversion light-to-electrical energy (Meyer, 1997). Besides, the interaction of $[Ru(phen)_3]^{2+}$ with nucleic acids showed two primary modes of binding (intercalation and surface binding) (Barton, *et al*., 1986)

Some bidentate and tridentate ligands based pyridine are interesting to be investigated. This is primarily due to their ability to stabilize metal center under a variety of oxidative and reductive conditions and the fact that pyridine ligands are on the borderline between hard and soft Lewis bases. For example, the well-known 2,2′:6′,2′′-terpyridine (tpy) ligand in the complexes of the type $[Ru(tpy)L_1L_2]^{(2-n)+}$ (L_1= apy (2,2′-azobispyridine), 2-phenylazopyridine, or 2-phenylpyridinylmethyleneamine, L_2= Cl^-, H_2O, or CH_3CN) are found to be able to coordinate to the DNA model base 9-ethylguanine. All compounds were screened for anticancer activity in variety of cancer cell lines. It was shown that in some cases activities are comparable to that of cisplatin (Corral, *et al*., 2009). Besides, 2,6-pyridily-diimines (pydim) has emerged as an alternative to tpy (Cetinkaya, *et al*., 1999). The pydim behaved as a tridentate ligand in complexes such as five-coordinate $[MX_2(pydim)]$ (M = Mn, Fe, Co, Ni, Cu, Zn, Cd; X = Cl, Br) complexes and six-coordinate $[M(pydim)_2]X_2$ (X = BF_4^-, $ClO4^-$) complexes. Pydim has been observed to function as a bidentate chelating ligand in certain carbonyl derivatives (Albon, *et al*., 1989).

In the last two decade, Ru(II) complexes containing 4,4′-dicarboxy-2,2′-bipyridine (H_2dcbpy) as an attaching group for the sensitization of nanocrystalline TiO_2 have been observed. This ligand is used in order to obtain sensitizers showing increased absorption coefficients for enhanced light harvesting (Nazeeruddin *et al*., 1993). In addition, it is now well established that H_2dcbpy serves as an interlocking group between the molecular ‘antenna’ (complex) and the

semiconductor's surface through an ester-like linkage between the -COOH group and the surface hydroxyl groups of TiO_2 (Falaras, 1998).

In this research, 2,6-(diphenylazo)pyridine (diazpy) is an azo compound similar to 2-(phenylazo)pyridine (azpy) containing two azo groups and it acted as both bidentate and tridentate ligands. The diazpy ligand was stronger π-acceptor than bpy and phen but less than azpy for stabilizing ruthenium(II) (Nookong., 2003). The structures of diazpy and H_2dcbpy ligands are shown in Figure 2.

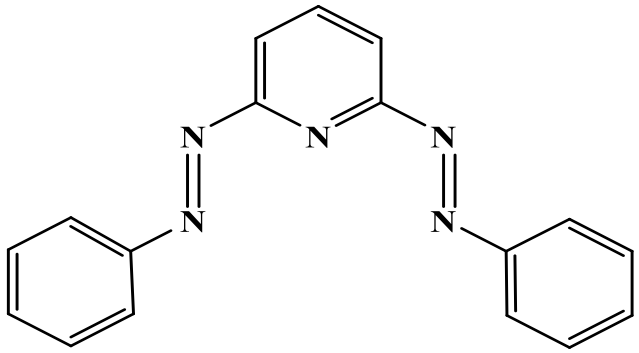

2,6-(diphenylazo)pyridine, (diazpy)

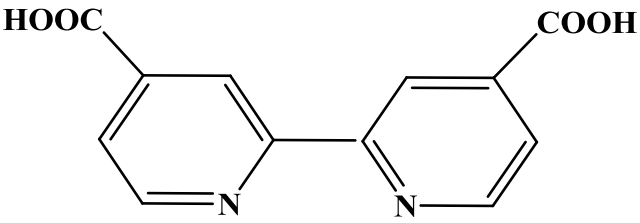

4,4′-dicarboxy-2,2′-bipyridine, (H_2dcbpy)

Figure 2 The structures of diazpy and H_2dcbpy ligands.

Therefore, in this work, it is our interest to investigate the chemistry of the ruthenium(II) complexes containing 2,6-(diphenylazo)pyridine (diazpy) and 4-4′-dicarboxy-2,2′-bipyridine (H_2dcbpy). These complexes have been synthesized and characterized by elemental analysis, infrared spectroscopy, UV-Visible absorption

spectroscopy, NMR spectroscopy and cyclic voltammetry. In addition, we hope that results from characterization of these complexes will be beneficial to insight information of these complexes and other researchers.

1.2 Review of Literatures

Krause and Krause, (1980) studied dichlorobis(2-(phenylazo)pyridine)-ruthenium(II) complexes, $[Ru(azpy)_2Cl_2]$. Three isomers of $[Ru(azpy)_2Cl_2]$ were obtained from reaction between 2-(phenylazo)pyridine (azpy) and $RuCl_3.3H_2O$. There were two *cis*-isomers (α and β) and one *trans*-isomer (γ). These complexes were characterized by IR spectroscopy, UV-Visible absorption spectroscopy and ^{13}C NMR techniques. The results from cyclic voltammetric data showed that the azpy ligand was a better π-acceptor than the bpy ligand (bpy = 2,2′-bipyridine).

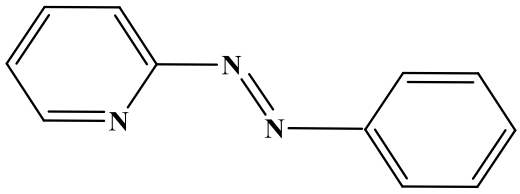

2-(phenylazo)pyridine, azpy

Goswami, *et al*., (1981) synthesized the complexes of $[Ru(bpy)_2L]^{2+}$ (L = 2-(phenylazo)pyridine, (azpy) and 2-(*m*-tolylazo)pyridine), (tap) and studied the chemical properties such as UV-Visible absorption which showed metal-to-ligand charge transfer (MLCT) in the visible region. The infrared spectra displayed the N=N azo stretching mode which was the important function group of azoimine ligands. Results from the cyclic voltemmetry showed that the azopyridine ligand gave rise to stabilize ruthenium(II).

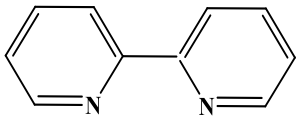

2,2′-bipyridine, (bpy)

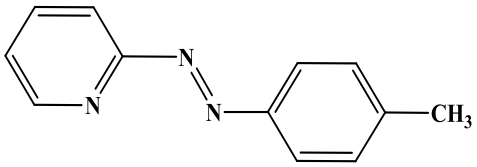

2-(*m*-tolylazo)pyridine), (tap)

Barton, *et al*., (1986) studied the binding of tris(1,10-phenanthroline)ruthenium(II), $[Ru(phen)_3]^{2+}$, enantiomers to nucleic acids of different base compositions and structures. Luminescence decay of $[Ru(phen)_3]^{2+}$ isomers in the presence of DNA shows components of two different lifetimes. Finite polarization in the emission of both Δ- and Λ- $[Ru(phen)_3]^{2+}$ in the presence of DNA is indicative of intercalation. Chiral discrimination for Δ-$[Ru(phen)_3]^{2+}$ increases both with the percent guanine-cytosine (GC) and with increasing Na^+ concentration. Based upon the stereoselectivities found by steady-state emission polarization, the variations are attributed to changes in chiral preferences for intercalation. Weak surface binding, having a preference for Λ- $[Ru(phen)_3]^{2+}$, is observed with double-stranded RNA. For both $[Ru(phen)_3]^{2+}$ and $[Ru(DIP)_3]^{2+}$ (DIP = 4,7-diphenylphenanthroline), binding to T4 DNA glycosylated in the major groove is markedly diminished compared to binding to calf thymus DNA. The chiral ruthenium complexes, with luminescence characteristics indicative of binding modes, and stereoselectivities that tuned to the helix topology, maybe useful molecular probes in solution for nucleic acid secondary structure.

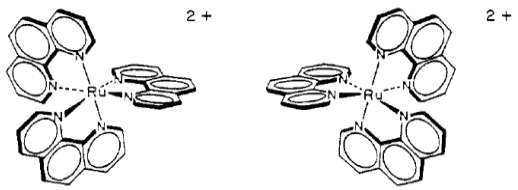

Λ Δ

Enantiomers of tris(1,10-phenanthroline)ruthenium(II), $[Ru(phen)_3]^{2+}$.

(*J. Am. Chem. Soc.*1986, **108**: 2081-2088.)

Albon, *et al*., (1989) reported the isolation and spectrosocopic characterization of six complexes, *cis*-$[M(CO)_4L^2]$ (M = Mo, W), *fac*-$[Mo(CO)_3(NCMe)L^2]$, *fac*-$[M'Br(CO)_3L^2]$ (M = Mn, Re) and *fac*-$[Re(CO)_3(NCMe)L^2]ClO_4$, with L^2= the Schiff base ligand 2,6-bis[1-(phenylimino)ethyl]pyridine. This ligand, which has previously been shown to act as a planar tridentate in a wide range of complexes, behaves as a bidentate chelating ligand in all the above complexes bonding through the pyridyl nitrogen and one imine nitrogen only.

Nazeeruddin, *et al*., (1993) synthesized the complexes of *cis*-$[Ru(II)L_2X_2]$ complexes (L= 2,2′-bipyridyl-4,4′-dicarboxylate and X = $C1^-$, Br^- , I^-, CN^-, and SCN^-) and characterized with respect to their absorption, luminescence, and redox behavior. They act as efficient charge-transfer sensitizers for nanocrystalline TiO_2 films of very high internal surface area, prepared by sintering of 15-30 nm colloidal titania particles on a conducting glass support. The performance of *cis*-di(thiocyanato)bis(2,2′-bipyridyl-4,4′-dicarboxylate)ruthenium(II) (**1**) was found to be outstanding and is unmatched by any other known sensitizer. Nanocrystalline TiO_2 films coated with a monolayer of **1** harvest visible light very efficiently, their absorption threshold being around 800 nm. Conversion of incident photons into electric current is nearly quantitative over a large spectral range. A solar-to-electric energy conversion efficiency of 10%.

Barf and Sheldon, (1995) studied the isomeric complexes of $[Ru(azpy)_2Cl_2]$ which were two *cis*-isomers (α, β) and one *trans*-isomer (γ). They were used as catalysts for epoxidation reactions of olefin to give epoxide. The different isomers showed different activity and selectivity. The results showed that the β-$[Ru(azpy)_2Cl_2]$ and γ-$[Ru(azpy)_2Cl_2]$ complexes gave better yields than the α-$[Ru(azpy)_2Cl_2]$ complex.

Meyer, (1997) studied the Ru(II) polypyridyl coordination compounds used as the most efficient and stable redox sensitizers on nanocrystalline TiO_2 solar cell for conversion light-to-electrical energy. These compounds possess metal-to-ligand charge transfer (MLCT) absorption bands that harvest a large fraction of visible light. The photophysical properties of the parent compound $[Ru(bpy)_3]^{2+}$,

where bpy is 2,2′-bipyridine, have been presented. Chemically related sensitizers where one or more of the bpy ligands is replaced by 4,4′-$(COOH)_2$-2,2′-bipyridine, dcbpy are anchored to semiconductor surfaces through the reaction of carboxylic acid groups with surfaces hydroxyl groups to form presumed ester linkages, as illustrated below. There now exist some spectroscopic data supporting the presence of ester links.

Falaras, (1998) investigated the surface interaction of TiO_2 powder particles sensitized with two of the most efficient sensitizers by using FT-IR spectroscopy, the mono-nuclear complex $[RuL_2(SCN)_2]$ and the tri-nuclear complex $[RuL_2[\mu\text{-}(CN)Ru(CN)L'_2]_2$ (L = 4,4′-dicarboxylicacid-2,2′-bipyridine and L′ = 2,2′-bipyridine), both having ligands substituted with carboxylic acid (-COOH) functional groups. The C=O band peak frequency shifts of about 20 cm^{-1} higher than that of bulk complexes and disappearance of the CN^- and SCN^- band vibrations were observed on derivative samples. The C=O shift was attributed to chemical adsorption of the dyes onto the oxide particles via ester-like binding between the carboxylic acid groups and the OH moieties on TiO_2.

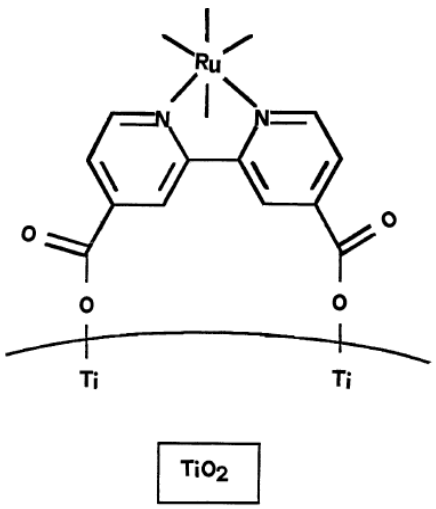

Adsorption of Ru-bpy sensitizes on TiO_2 particles via formation of ester-like linkages.

(*Sol. Energy Mater, Sol. Cells.*1998, **53**: 163-175.)

Cetinkaya, *et al*., (1999) studied the reaction of $[RuCl_2(p\text{-cymene})]_2$ with tridentate *N,N'-N* ligands, 2,6- pyridyl-diimines (pydim). This led to substitution of *p*-cymene. These complexes exhibited efficient activity for epoxidation of cyclohexene in the presence of iodosobenzene (PhIO). The molecular structure for one of complexes, (acetonitrile){2,6-bis-[1-(4-methoxyphenylimino)ethyl] pyridine} dichlororuthenium(II) has been determined by X-ray diffraction.

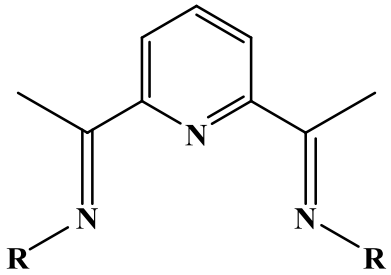

Pydim (R = alkyl or aryl)

Maruthamuthu, *et al*., (1999) reported the preparation, characterization and photoconversion properties of $[Ru(II)(dcbpy)(terpy)X]X\cdot 3H_2O$ where X = Cl^-, SCN^-, and CN^-. For the fabrication of a solar cell, TiO_2 and platinum coated conducting glasses were used. The performance of the complexes for the conversion of solar radiation into electricity was found to be good, with maximum output voltage (V_{oc}) and short circuit current (I_{sc}).

Hotze, *et al*., (2000) reported the new water-soluble compound α-$[Ru(azpy)_2(NO_3)_2]$ (azpy = 2-phenylazo)pyridine; α indicated that isomer in which the coordinating pairs ONO_2, N(py) and N(azo) were *cis*, *trans* and *cis*, respectively. The solid-state structure of this compound has been determined by X-ray crystallography. The binding of DNA-model bases 9-ethylguanine (9egua) and guanosine (guo) to this complex has been studied and compared with the complex of *cis*-$[Ru(bpy)_2Cl_2]$. The binding DNA complex has been identified by ^1H NMR and 2D NMR spectroscopy.

Velders, *et al*., (2000) investigated the three isomeric of $[Ru(azpy)_2Cl_2]$ complexes (α-$[Ru(azpy)_2Cl_2]$; β-$[Ru(azpy)_2Cl_2]$; γ-$[Ru(azpy)_2Cl_2]$ which α, β, γ referred to *ctc*, *ccc*, *tcc* configurations). These complexes showed different in Vitro cytotoxicity activity. The *ctc*-$[Ru(azpy)_2Cl_2]$ isomer showed high cytotoxicity against a series of tumor cell lines. While the *ccc* and *tcc* showed low to moderate cytotoxicity. In addition, the structure of *tcc* isomer was confirmed by single crystal X-ray diffraction. The *tcc* had two chloride atoms in *trans* position, but the N(pyridine) and N(azo) groups were in *cis* geometry. Futhermore, the binding of DNA bases to the *ctc*-$[Ru(azpy)_2Cl_2]$ was studied and compared with the similar complexes such as *cis*-$[Ru(bpy)_2Cl_2]$. The binding of the *ctc* isomer with guanine and purine base was sterically less hindered than that in *cis*-$[Ru(bpy)_2Cl_2]$ complexes. Therefore the *ctc*-isomer was found to show high cytotoxicity against a series of tumor-cell lines.

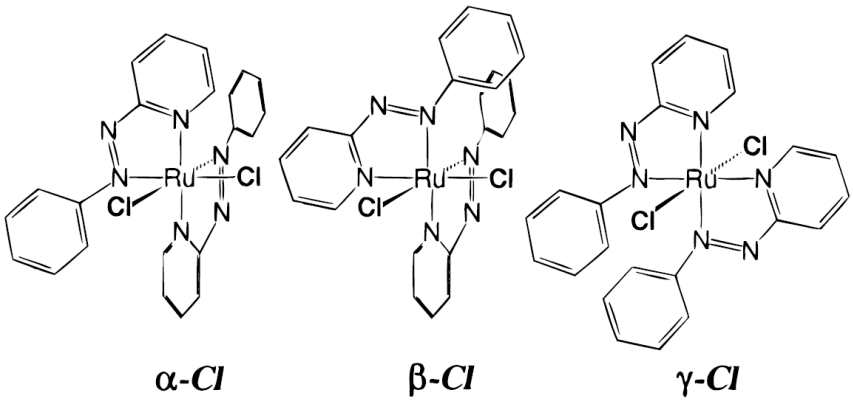

Structural representation of (the Δ enantiomers of) α-[Ru-$(azpy)_2Cl_2$] (left), β-$[Ru(azpy)_2Cl_2]$ (middle) and γ-$[Ru(azpy)_2Cl_2]$ (right).

(*Inorg. Chem.* 2000, **39**: 2966-2967.)

Hansongnern, *et al*., (2001) synthesized and characterized the complex [Ru(tpy)(L)Cl]Cl (where L is 2-(phenylazo)pyridine = azpy). [Ru(tpy)(azpy)Cl]Cl was characterized by X-ray crystallography. The chlorine atom is *trans* to the nitrogen atom of the pyridine ring.

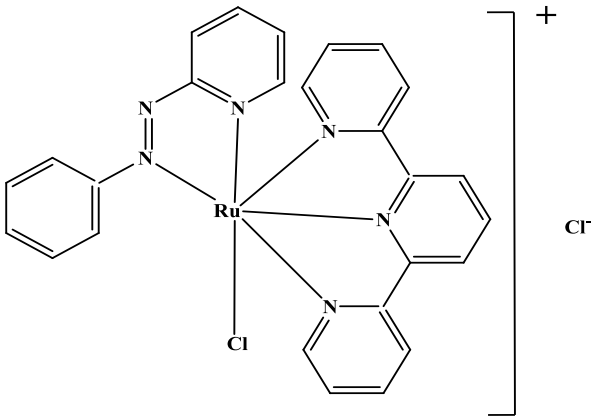

[Ru(tpy)(azpy)Cl]Cl, (azpy = 2-(phenylazo)pyridine).

Chryssou, *et al*., (2002) synthesized a new complex, [Ru(II)(dcbpyH_2)(bdmpp)Cl] (PF_6) (where bdmpp is 2,6-bis(3,5-dimethyl-*N*-pyrazoyl)pyridine, dcbpyH_2 is 2,2′-bipyridine-4,4′-dicarboxylic acid). This complex was characterized by mass spectroscopy, IR, ES-MS and ^{1}H NMR (1D and 2D) spectroscopies. The broad and very high intensity MLCT absorption band in the visible made this dye potentially beneficial for the photosensitization process. Cyclic voltammetry analysis displays a well reversible oxidation–reduction wave. Transparent TiO_2 thin film electrodes could easily be chemically modified by the complex and the incorporation of the resulting photoelectrodes in wet regenerative solar cells produced a stable photovoltage of 550 mV and gave a continuous photocurrent of 140 μA cm^{-2}.

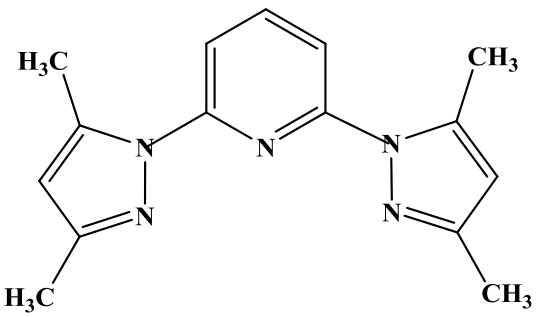

2,6-bis(3,5-dimethyl-*N*-pyrazoyl)pyridine, (bdmpp)

Nookong, (2003) synthesized a new ligand, containing an azo moiety. Structure of the 2,6-(diphenylazo)pyridine (diazpy) was similar to 2-(phenylazo)pyridine (azpy) but contained two azo groups and it acted as both tridentate and bidentate ligands. Results from IR spectroscopic data and cyclic voltammetry showed that the bidentate diazpy ligand was stronger π-acceptor than bpy and phen but less than azpy.

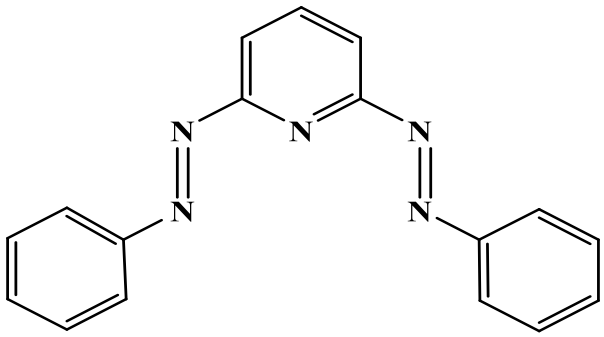

2,6-(diphenylazo)pyridine, (diazpy)

Anandan, *et al*., (2004) synthesized naphthyridine and acridinedione coordinated ruthenium(II) complexes and characterized by using UV-Visible absorption, FTIR and CHN analysis. Their applications in dye-sensitized solar cells were demonstrated. From the *I*–*V* curves, the short-circuit photocurrent (I_{SC}) and the open-circuit photovoltage (V_{OC}) were measured. A maximum current conversion efficiency (η) of about 7.7% was obtained for 5-amino-4-phenyl-2-(4-methylphenyl)-7-(pyrrolidin-1-yl)-1,6-naphthyridine-8-carbonitrile (*pmpn*) coordinated ruthenium (II) complex.

Stergiopoulos, *et al*., (2004) reported the new dyes of the type [Ru(II)(bdmpp)(dcbpy)X](PF_6) (where bdmpp is 2,6-bis(3,5-dimethyl-*N*-pyrazoyl)pyridine, dcbpy is 2,2′-bipyridine-4,4′-dicarboxylic acid and X = Cl^- (Ru-Cl) or NCS^- (Ru–NCS)) have been tested with success as molecular antennas in titania nanocrystalline photoelectrochemical cells (DSSCs) and compared with the Grätzel's N3 photosensitizer. The solar cells made using the complex with the –NCS ligand have a significantly better performance than those fabricated with the dye

containing the Cl^- ligand. The comparison of their action spectra has revealed that the Ru–NCS dye presents higher incident monochromatic photon-to-current conversion efficiency (IPCE) values. The Ru–NCS cells has an overall energy conversion cell efficiency (η) as high as 1.64%.

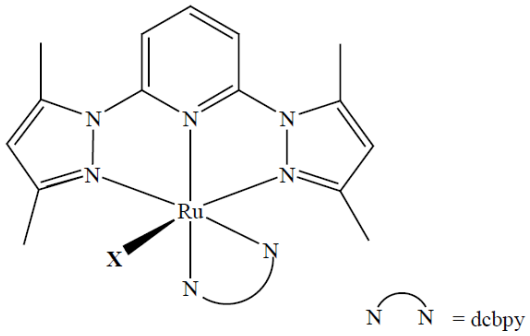

Molecular structure for the Ru–Cl and Ru–NCS complexes.
(*J. Photochem. Photobiol. A: Chem.* 2004, **163**: 331-340.)

Chatzivasiloglou, *et al.*, (2005) synthesized the complex of $[Ru(II)(H_2dcbpy)Cl_2]\cdot 2H_2O$ (H_2dcbpy = 4,4′-dicarboxy-2,2′-bipyridine) and characterized by using ^1H NMR, FT-IR and UV–vis spectroscopies. This complex used as the dye to sensitize nanocrystalline TiO_2 film electrodes. The cells under direct sunlight illumination has an overall energy conversion efficiency of 0.27%.

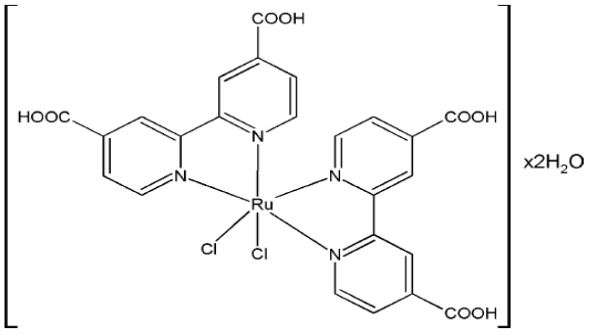

Molecular configuration for the $[Ru(II)(dcbpyH_2)_2Cl_2]\cdot 2H_2O$ complex.
(*J. Mat.Pro.Tech.* 2005, **161**: 234-240.)

Sahavisit and Hansongnern, (2005) synthesized a new bidentate ligand, containing an azo moiety. Structure of the 5-chloro-2-(phenylazo)pyridine (Clazpy) was similarly to 2-(phenylazo)pyridine (azpy) but the hydrogen atom on the fifth position on the pyridine ring was replaced by a chlorine atom. They reported the bidentate Clazpy ligand is a better π-acceptor than azpy in order to stabilize Ru(II) center.

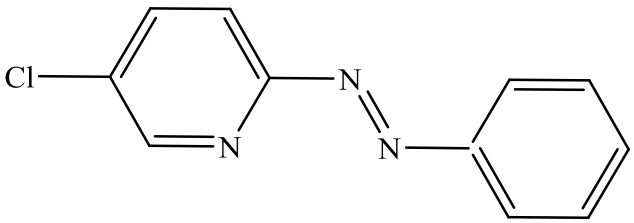

5-Chloro-2-(phenylazo)pyridine (Clazpy)

Corral, *et al*., (2006) synthesized and characterized the complexes $[Ru(tpy)(apy)L^{n-}](ClO_4)_{(2-n)}$ (apy = 2,2′-azobispyridne; tpy = 2,2′:6′,2″-terpyridine; L = Cl^-, H_2O, CH_3CN). These complexes were characterized by 1D and 2D ^1H NMR spectroscopy, spectrometry, and elemental analysis. The molecular structures of the compounds were elucidated by single-crystal X-ray diffraction.

Philippopoulos, *et al*., (2007) reported the synthesis and spectroscopic characterization of a series of neutral [Ru(bpp)(dcbpyH)(X)] ($X = Cl^-, NCS^-$) cationic $[Ru(bpp)(dcbpyH_2)Cl]Cl$, and anionic Na[Ru(bpp)-(dcbpy)(CN)] ruthenium(II) complexes containing the tridentate ligand 2,6-bis(1-pyrazolyl)pyridine. All complexes were characterized by FT-IR, FT-Raman, UV/Vis, ^1H NMR spectroscopy, elemental analysis, and mass spectrometry. Furthermore, their photo-electrochemical properties have been studied in sandwich-type solid-state nanocrystalline TiO_2 cells using a composite polymer redox electrolyte.

Seok, *et al*., (2007) synthesized novel Ru(II) polypyridyl dyes and described their characterization. The photo-electrochemical properties of DSCs using these sensitizers were investigated. New dyes contain chromophore unit of dafo (4,5-diazafluoren-9-one) or phen-dione (1,10-phenanthroline-5,6-dione) instead of the

nonchromophoric donor unit of thiocyanato ligand in *cis*-[Ru^{II}(dcbpy)$_2$(NCS)$_2$] (dcbpy = 4,4'-dicarboxy-2,2'-bipyridine) coded as N3 dye. For example, the photovoltaic data of DSCs using [Ru^{II}(dcbpy)2(dafo)](CN)$_2$ as a sensitizer show 6.85 mA/cm^2, 0.70 V, 0.58 and 2.82% in short-circuit current (J_{sc}), open-circuit voltage (V_{oc}), fill factor (*FF*) and power conversion efficiendy (E_{ff}), which can be compared with those of 7.90 mA/cm^2, 0.70 V, 0.53 and 3.03% for N3 dye.

Hamaguchi, *et al*., (2008) prepared the [Ru(tpy)(bpy)(2-OpyS)]PF_6 (where bpy = 2,2′-bipyridine; tpy = 2,2′:6′,2″-terpyridine; 2-OpyS = 2-mercaptopyridine *N*-oxide). The complex contains a 2-OpyS- ligand coordinating only with the sulfur atom. Electrochemically induced linkage isomerisation was examined for this complex.

Corral, *et al*., (2009) studied the various interaction modes between a group of six ruthenium polypyridyl complexes and DNA. Five mononuclear species were selected with formula [Ru(tpy)L_1L_2]$^{(2-n)+}$, and one closely related to dinuclear cation of formula [{Ru(apy)(tpy)}$_2${μ-$H_2N(CH_2)_6NH_2$}]$^{4+}$. The ligand tpy is 2,2′:6′,2″-terpyridine and the ligand L_1 is a bidentate ligand, namely, apy (2,2′-azobispyridine), 2-phenylazopyridine, or 2-phenylpyridinylmethyleneamine. The ligand L_2 is a labile monodentate ligand, being Cl^-, H_2O, or CH_3CN. All six species containing a labile L_2 able to coordinate to the DNA model base 9-ethylguanine. These compounds were studied by ^{1}H NMR and mass spectrometry.

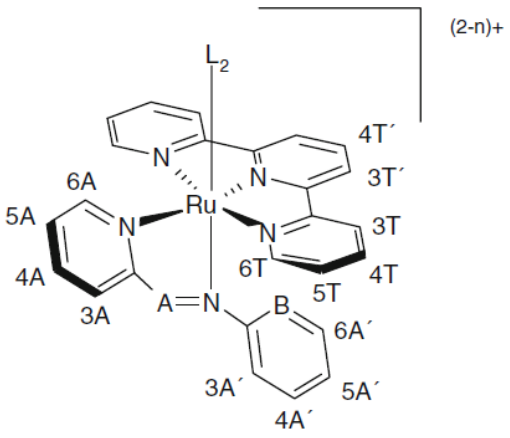

1a: A = N, B = N, $L_2 = Cl^-$

1b: A = N, B = N, $L_2 = H_2O$

1c: A = N, B = N, $L_2 = CH_3CN$

1d: A = N, B = CH, $L_2 = Cl^-$

1e: A = CH, B = CH, $L_2 = Cl^-$

[Ru(tpy)L_1L_2]$^{(2-n)+}$ compounds (**1a**, **1b**, **1c**, **1d**, **1e**), (tpy is 2,2′:6′,2′′-terpyridine).

(*J. Biol. Inorg. Chem.*2009, **14**: 439-448.)

Onozawa-Komatsuzaki, *et al*., (2011). synthesized the new ruthenium(II)–polypyridyl complexes, [Ru{2,6-bis(4-carboxy-quinolin-2-yl)pyridine}$(NCS)_3$] (**1a** (X=H)) and [Ru{2,6-bis(4-carboxy-5-chloroquinolin-2-yl)pyridine} $(NCS)_3$] (**1b** (X=Cl)). These complexes were characterized their photophysical, photochemical properties and as a sensitizer for dye-sensitizedsolarcells (DSCs). Both of the complexes showed broad electronic absorption bands in the near-IR region, which were assigned to the metal-to-ligand charge transfer (MLCT) transitions. The DSC sensitized with **1a** exhibited higher IPCE value than that of the one sensitized with **1b**.

1.3 Objectives

1. To synthesize the 2,6-(diphenylazo)pyridine (diazpy) ligand, the [Ru(diazpy)(H_2dcbpy)Cl]Cl·H_2O, and [Ru(H_2dcbpy)$_2$(diazpy)]Cl_2·$6H_2O$ complexes.
2. To characterize and to analyze the chemistry of the [Ru(diazpy)-(H_2dcbpy)Cl]Cl·H_2O, and [Ru(H_2dcbpy)$_2$(diazpy)]Cl_2·$6H_2O$ complexes.

CHAPTER 2
MATERIALS AND METHODS

2.1 Materials

2.1.1 Chemical substances

Material from Ajax Finechem

Sodium hydroxide, NaOH, A.R. grade

Material from A Johnson Metthey Company

2,2′-Bipyridine-4,4′-dicarboxylic acid, $C_{12}H_8N_2O_4$, A.R. grade

Materials from Fluka

2,6-Diaminopyridine, $C_5H_7N_3$, A.R. grade

Lithium chloride anhydrous, LiCl, A.R. grade

Nitrosobenzene, C_6H_5NO, A.R. grade

Materials from Merck

Nitrosobenzene, C_6H_5NO, A.R. grade

Silica gel 60 (0.040-0.063 mm)

Silica gel 100 (0.060-0.200 mm)

Material from Sigma-Aldrich

Dichloro(*p*-cymene)ruthenium(II) dimer, $C_{20}H_{28}C_{l4}Ru_2$, A.R. grade

2.1.2 Solvents

Solvent from Ajax Finechem

N, *N*-Dimethylformamide, DMF, C_3H_7NO, A.R. grade

Solvents from J.T. Baker

Ethanol, C_2H_5OH, A.R. grade

Ether, $((C_2H_5)_2O)$, A.R. grade

Solvents from Lab.Scan Analytical Science

Acetone, CH_3COCH_3, A.R. grade

Acetonitrile, CH_3CN, A.R. grade

Chloroform, $CHCl_3$, A.R. grade

Ethanol, C_2H_5OH, A.R. grade

Ethyl acetate, $C_4H_8O_2$, A.R. grade

Hexane, C_6H_{14}, A.R. grade

N, *N*-Dimethylformamide, DMF, C_3H_7NO, A.R. grade

Solvents from Merck

Methanol, CH_3OH, A.R. grade

Toluene, $C_6H_5CH_3$, A.R. grade

Solvent from RANKEM

Benzene, C_6H_6, A.R. grade

2.2 Instruments

2.2.1 Melting Point Apparatus

Melting points of all compounds were measured in range 30 - 300˚C on the Thomas Hoover Capillary melting point apparatus, ARTHUR H. THOMAS COMPANY. PHILADELPHIA PA., U.S.A.

2.2.2 Elemental Analysis

Elemental analytical data were obtained by using a CHNS-O Analyzer, CE Instruments Flash EA 1112 Series, Thermo Quest, Italy.

2.2.3 Infrared Spectroscopy

Infrared spectra were collected by using KBr pellets on a Perkin Elmer Spectrum BX FT-IR Spectrophotometer from 400-4,000 cm^{-1}.

2.2.4 UV-Visible Absorption Spectroscopy

UV-Visible absorption spectra were recorded in the range 200-800 nm by Hewlett Peckard 8453 UV-Visible spectrophotometer.

2.2.5 Nuclear Magnetic Resonance Spectroscopy

1D and 2D NMR spectra were recorded in methanol-d_4 solution with a BRUKER AVANCE 300 FT-NMR instrument. Tetramethysilane ($Si(CH_3)_4$) was used as an internal standard.

2.2.6 Cyclic Voltammetry

Electrochemical experiments were carried out using MacLab (4e AD Instruments with potentionstate/Serial No. p 068). Software of the MacLab is ECHEM program version 1.5.1. Cyclic voltammograms were obtained using a glassy carbon as a working electrode, a platinum flag as an auxiliary electrode and a platinum wire as a reference electrode. The supporting electrolyte was tetrabutylammonium hexafluorophosphate, $[NBu_4]PF_6$, (TBAH) in acetonitrile and dimethylformamide. At the end of each experiment, ferrocene was added as an internal standard. The argon gas was bubbled through the solution for 10 minutes prior to each measurement.

2.3 Synthesis of ligand

The 2,6-(diphenylazo)pyridine ligand was prepared by literature methods (Nookong, 2003).

2,6-(diphenylazo)pyridine ligand (Diazpy)

2,6-diaminopyridine (0.109 g, 1 mmol) and nitrosobenzene (0.214 g, 2 mmol) were added to the benzene solution with the presence of sodium hydroxide

(NaOH) solution. The mixture was refluxed under stirring continuously for 5 h. The green solution gradually turned to dark brown. The product was extracted with benzene and purified by using column chromatography on a silica gel. The orange band was collected after elution with ethyl acetate and hexane (1:9 by volume) and evaporated to dryness. The yield was 65 mg (22%).

2.4 Syntheses of complexes

[Ru(diazpy)Cl_2] complex was prepared by the modified literature method (Nookong, 2003). The [Ru(diazpy)(H_2dcbpy)Cl]Cl·H_2O complex was prepared by using published procedures (Chryssou, *et al*., 2002). [Ru(H_2dcbpy)$_2Cl_2$] complex was prepared by the modified literature method (Liska, *et al.*, 1988). The [Ru(H_2dcbpy)$_2$(diazpy)]Cl_2·$6H_2O$ complex was prepared by modified literature methods (Seok, *et al*., 2007).

Synthesis of [Ru(diazpy)Cl_2] complex

The dichloro(*p*-cymene) ruthenium(II) dimer (0.061 g, 0.1 mmol) and 2,6-(diphenylazo)pyridine (0.058 g, 0.2 mmol) were added to 50 mL of absolute ethanol in a 250 round-bottom flask and the mixture was refluxed for 3 h under stirring. Then the reaction mixture was evaporated to dryness and the crude product was dissolved in 30 mL of a acetonitrile:toluene solvent mixture (2:1 by volume). The solution was left at room temperature for 2 days. The resulting deep green precipitate was collected on a sintered glass funnel and washed with hexane and ether, respectively. The yield was 35 mg (76%).

Synthesis of [Ru(diazpy)(H_2dcbpy)Cl]Cl·H_2O complex

[Ru(diazpy)Cl_2] (0.100 g, 0.218 mmol), 2,2′-bipyridine-4,4′-dicarboxylic acid, H_2dcbpy (0.066 g, 0.270 mmol) and LiCl (0.021 g, 0.50 mmol) were added to 40 mL of an ethanol:H_2O solvent mixture (3:1 by volume). The solution was refluxed with stirring continuously for 4 h. Then the reaction mixture

was filtered while it was hot and evaporated to dryness. After dissolving the crude product in ethanol, the solution was left at 0 °C for 20 days. The resulting deep brown precipitate was collected on a sintered glass funnel and washed with cooled water, and ether, respectively. The precipitate was dried and recrystallized with acetone and ethanol. The yield was 112 mg (71%).

Synthesis of [Ru(H_2dcbpy)$_2$$Cl_2$] complex

The 20 mL of *N*,*N*-dimethylformamide (DMF) was added to a dichloro(*p*-cymene)ruthenium(II) dimer (0.061 g, 0.1 mmol) and 2,2′-bipyridine 4,4′-dicarboxylic acid (H_2dcbpy) (0.102 g, 0.42 mmol). The mixture was refluxed for 4 h. After this time the reaction was filtered and then ethanol was added to the filtrate solution. The mixture was allowed to stand overnight. The solution was filtered, evaporated to dryness and washed with $CHCl_3$. The purple solid was obtained. The yield was 23 mg (69%).

Synthesis of [Ru(H_2dcbpy)$_2$(diazpy)]Cl_2·6H_2O complex

[Ru(H_2dcbpy)$_2$$Cl_2$] (0.066 g, 0.1 mmol) and 2,6-(diphenylazo)pyridine (0.037 g, 0.13 mmol) were added to 40 mL of a methanol:H_2O solvent mixture (1:1 by volume). The solution was refluxed with stirring continuously for 14 h. Then the reaction mixture was evaporated to dryness and purified by column chromatography on a silica gel using a methanol:ethanol solvent mixture (1:1 by volume) as the eluent. The resulting orange-brown solid was obtained. The yield was 43 mg (41%).

CHAPTER 3
RESULTS AND DISCUSSION

3.1 Synthesis and characterization of ligand

3.1.1 Synthesis of ligand

The 2,6-(diphenylazo)pyridine ligand was synthesized by using the literature procedure (Nookong, 2003). This ligand was generally obtained by the condensation of nitrosobenzene with 2,6-diaminopyridine in 2:1 mole ratio in the mixture of sodium hydroxide and benzene solution. The reaction was refluxed for 5 h. Then, the mixture was extracted with benzene and purified by column chromatography as described previously. The orange band was collected. The reaction is shown in equation (1).

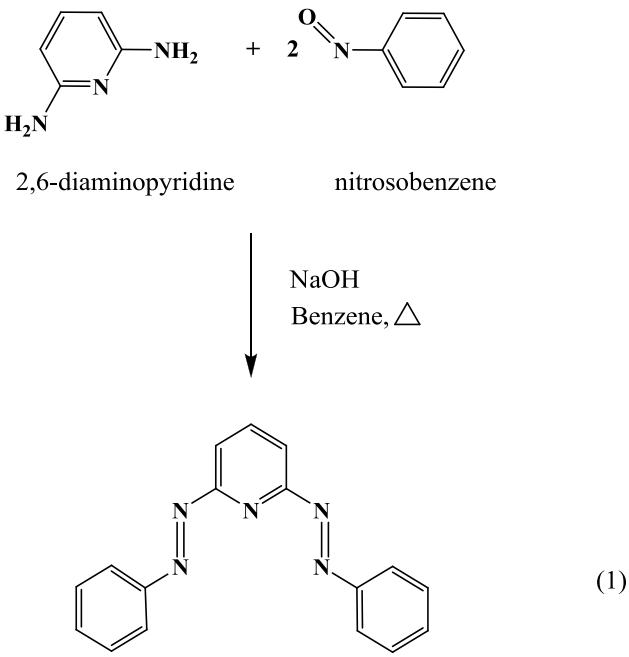

2,6-diaminopyridine nitrosobenzene

2,6-(diphenylazo)pyridine (diazpy)

(1)

The yield of diazpy is 22 %. The physical properties of the diazpy ligand are summarized in Table 1.

Table 1 The physical properties of the diazpy ligand

Compound	Physical properties		
	Appearance	Color	Melting point (°C)
Diazpy	solid	Red-orange	104-105

The melting point of the diazpy ligand was in the range of 104-105°C. The solubility of ligand was tested in various solvents. The ligand was very soluble in the methanol (MeOH), ethanol (EtOH), acetonitrile (CH_3CN), acetone (CH_3COCH_3), ethyl acetate (EtOAc), dichloromethane (CH_2Cl_2) and hexane, but it is insoluble in water (Nookong, 2003).

3.1.2 Characterization of ligand

The chemistry of the diazpy ligand was determined by using these techniques.

3.1.2.1 Infrared spectroscopy

3.1.2.2 UV-Visible absorption spectroscopy

3.1.2.3 Nuclear Magnetic Resonance spectroscopy (1D and 2D)

3.1.2.4 Cyclic Voltammetry

3.1.2.1 Infrared spectroscopy

Infrared spectroscopy is a technique to study the functional groups of compounds. Infrared spectra were collected by using KBr pellets in the range of 4000-400 cm^{-1}. The important vibrational frequencies are C=C, C=N, N=N (azo) stretching modes and C-H bending in monosubstituted benzene.The infrared spectroscopic data of the diazpy ligand are listed in Table 2.

Table 2 Infrared spectroscopic data of the diazpy ligand

Vibration modes	Frequencies (cm^{-1})
C=N, C=C stretching	1571 (s) 1489 (m) 1474 (m)
N=N stretching	1448 (m) 1420 (s)
C-H bending of monosubstituted benzene	828 (s) 768 (s) 687 (s)

s = strong, m = medium

The infrared spectrum of diazpy exhibit intense bands at 1600-400 cm^{-1}. The ligand showed strong peaks at 1571, 1489 and 1474 cm^{-1} corresponding to C=C and C=N stretching in the pyridine ring of the ligand. The most important band was N=N stretching which used to be considered for the π-acidity property in azo complexes. The N=N stretching of diazpy showed two intense bands at 1448 cm^{-1} and 1420 cm^{-1}. This corresponded to the vibration energies of both N=N (azo) in diazpy molecule. The vibration energies of both N=N (azo) were different frequencies maybe due to nonplanarity in diazpy molecule. The infrared spectrum is shown in Figure 3.

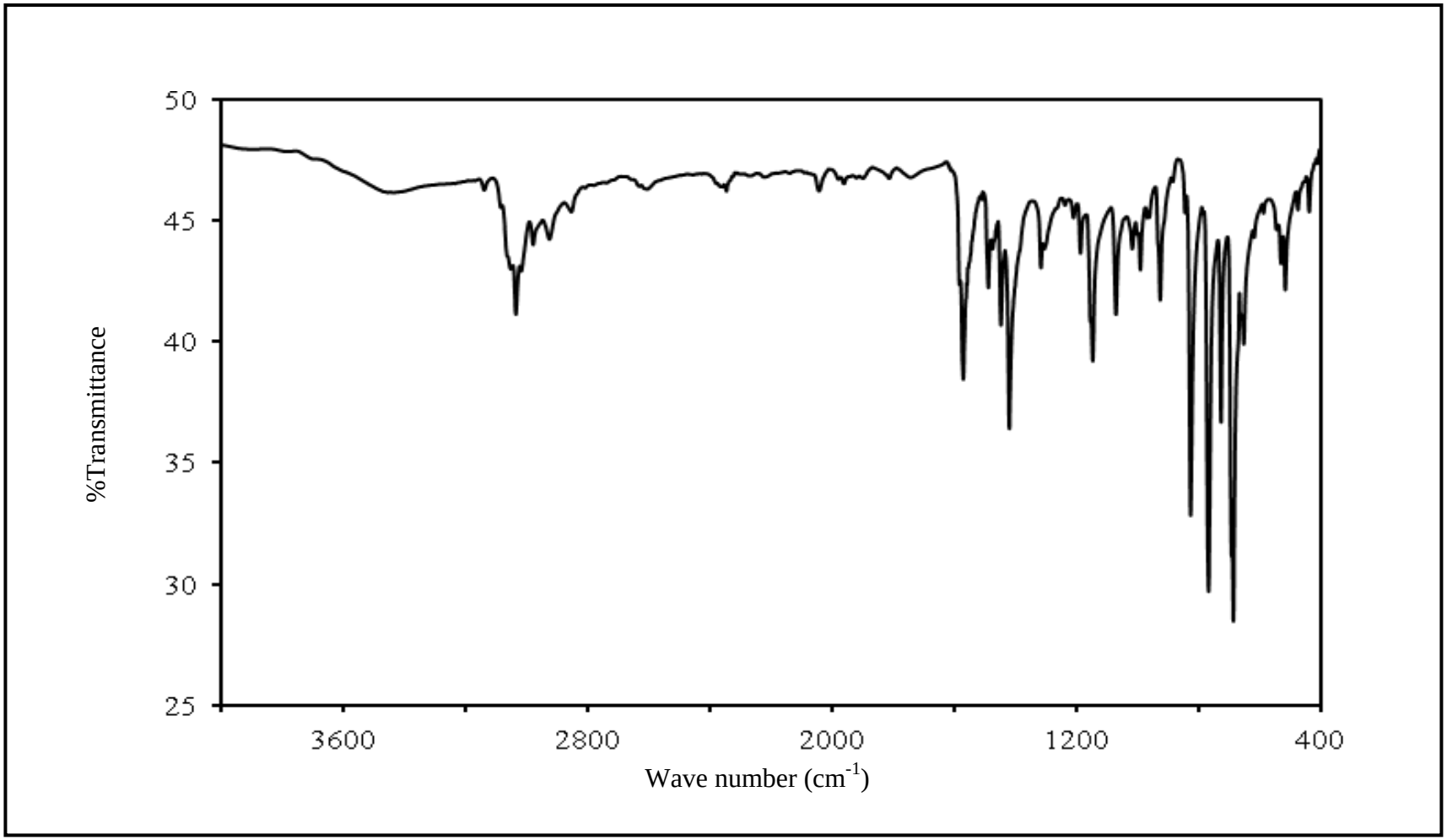

Figure 3 IR spectrum of diazpy.

3.1.2.2 UV-Visible absorption spectroscopy

UV-Visible absorption spectroscopy is a technique to study the electronic transition of compound. The electronic absorption spectrum of the ligand in five solvents were recorded in the range of 200-800 nm. The spectral data are summarized in Table 3. The absorption spectrum of diazpy in CH_3CN is shown in Figure 4.

Table 3 UV-Visible absorption spectroscopic data of the diazpy ligand (10^{-5} M)

Solvents	λ_{max}, nm, (ε^a, x 10^4 $M^{-1}cm^{-1}$)
MeOH	332(3.73) 453(0.08)
EtOH	331(3.53) 456(0.09)
CH_3CN	325(3.28) 459(0.11)
CH_2Cl_2	328(3.49) 460(0.15)
DMSO	332(3.15) 458(0.01)

[a]Molar extinction coefficient

The absorption spectra of diazpy ligand were recorded in the range of 200-800 nm in five different solvents; methanol, ethanol, acetonitrile, dichloromethane and dimethyl sulfoxide. The absorption occurring in UV region displayed absorption bands in the range 325-322 nm (ε ≈3.15-3.73 ($x10^4$ $M^{-1}cm^{-1}$)) attributed to $\pi \rightarrow \pi^*$ transition. In addition , the diazpy ligand showed absorption bands in the range 453-460 nm (ε ≈0.01-0.15 ($x10^4$ $M^{-1}cm^{-1}$)) in the visible region which referred to $n \rightarrow \pi^*$ transition.

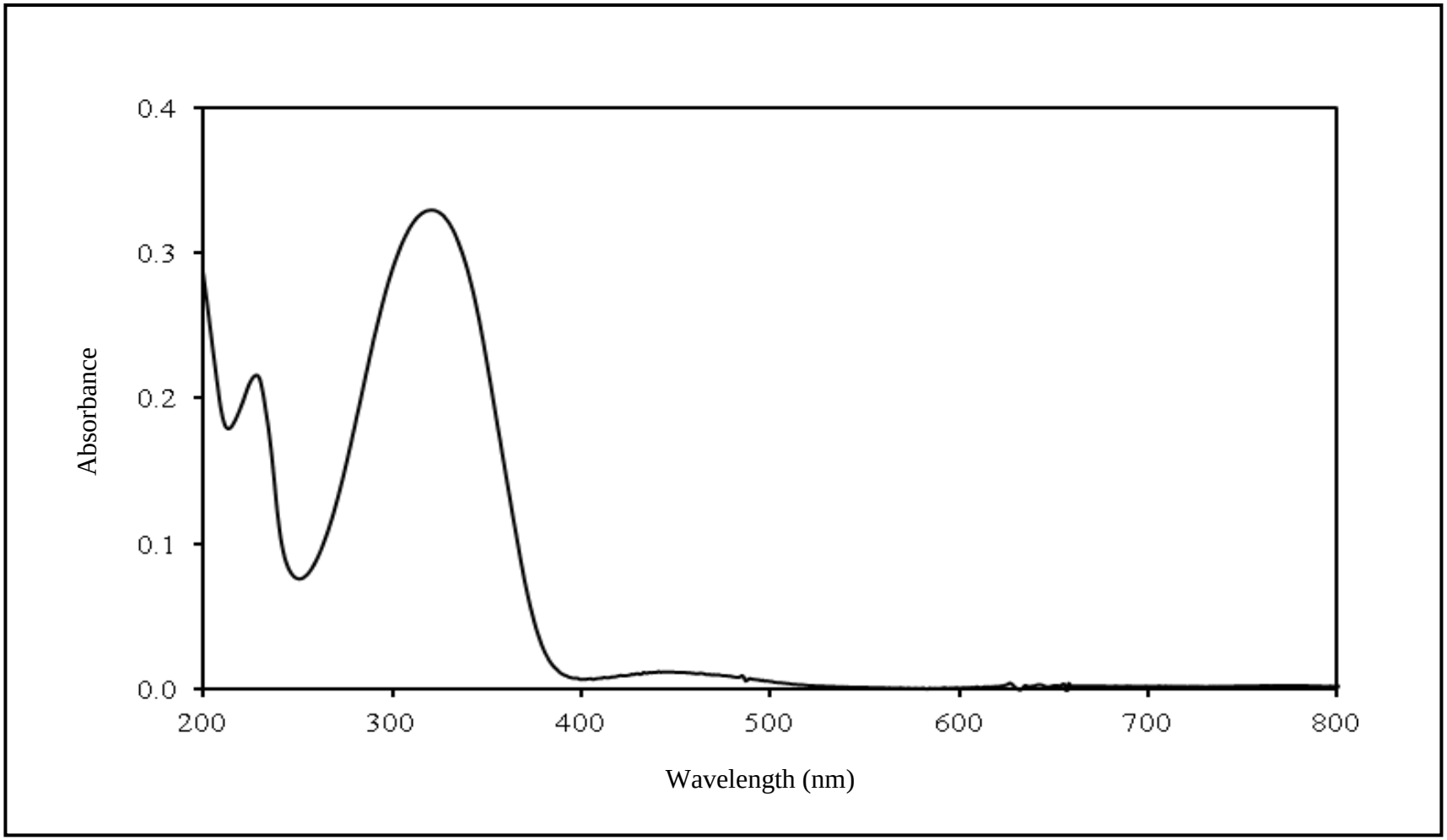

Figure 4 UV-Visible absorption spectrum of diazpy (10^{-5} M) in CH_3CN.

3.1.2.3 Nuclear Magnetic Resonance spectroscopy (1D and 2D)

Nuclear Magnetic Resonance (NMR) spectroscopy is an important technique to determine the molecular structure of the compounds. The structure of diazpy ligand was investigated by using 1D and 2D NMR spectroscopic techniques (^{1}H NMR, ^{1}H-^{1}H COSY NMR, ^{13}C NMR, DEPT NMR and ^{1}H-^{13}C HMQC NMR). The NMR spectra of the ligand was recorded in methanol-d_4 on BRUKER AVANCE 300 FT-NMR instrument 300 MHz and tetramethylsilane (TMS, $Si(CH_3)_4$) was used as an internal reference. The chemical shift (δ) of the ligand was reported in part per million (ppm) downfield from TMS and *J*-coupling were reported in hertz (Hz).

Nuclear Magnetic Resonance spectroscopy of the
2,6-(diphenylazo)pyridine ligand

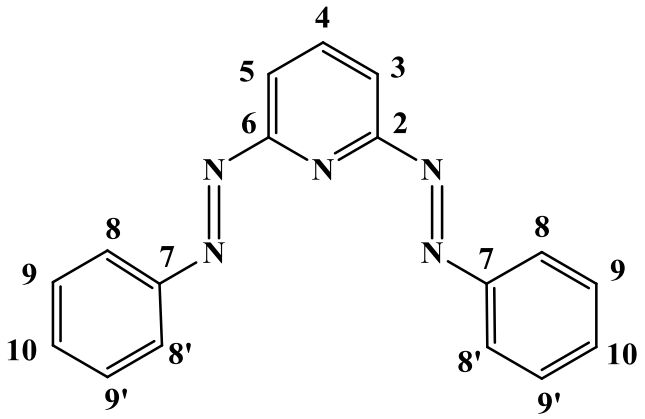

The chemical shift and proton, carbon assignments of diazpy ligand are summarized in Table 4 and NMR spectra are shown in Figure 5 to Figure 10.

Table 4 ^{1}H and ^{13}C NMR spectroscopic data of the diazpy ligand

H-Position	^{1}H NMR			^{13}C NMR
	δ (ppm)	*J* (Hz)	Number of H	δ (ppm)
4	8.26 (*t*)	7.8	1	141.4
8	8.07 (*m*)	-	4	123.2
3, 5	7.98 (*d*)	7.8	2	115.0
9	7.62 (*m*)	-	6	129.1
10				132.5
Quaternary carbon (C)			C2, 6	162.4
			C7	152.3

d = doublet, *t* = triplet, *m* = multiplet

The 2,6-(diphenylazo)pyridine (diazpy) has thirteen protons on the molecule. The ^{1}H NMR spectrum of diazpy showed four resonance signals for thirteen protons (Figure 5).

The proton H4 was effected from resonance results. Therefore, the chemical shift of proton H4 occurred at most downfield. This signal was splitted by proton H3 (*J*= 7.8Hz), H5 (*J*= 7.8 Hz) and appeared as triplet (*t*) peak at 8.26 ppm.

The chemical shift proton H3 and H5 occurred at higher field than proton H4 because it was less effected from resonance results than proton H4. The resonance occurred as doublet (*d*) at 7.98 ppm. It was splitted by proton H4 (*J*=7.8 Hz)

The protons H8 were two equivalent protons on both phenyl rings located closed to the azo nitrogens. The resonance occurred as multiplet (*m*) at 8.07 ppm. They appeared at lower than that the proton H9 and H10.

The protons H9 were two equivalent protons located next to the proton H8. The protons H9 resonance appeared as multiplet (*m*) at 7.62 ppm.

The proton H10 located next to the proton H9. The proton H10 resonance appeared as multiplet (*m*) at the same position with signal of the proton H9 (7.62 ppm).

In addition, the peak assignments were confirmed using ^{1}H-^{1}H COSY NMR spectrum, which showed the correlation of ^{1}H-^{1}H COSY NMR signals are presented in Figure 6.

The results from ^{13}C NMR spectrum (Figure 7) corresponded to the results of DEPT-90 and DEPT-135 NMR (Figure 8, 9), which showed only methine carbon signals. The ^{13}C NMR spectrum of the diazpy ligand appeared 7 signals for 17 carbons. The signal of two equivalent quaternary carbons (C2 and C6) of the pyridine ring appeared at the most downfield (162.4 ppm) due to its position between nitrogen of the pyridine ring and nitrogen of the azo function. The signal at 152.3 ppm belonged to two equivalent quaternary carbons (C7 of both phenyl rings). The signals of two equivalent carbons C3, C5 and carbon C4 on pyridine ring occurred at 115.0 and 141.4 ppm, respectively. The carbon signals at 123.2, 129.1 and 132.5 ppm were attributed to four equivalent carbons of C8, C9 and two equivalent carbons of C10, respectively.

Moreover, the ^{13}C NMR signals assignments were based on the ^{1}H-^{13}C HMQC NMR spectrum (Figure 10), which exhibited a correlation between ^{1}H NMR spectrum and ^{13}C NMR spectrum. Therefore, the result of 1D and 2D NMR spectra were good evidence to confirm the structure of the diazpy ligand.

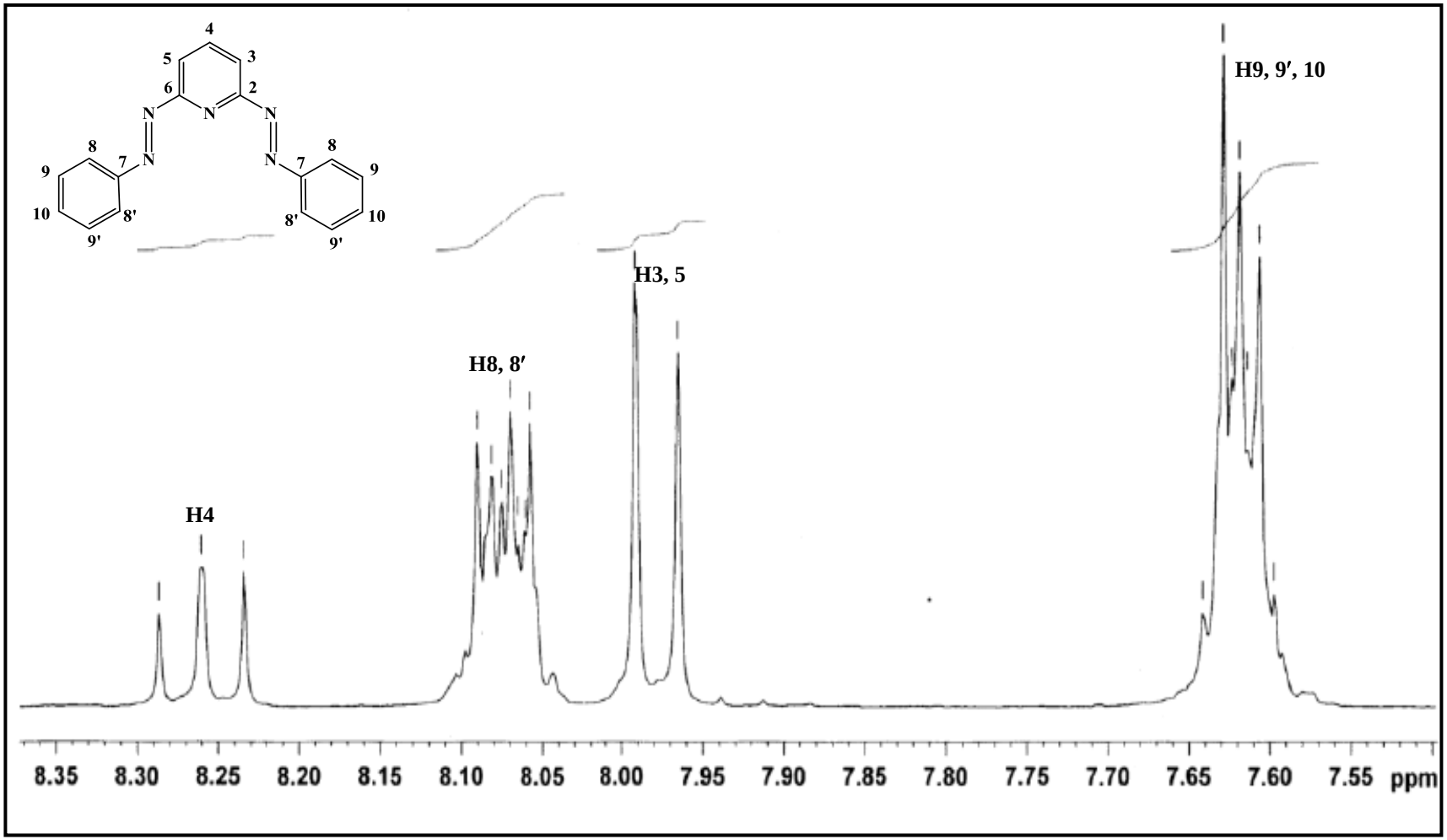

Figure 5 ^{1}H NMR spectrum of diazpy in methanol-d_4 (300 MHz).

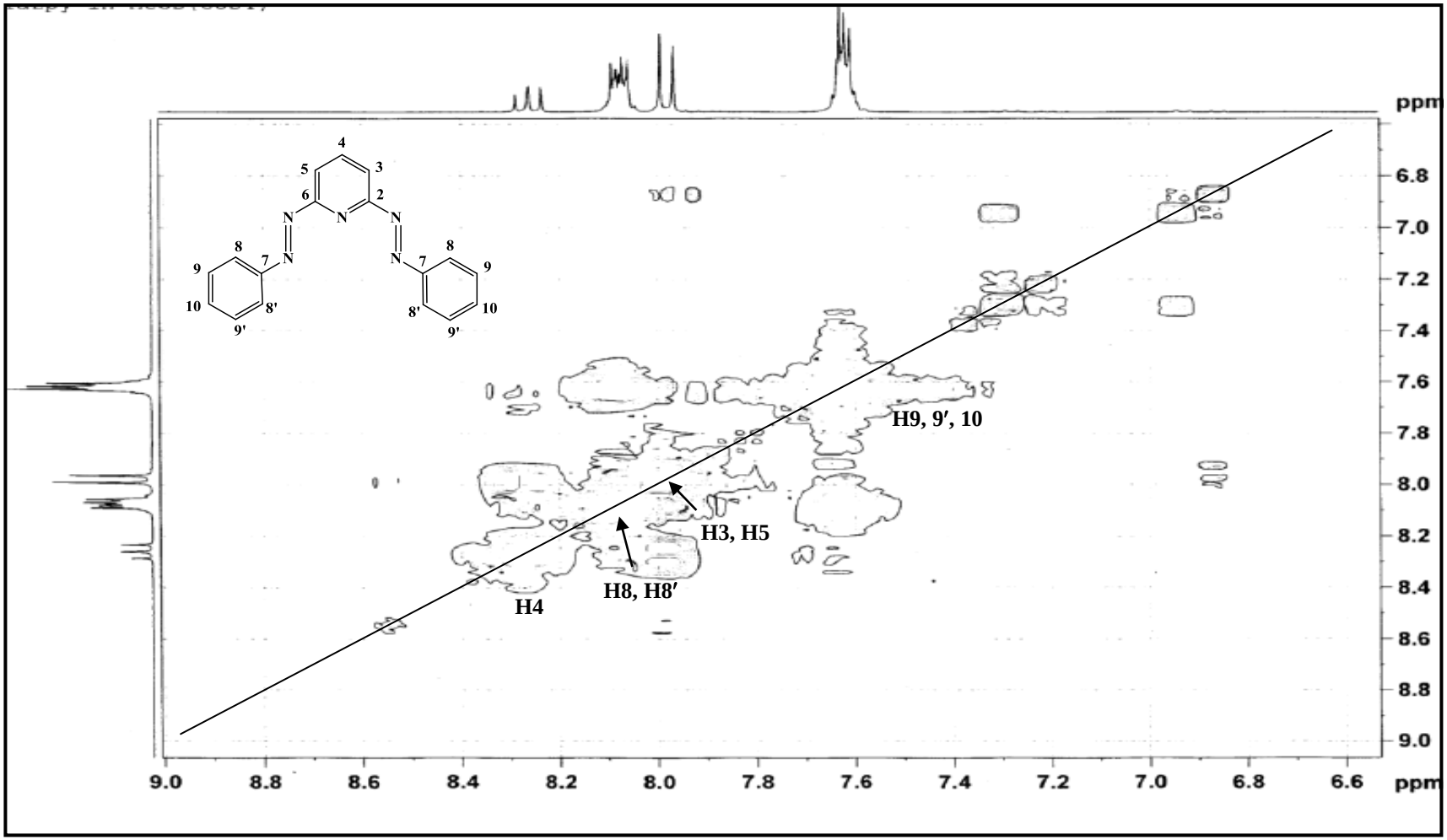

Figure 6 ^{1}H-^{1}H COSY NMR spectrum of diazpy in methanol-d_4 (300 MHz).

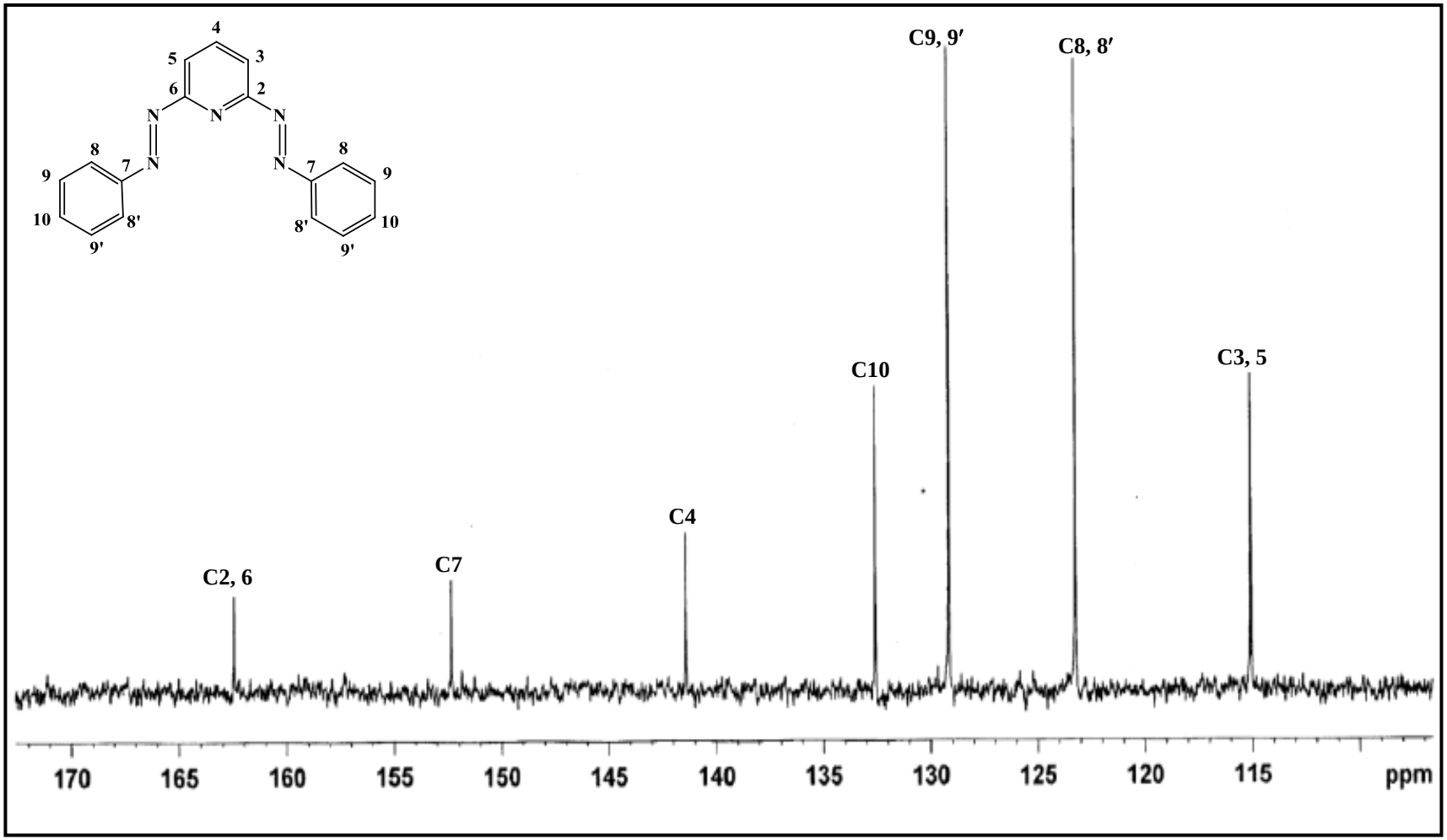

Figure 7 ^{13}C NMR spectrum of diazpy in methanol-d_4 (300 MHz).

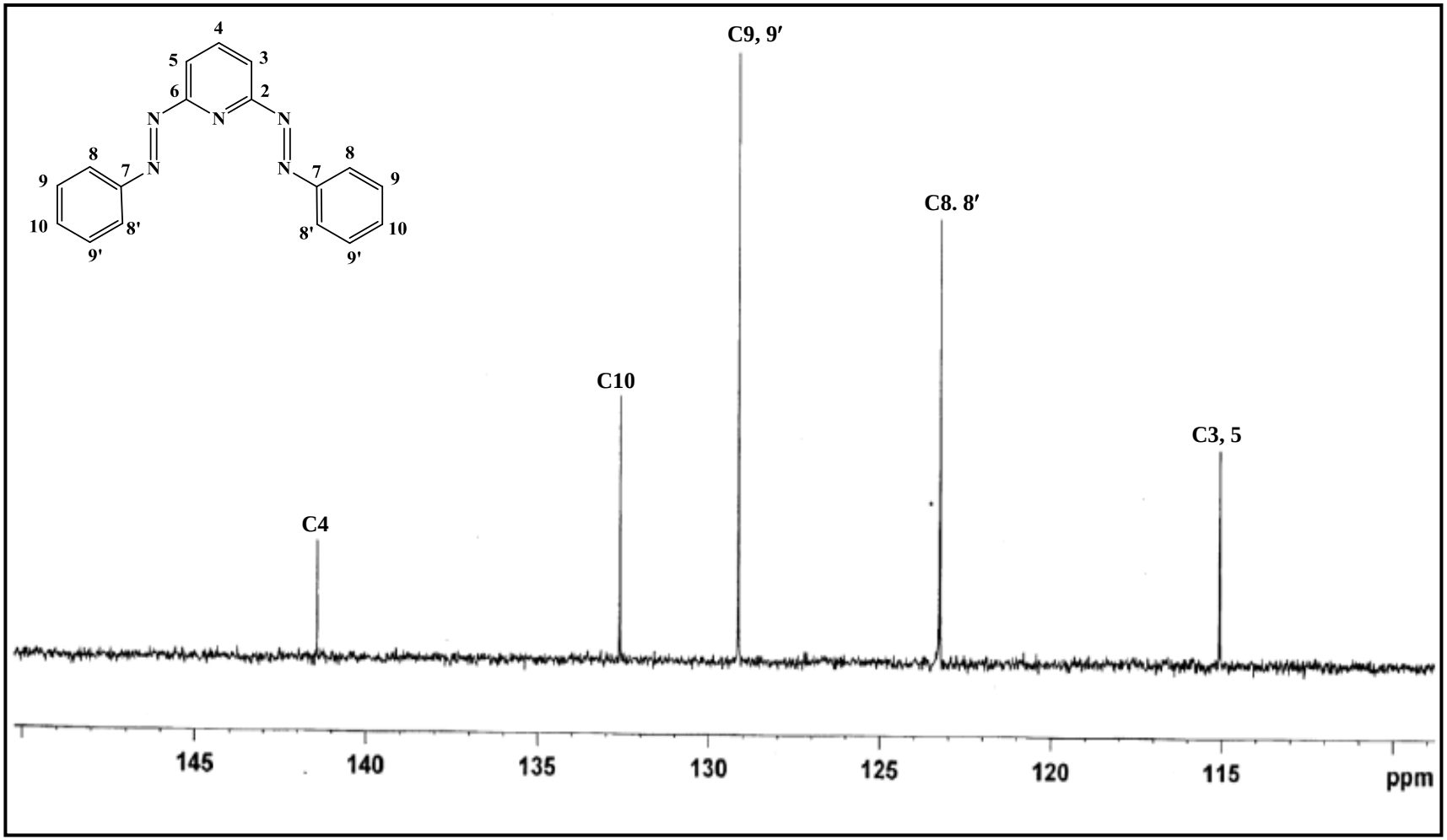

Figure 8 DEPT-90 NMR spectrum of diazpy in methanol-d_4 (300 MHz).

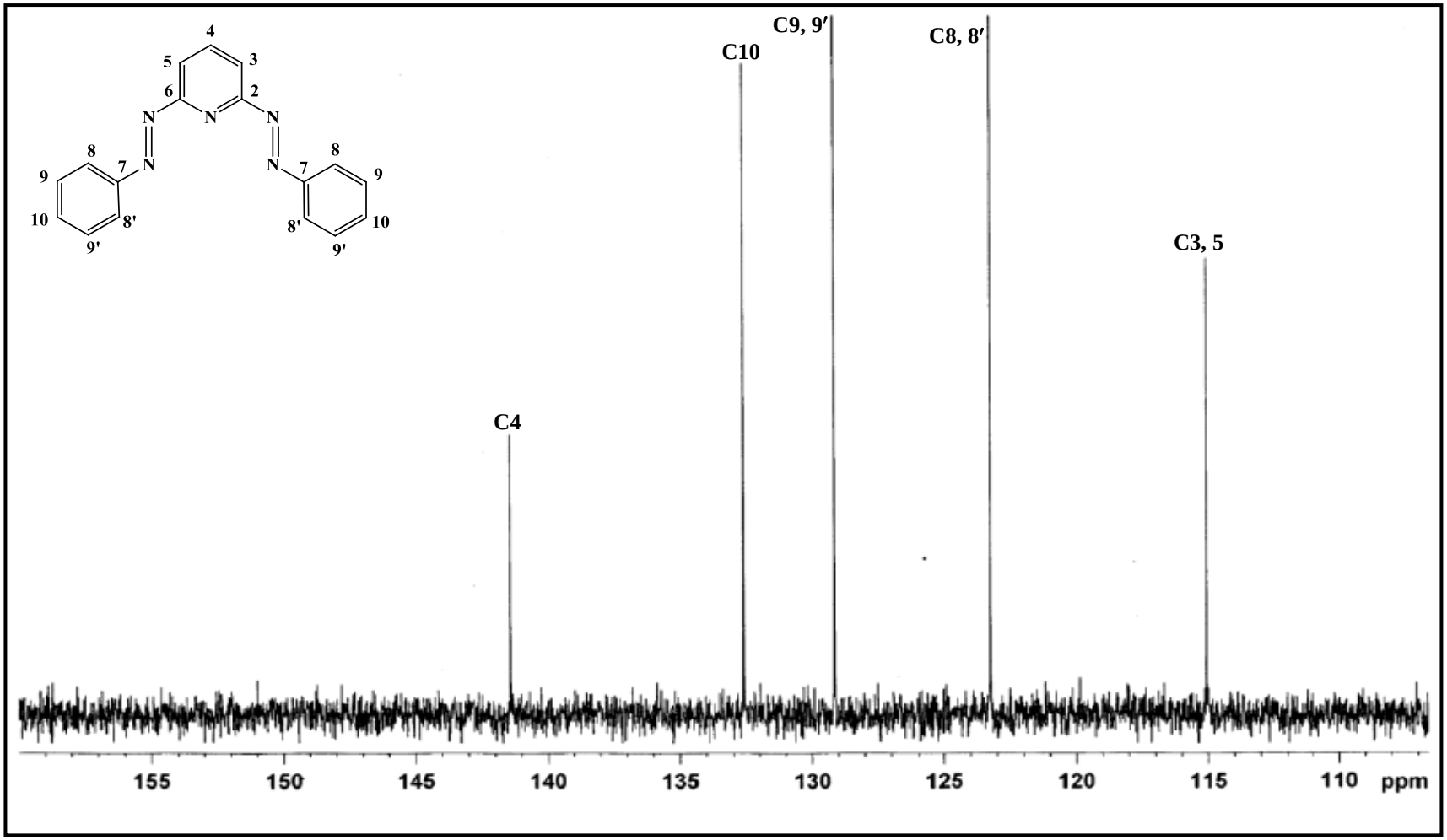

Figure 9 DEPT-135 NMR spectrum of diazpy in methanol-d_4 (300 MHz).

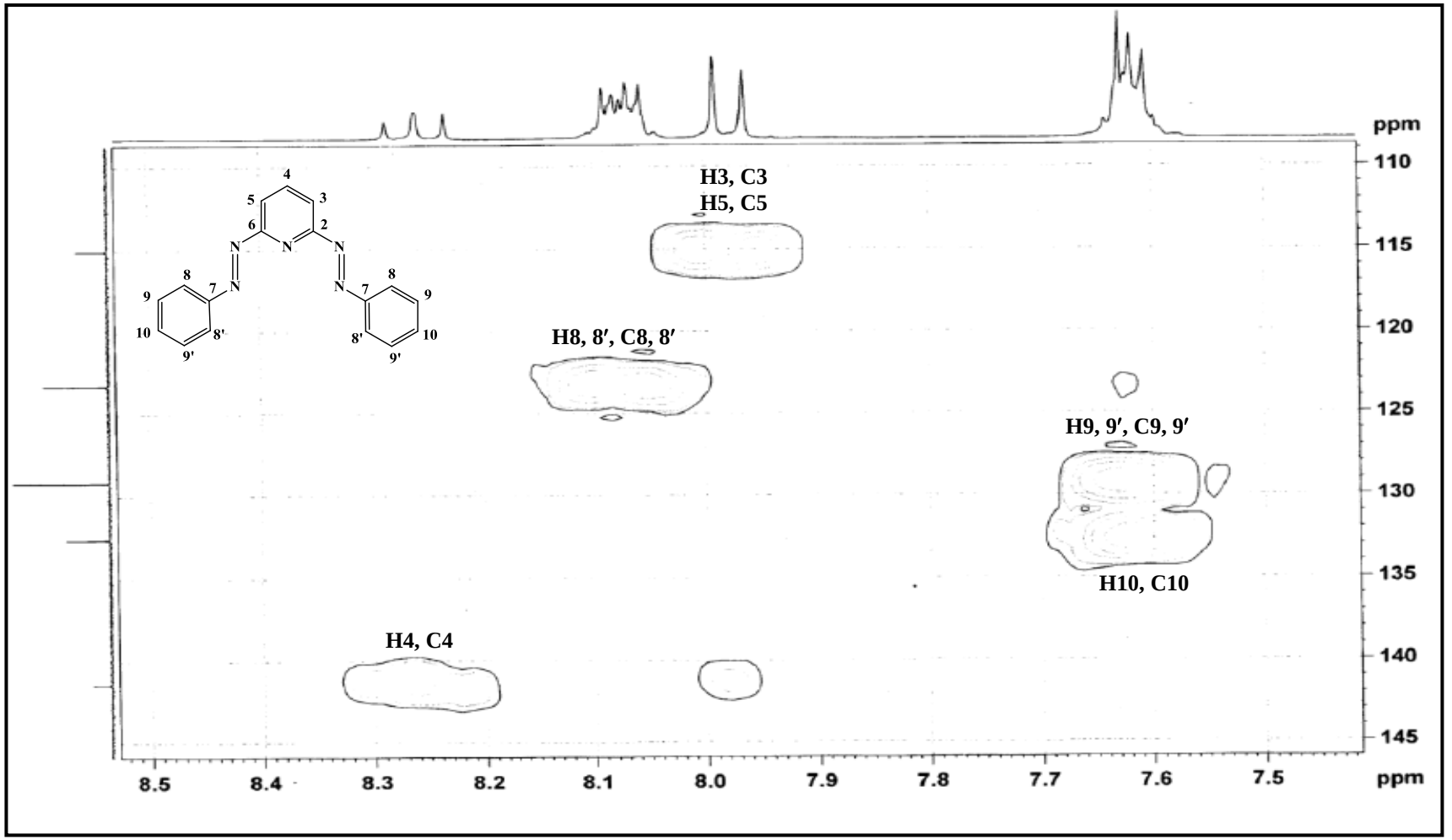

Figure 10 ^{1}H-^{13}C HMQC NMR spectrum of diazpy in methanol-d_4 (300 MHz).

3.1.2.4 Cyclic Voltammetry

Cyclic voltammetry is a technique to study the oxidation-reduction processes of the ligands. Electrochemical properties of the diazpy ligand were studied by using a glassy carbon as a working electrode, platinum wire as a reference electrode, a platinum flage as an auxiliary electrode and was examined in acetonitrile (CH_3CN) using tetrabutylammonium hexafluorophosphate (TBAH) as a supporting electrolyte at the scan rate of 50 mV/s. The reported potential data was compared with the values for the ferrocenium-ferrocence couple, under our experimental conditions.

In this experiment, the different scan rates were used to check whether the couple is arising from reversible couple. The couple which have an almost equal anodic current (i_{pa}) and cathodic current (i_{pc}) was referred as a reversible couple. Besides, the ΔE (E_{pa}-E_{pc}) should be approximately less than 60 mV. While, unequal current was referred to the unequally transfer of electron in reduction and oxidation. This is quasi-reversible couple. In addition, the different scan rates were applied to the unequal current, these currents gave anodic or cathodic peak. This led to irreversible couple. The cyclic voltammetric data are given in Table 5.The cyclic voltammogram in acetonitrile solution of the diazpy ligand is shown in Figure 11.

Table 5 Cyclic voltammetric data of diazpy ligand in 0.1 M TBAH CH_3CN at scan rate 50 mV/s (ferrocence as an internal standard)

Compounds	Oxidation		Reduction	
	E_{pa}, V	E_{pc}, V	E_{pa}, V	E_{pc}, V
azpy	-	-	-1.47	-1.61
diazpy	-	-	-1.26 -1.46	-1.44 -1.56

E_{pa} = anodic peak potentials, E_{pc} = cathodic peak potentials

Oxidation range

The cyclic voltammograms of the diazpy ligand showed no signal in the potential range 0.00 V to + 1.50 V

Reduction range

The electrochemistry of diazpy ligand was measured in the potential range 0.00 V to -2.00 V (Figure 11). The scan rates were varied from 50 mV/s up to 500 mV/s (Figure 30). The cyclic voltammogram of diazpy shows two quasi-reversible couple at the E_{pa} = -1.26 V, E_{pc} = -1.44 V (ΔE = 180 mV) and E_{pa} = -1.46 V, E_{pc} = -1.56 V (ΔE = 100 mV). The first cathodic peak of diazpy appeared at -1.44 V more positive potential than azpy (-1.61 V). It shows that diazpy can be better π-accepter than that of azpy owing to its higher reduction potential (Nookong, 2003).

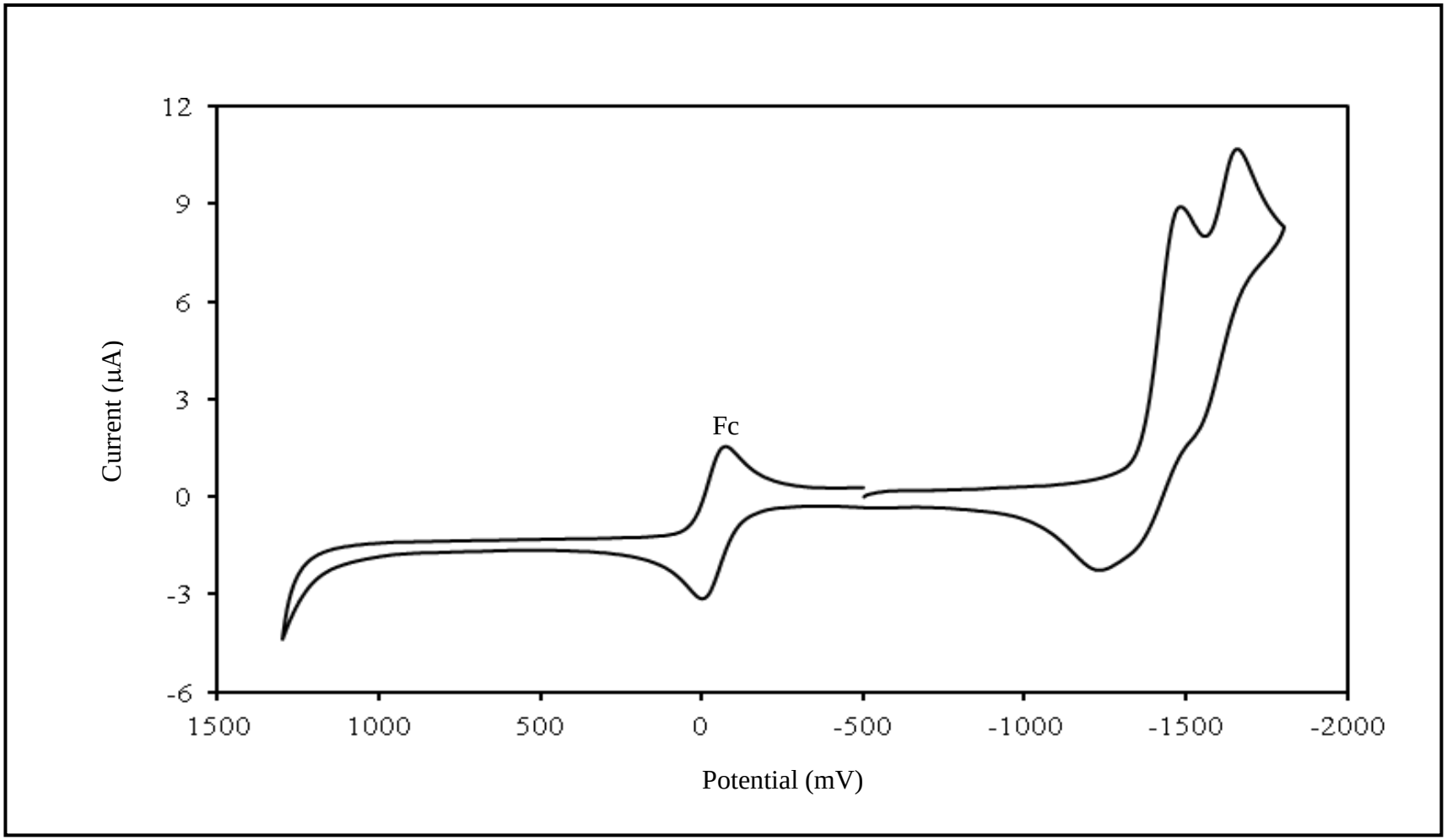

Figure 11 Cyclic voltammogram of diazpy in 0.1 M TBAH CH_3CN at scan rate 50 mV/s (ferrocence as an internal standard).

3.2 Syntheses and characterization of the complexes

3.2.1 Syntheses of complexes

The [Ru(diazpy)(H_2dcbpy)Cl]Cl·H_2O complex was synthesized by reaction of the Ru(diazpy)Cl_2 with 2,2′-bipyridine-4,4′-dicarboxylic acid, H_2dcbpy ligand under the refluxing condition in ethanol/water in a presence of LiCl. The reaction is shown in equation (2).

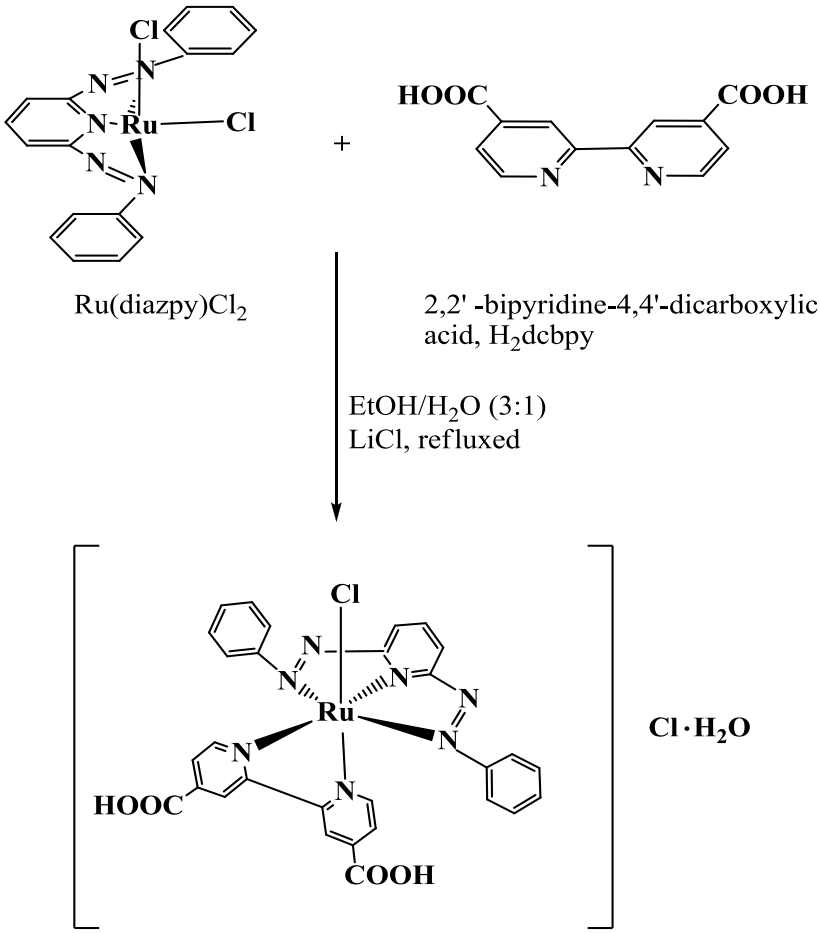

The yield of [Ru(dizpy)(H_2dcbpy)Cl]Cl·H_2O is 71 %.

The $[Ru(H_2dcbpy)_2(diazpy)]Cl_2 \cdot 6H_2O$ complex was synthesized by reaction of the $Ru(H_2dcbpy)_2Cl_2$ with 2,6-(diphenylazo)pyridine, diazpy ligand under the refluxing condition in methanol/water. The reaction is shown in equation (3).

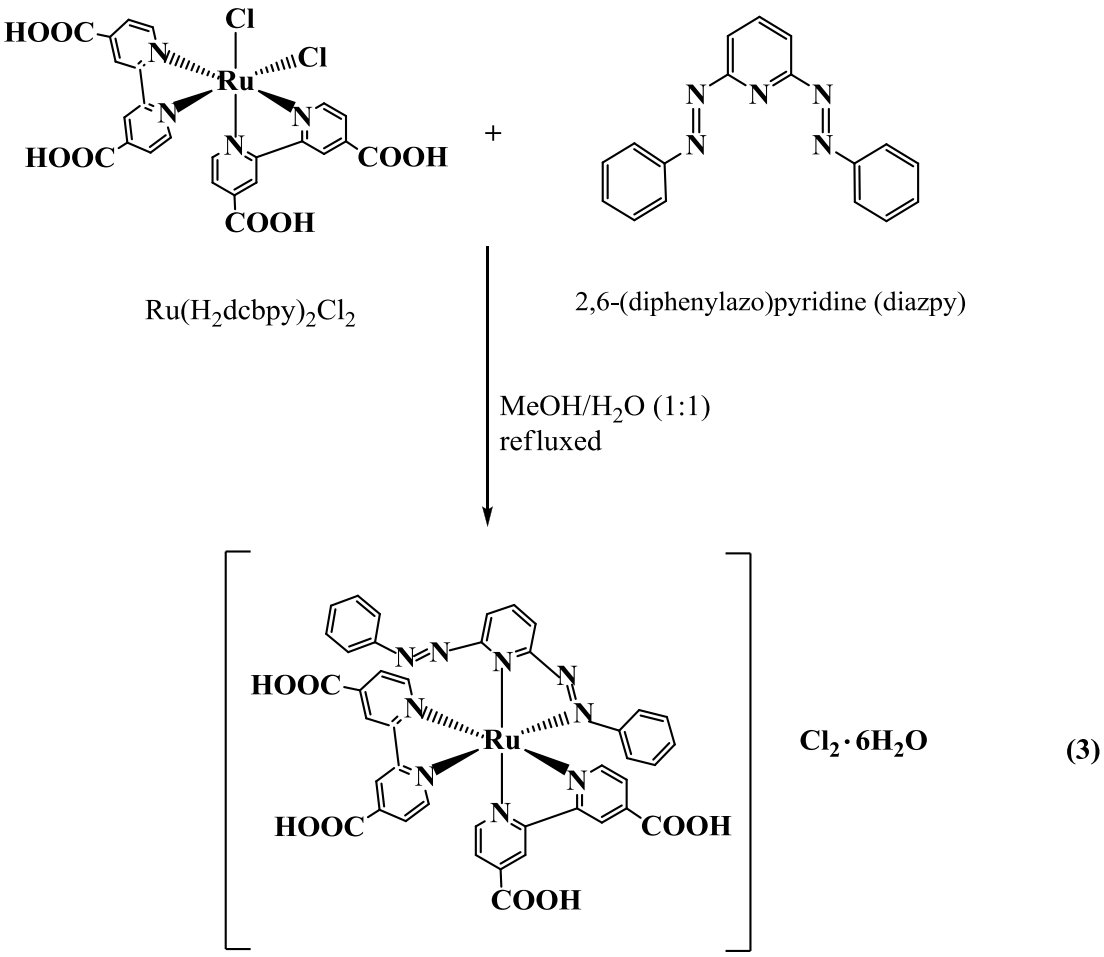

The yield of $[Ru(H_2dcbpy)_2(diazpy)]Cl_2 \cdot 6H_2O$ is 41 %. The physical properties of the complexes are summarized in Table 6.

Table 6 The physical properties of complexes

Complex	Physical properties		
	Appearance	Color	Melting point (°C)
[Ru(diazpy)(H_2dcbpy)Cl]Cl·H_2O	solid	black	>300
[Ru(H_2dcbpy)$_2$(diazpy)]Cl_2·$6H_2O$	solid	orange-brown	>300

The solubility of [Ru(diazpy)(H_2dcbpy)Cl]Cl·H_2O complex was tested in various solvents. The results showed that complex was slightly soluble in water (H_2O), acetone (CH_3COCH_3) and dichloromethane (CH_2Cl_2). It was completely soluble in methanol (CH_3OH), acetonitrile (CH_3CN), ethanol (C_2H_5OH), chloroform ($CHCl_3$) and DMSO $(CH_3)_2SO$ but insoluble in ethyl acetate ($CH_3COOC_2H_5$) and hexane (C_6H_{14}).

The solubility of [Ru(H_2dcbpy)$_2$(diazpy)]Cl_2·$6H_2O$ complex was tested in various solvents. The results showed that complex was completely soluble in water, methanol, ethanol and DMSO but insoluble in acetonitrile, acetone, chloroform, ethyl acetate, dichloromethane and hexane.

3.2.2 Characterization of complexes

The chemistry of complexes were determined by using these techniques.

3.2.2.1 Elemental analysis

3.2.2.2 Infrared spectroscopy

3.2.2.3 UV-Visible absorption spectroscopy

3.2.2.4 Nuclear Magnetic Resonance spectroscopy (1D and 2D)

3.2.2.5 Cyclic Voltammetry

3.2.2.1 Elemental analysis

Elemental analysis is a technique to study the composition of elements in a compound. It is shown that the analytical data of the compounds corresponded to the calculated values. Therefore, the elements in the complexes are confirmed by this method. The elemental analysis data are listed in Table 7.

Table 7 Elemental analysis data of the [Ru(diazpy)(H_2dcbpy)Cl]Cl·H_2O and [Ru(H_2dcbpy)$_2$(diazpy)]Cl_2·$6H_2O$ complexes

Compounds	% C		% H		% N	
	Calc.	Found	Calc.	Found	Calc.	Found
[Ru(diazpy)(H_2dcbpy)Cl]Cl·H_2O	48.28	48.18	3.21	3.05	13.59	13.33
[Ru(H_2dcbpy)$_2$(diazpy)]Cl_2·$6H_2O$	46.64	47.08	3.91	3.79	11.94	11.06

3.2.2.2 Infrared spectroscopy

Infrared spectroscopy is an useful technique to study the functional groups of compounds. Infrared spectra were collected by using KBr pellets in the range of 4000-400 cm^{-1}. The important vibrational frequencies are C=C, C=N, N=N (azo) stretching modes, C-H bending in monosubstituted benzene and C=O stretching on the carboxylate group. The infrared spectroscopic data of the complexes are listed in Table 8 and these spectra are shown in Figure 12 and Figure 13.

Table 8 Infrared spectroscopic data of the $[Ru(diazpy)(H_2dcbpy)Cl]Cl\cdot H_2O$ and $[Ru(H_2dcbpy)_2(diazpy)]Cl_2\cdot 6H_2O$ complexes

Vibration modes	Frequencies (cm^{-1})	
	$[Ru(diazpy)(H_2dcbpy)Cl]Cl\cdot H_2O$	$[Ru(H_2dcbpy)_2(diazpy)]Cl_2\cdot 6H_2O$
C=N, C=C stretching	1616 (m) 1546 (m) 1456 (m)	1613 (m) 1547 (m)
N=N stretching	1260 (s) 1233 (s)	1403 (s) 1376 (s)
C-H bending of monosubstituted benzene	802 (m) 768 (s) 693 (s)	844 (s) 772 (m) 701(m)
C=O stretching on the carboxylate group	1723 (s)	1723 (s)

s = strong, m = medium, w = weak

Infrared spectrum of $[Ru(diazpy)(H_2dcbpy)Cl]Cl\cdot H_2O$ is shown in Figure 12. In the $[Ru(diazpy)(H_2dcbpy)Cl]Cl\cdot H_2O$ complex, the infrared spectra exhibited medium peaks at 1616, 1546 and 1456 cm^{-1}. These frequencies were assigned to the streching of C=N and the C=C vibrational modes. The streching of N=N (azo) vibrational frequency at 1260 and 1233 cm^{-1} are lower than that of the free diazpy ligand (cal. 188 and 187 cm^{-1}, respectively). This is a good indication of N-azo coordination. It was due to the π-back bonding between diazpy ligand and ruthenium (II) resulted in a decrease of the vibrational energy of the N=N (azo) stretching mode. Infrared spectrum of $[Ru(H_2dcbpy)_2(diazpy)]Cl_2\cdot 6H_2O$ is shown in Figure 13. In the $[Ru(H_2dcbpy)_2(diazpy)]Cl_2\cdot 6H_2O$ complex, the infrared spectra exhibited medium peaks at 1613 and 1547 cm^{-1}. These frequencies were assigned to the C=N and the C=C vibrational modes. Intense bands at 1403 and 1376 cm^{-1} are attributed to the N=N (azo) stretching frequencies, the red shifted from the diazpy ligand about 45 and 44 cm^{-1}. The N=N stretching modes in both complexes appeared at lower frequency than that in the free ligand. It was due to the π-back bonding occurring from the t_{2g} orbitals of metal to the π* orbitals of azo. From this result, the bond order of N=N (azo) decreased and the bond length increased, therefore, the vibrational energies decreased. Moreover, the 1723 cm^{-1} vibration is characteristic of the C=O bond stretching on the carboxylate group due to the presence of H_2dcbpy ligand in both complexes. However, the vibration at 325 $cm^{-1}$of Ru-Cl stretching (Pramanik, *et al*., 1998) could not be observed because the spectrum was out of range.

In the $[Ru(diazpy)(H_2dcbpyCl)]Cl\cdot H_2O$ complex, diazpy acted as tridentate ligand, the N=N stretching frequencies appeared at lower energies (1260 cm^{-1} and 1233 cm^{-1}) than $[Ru(H_2dcbpy)_2(diazpy)]Cl_2\cdot 6H_2O$ complex. Because of both N=N stretching frequencies corresponded to two N=N azo of diazpy which coordinated with ruthenium metal center. Since, diazpy acted as a bidentate ligand in the $[Ru(H_2dcbpy)_2(diazpy)]Cl_2\cdot 6H_2O$ complex by using N-pyridine and N-azo bonded with ruthenium center. Therefore, another N=N azo was free. In the case of the $[Ru(H_2dcbpy)_2(diazpy)]Cl_2\cdot 6H_2O$ complex showed the N=N stretching frequencies of coordinated N=N azo at 1376 cm^{-1}. Whereas, the N=N stretching frequencies of free N=N azo occurred at 1403 cm^{-1}. The coordinated N=N

frequencies was shifted to lower energies than free N=N because of the strong $d\pi(Ru) \rightarrow \pi^*(L)$ back bonding (Nookong, 2003). The N=N (azo) stretching vibration frequency values of diazpy ligand and complexes are listed in Table 9.

Table 9 The N=N (azo) stretching vibrational frequencies values of diazpy ligand and complexes

Compounds	Frequencies (cm^{-1})
diazpy	1448, 1420
$[Ru(diazpy)(H_2dcbpyCl)]Cl \cdot H_2O$	1260, 1233
$[Ru(H_2dcbpy)_2(diazpy)]Cl_2 \cdot 6H_2O$	1403, 1376

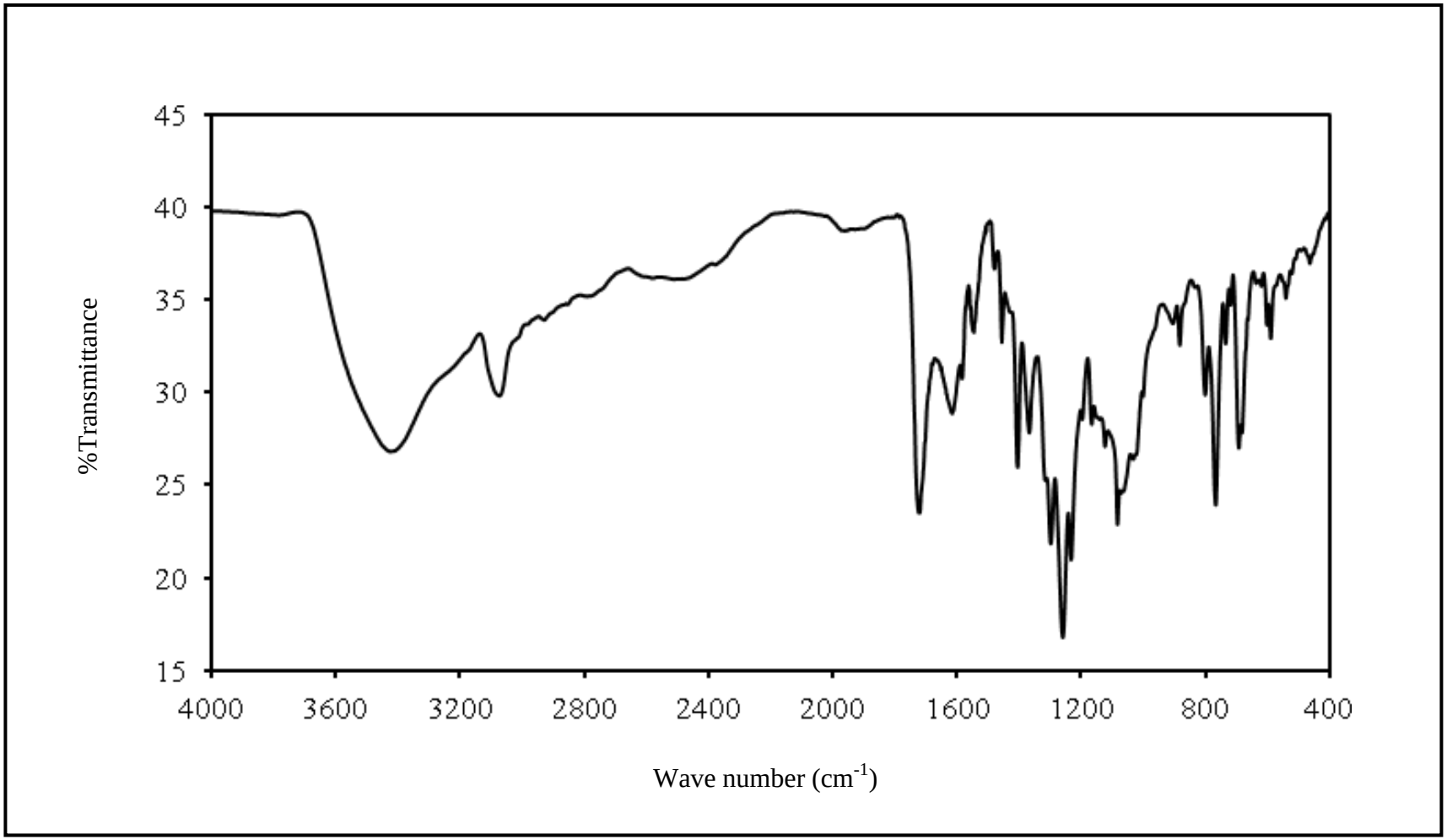

Figure 12 IR spectrum of [Ru(diazpy)(H_2dcbpy)Cl]Cl·H_2O.

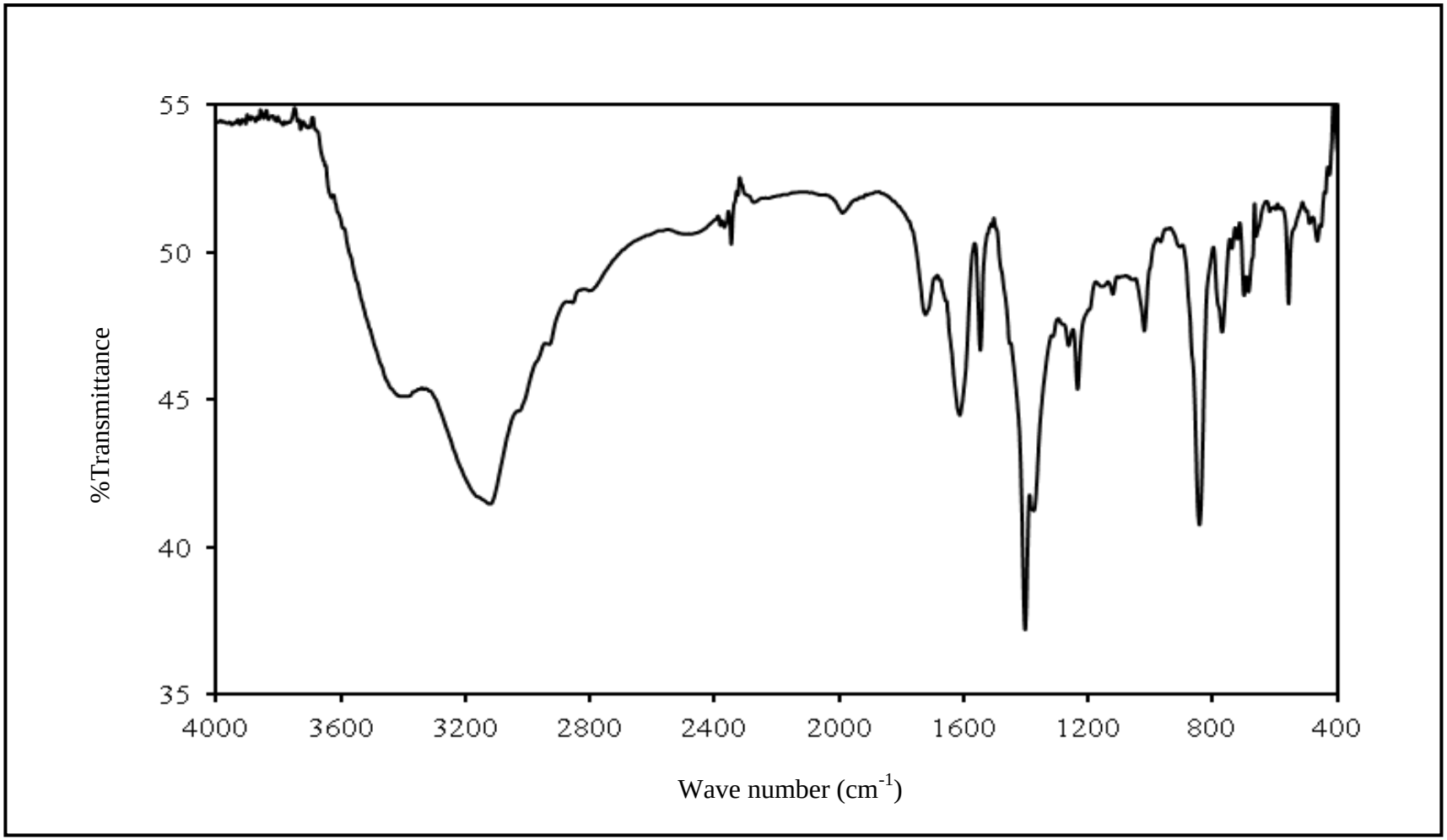

Figure 13 IR spectrum of [Ru(H_2dcbpy) $_2$(diazpy)]Cl_2·6H_2O.

3.2.2.3 UV-Visible absorption spectroscopy

UV-Visible absorption spectroscopy is a technique to study the electronic transition of compound. The electronic absorption spectra of the complexes in four solvents were recorded in the range of 200-800 nm. The spectral data are summarized in Table 10. The absorption spectrum of $[Ru(diazpy)(H_2dcbpy)Cl]Cl\cdot H_2O$ complexes in CH_3CN is shown in Figure 14 and The absorption spectrum of $[Ru(H_2dcbpy)_2(diazpy)]Cl_2\cdot 6H_2O$ in methanol is shown in Figure 15.

Table 10 UV-Visible absorption spectroscopic data of the complexes (10^{-5} M)

Complexes	Solvents	λ_{max}, nm (ε^a, x 10^4 $M^{-1}cm^{-1}$)	
		UV region	Visible region
$[Ru(diazpy)(H_2dcbpy)Cl]Cl\cdot H_2O$	Methanol	305(4.89)	422(2.31) 502(0.96)
	Ethanol	304(3.38)	422(1.57) 503(0.67)
	CH_3CN	311(3.97)	424(1.81) 502(0.94)
	DMSO	297(6.00)	436(2.41) 502(1.11)

[a]Molar extinction coefficient

Table 10 UV-Visible absorption spectroscopic data of the complexes (10^{-5} M) (Continued)

Complexes	Solvents	λ_{max}, nm (ε^a, x 10^4 $M^{-1}cm^{-1}$)	
		UV region	Visible region
$[Ru(H_2dcbpy)_2(diazpy)]Cl_2 \cdot 6H_2O$	Methanol	297(2.72) 388(0.98)	511(0.55)
	Ethanol	295(2.38) 385(0.93)	516(0.51)
	CH_3CN	-	-
	DMSO	288(2.80) 377(1.05)	517(0.58)

[a]Molar extinction coefficient

The absorption spectra of $[Ru(diazpy)(H_2dcbpy)Cl]Cl \cdot H_2O$ and $[Ru(H_2dcbpy)_2(diazpy)]Cl_2 \cdot 6H_2O$ complexes were recorded in both ultraviolet (200-400 nm) and visible regions (400-800 nm) in four different solvents; methanol, ethanol, acetonitrile and dimethyl sulfoxide. The spectra of $[Ru(diazpy)(H_2dcbpy)Cl]Cl \cdot H_2O$ and $[Ru(H_2dcbpy)_2(diazpy)]Cl_2 \cdot 6H_2O$ complexes displayed absorption bands in the range of 288-311 nm ($\varepsilon \approx 2.80\text{-}3.97$ (x 10^4 $M^{-1}cm^{-1}$)), which have been assigned as intraligand $\pi \rightarrow \pi^*$ transitions. Whereas, the intense band around at 436 nm ($\varepsilon \approx 2.41$ x 10^4 $M^{-1}cm^{-1}$) and the broad band centered around at 517 nm ($\varepsilon \approx 0.58$ x 10^4 $M^{-1}cm^{-1}$) were assigned to matal-to-ligand charge transfer transition (MLCT) band involving transfer of an electron from the metal d orbitals to π^* orbitals of the ligands [$Ru_{t2g} \rightarrow L(\pi^*)$] with high molar extinction coefficient (ε, 10^4 M^{-1} cm^{-1}).

In addition, when the solvents have been varied. Absorption spectra show that the intense metal-to-ligand charge transfer (MLCT) in the visible region are not effected. These solvents have slightly difference in polarity. Figure 14 and 15 show the UV-Visible absorption spectra for the [Ru(diazpy)(H_2dcbpy)Cl]Cl·H_2O and [Ru(H_2dcbpy)$_2$(diazpy)]Cl_2·$6H_2O$ complexes in acetonitrile and methanol, respectively.

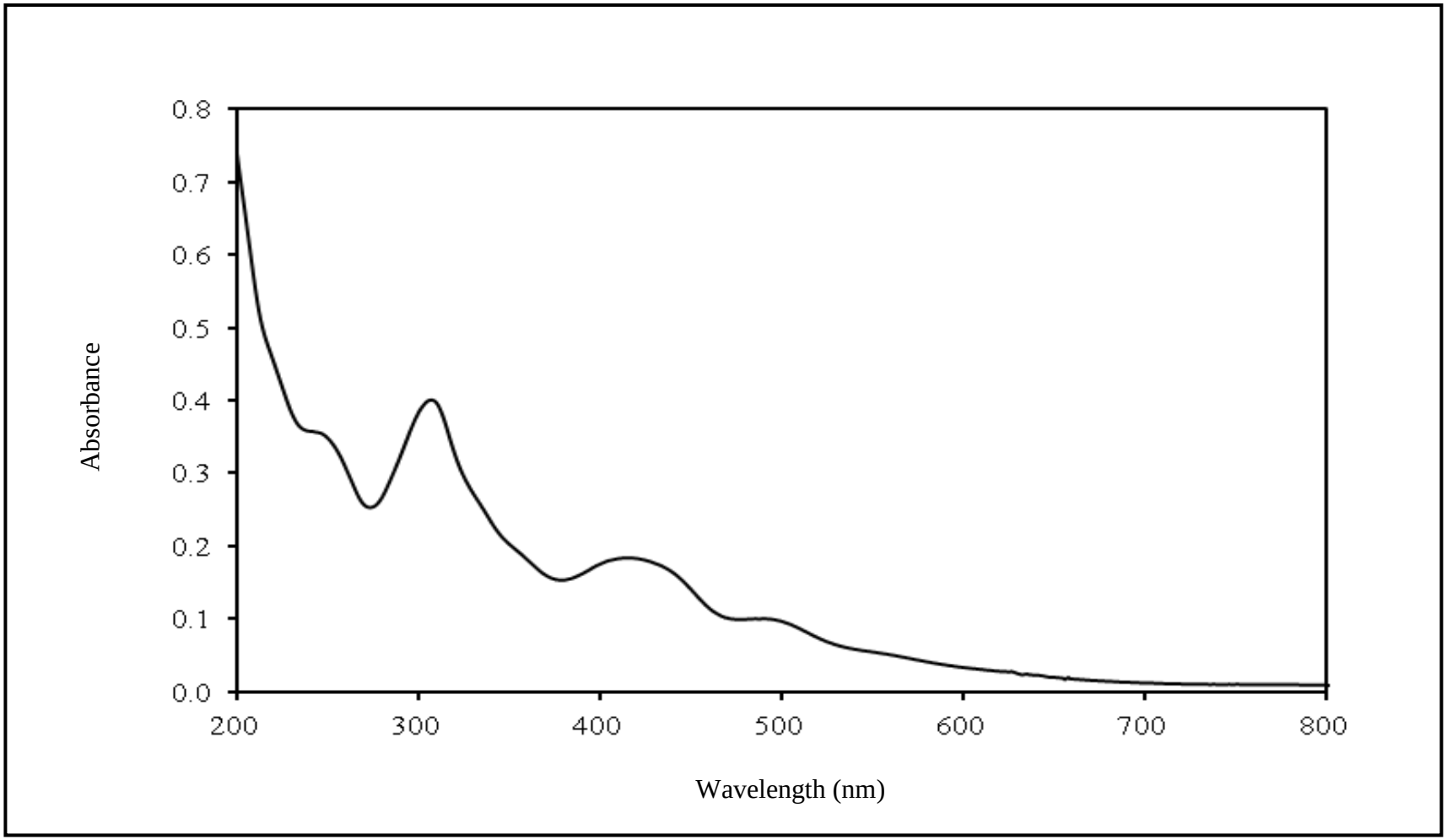

Figure 14 UV-Visible absorption spectrum of $[Ru(diazpy)(H_2dcbpy)Cl]Cl \cdot H_2O$ (10^{-5} M) in CH_3CN.

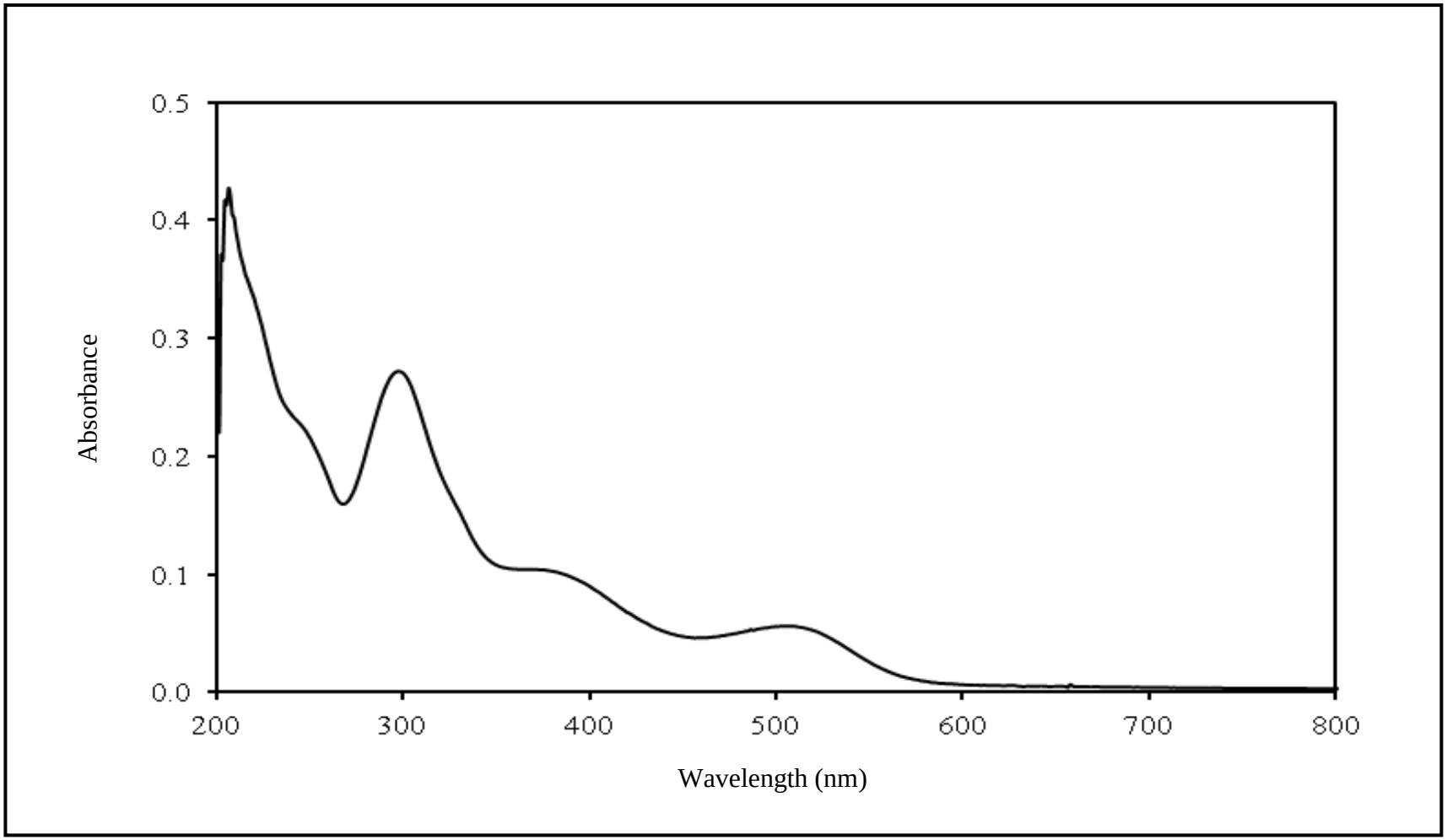

Figure 15 UV-Visible absorption spectrum of $[Ru(H_2dcbpy)_2(diazpy)]Cl_2 \cdot 6H_2O$ (10^{-5} M) in methanol.

3.2.2.4 Nuclear Magnetic Resonance spectroscopy (1D and 2D)

Nuclear Magnetic Resonance (NMR) spectroscopy is an important technique to determine the molecular structure of the compounds. The structures of complexes were investigated by using 1D and 2D NMR spectroscopic techniques (^{1}H NMR, ^{1}H-^{1}H COSY NMR, ^{13}C NMR, DEPT NMR and ^{1}H-^{13}C HMQC NMR). The NMR spectra of the complexes were recorded in methanol-d_4 on BRUKER AVANCE 300 FT-NMR instrument 300 MHz and tetramethylsilane (TMS, $Si(CH_3)_4$) was used as an internal reference. The chemical shifts (δ) of the complexes were reported in part per million (ppm) downfield from TMS and *J*-coupling were reported in hertz (Hz).

Nuclear Magnetic Resonance spectroscopy of the
[Ru(diazpy)(H_2dcbpy)Cl]Cl·H_2O complex

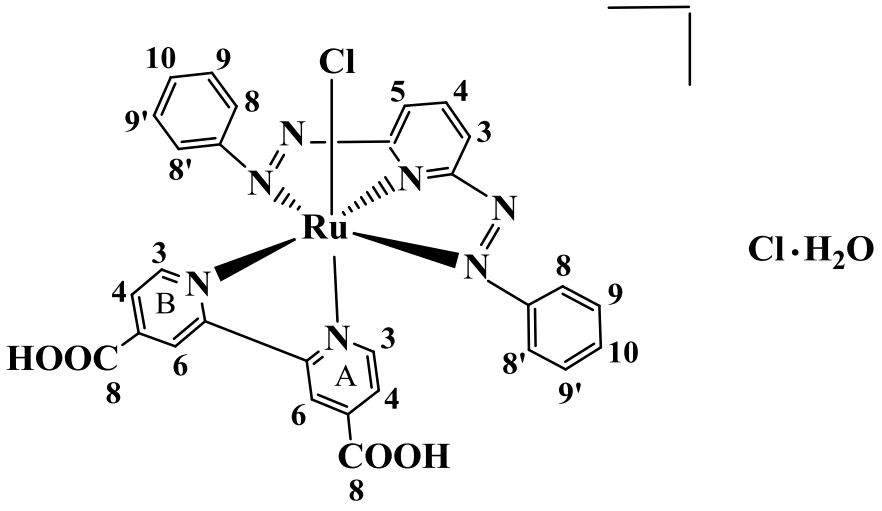

The chemical shift and *J*-coupling constant data of the [Ru(diazpy)(H_2dcbpy)Cl]Cl·H_2O complex are summarized in Table 11 and NMR spectra are shown in Figure 16 to Figure 21.

The ^{1}H NMR spectrum of the [Ru(diazpy)(H_2dcbpy)Cl]Cl·H_2O complex recorded in methanol-d_4, shows many sharp resonances (Figure 16). The NMR spectroscopic data of [Ru(diazpy)(H_2dcbpy)Cl]Cl·H_2O are summarized in Table 11. Twelve resonances are expected for nineteen hydrogens in the [Ru(diazpy)(H_2dcbpy)Cl]Cl·H_2O complex, six signals for thirteen hydrogens of diazpy ligand and six signals for six hydrogens of H_2dcbpy ligand. Integration of the signals corresponds to nineteen hydrogens present in complex. The complex exhibits downfield signals near 10 ppm that can be assigned to the resonances from the hydrogen atoms closest to the chloride ligand (Chryssou *et al*., 2002). More specifically H3B is shifted more downfield than any other proton because it is nearer the chloride atom. The proton H3B resonance appeared at 10.28 ppm as doublet (*d*) due to the coupling with the proton H4B (J = 1.8 Hz). A chemical shift of proton on pyridine ring in the diazpy ligand exhibited at lower field than phenyl rings because of inductive effect of N atom in pyridine ring. The H3 and H5 on pyridine ring of the diazpy ligand appeared at lowest field (9.07 ppm and 9.05 ppm, respectively). In addition, the peak assignments were confirmed using ^{1}H-^{1}H COSY NMR spectrum, which showed the correlation of ^{1}H-^{1}H coupling and the spectrum is shown in Figure 17.

The ^{13}C NMR of [Ru(diazpy)(H_2dcbpy)Cl]Cl·H_2O was shown in Figure 18. The result of spectrum corresponded to the DEPT NMR spectrum (Figure 19, 20). The ^{13}C NMR spectrum of [Ru(diazpy)(H_2dcbpy)Cl]Cl·H_2O showed twenty signals of twenty-nine carbons, twelve signals from nineteen methine carbons, six signals from eight quaternary carbons and two signals from two carbons on the carboxylate group. The quaternary carbons of 2C(C2, C6), C7, C5B, C7B, C7A and C5A were assigned to the signals at 167.7, 154.6, 143.5, 156.1, 158.2 and 143.8 ppm, respectively. The signals of carbon C2, C6 occurred at a lowest field because it located between the nitrogen atoms on pyridine ring. The ^{13}C NMR signal assignments were based on the ^{1}H-^{13}C HMQC spectrum (Figure 21).

Table 11 ^{1}H and ^{13}C NMR spectroscopic data of the [Ru(diazpy)(H_2dcbpy)Cl]Cl·H_2O complex

Position (complex)	δ_H (ppm), (Multiplicity, *J* in Hz), (Number of H)	δ_C (ppm), (C-type)
2, 6(diazpy)	-	167.7 (C)
3(diazpy)	9.07, (*d*, 8.1), (1H)	125.0 (CH)
4(diazpy)	8.60, (*t*, 8.1), (1H)	138.0 (CH)
5(diazpy)	9.05, (*d*, 8.1), (1H)	125.5 (CH)
7(diazpy)	-	154.6 (C)
8, 8′(diazpy)	7.21, (*m*), (4H)	124.3 (CH)
9, 9′(diazpy)	7.20, (*m*), (4H)	130.4 (CH)
10(diazpy)	7.41, (*tt*, 6.3, 2.4), (2H)	134.2 (CH)
3A	7.02, (*d*, 6.0), (1H)	154.3 (CH)
4A	7.62, (*dd*, 6.0, 1.8), (1H)	127.9 (CH)
5A	-	143.8 (C)
6A	8.80, (*d*, 1.2), (1H)	124.8 (CH)
7A	-	158.2 (C)
8A	-	165.8 (C=O)

brs = broad singlet, *d* = doublet, *dd* = doublet of doublet, *t* = triplet, *tt* = triplet of triplet, *m* = multiplet

Table 11 ^{1}H and ^{13}C NMR spectroscopic data of the $[Ru(diazpy)(H_2dcbpy)Cl]Cl \cdot H_2O$ complex (Continued)

Position (complex)	δ_H (ppm), (Multiplicity, *J* in Hz), (Number of H)	δ_C (ppm), (C-type)
3B	10.28, (*d*, 6.0), (1H)	154.2 (CH)
4B	8.54, (*dd*, 6.0, 1.8), (1H)	128.4 (CH)
5B	-	143.5 (C)
6B	9.07, (*brs*), (1H)	125.0 (CH)
7B	-	156.1 (C)
8B	-	166.3 (C=O)

brs = broad singlet, *d* = doublet, *dd* = doublet of doublet, *t* = triplet, *tt* = triplet of triplet, *m* = multiplet

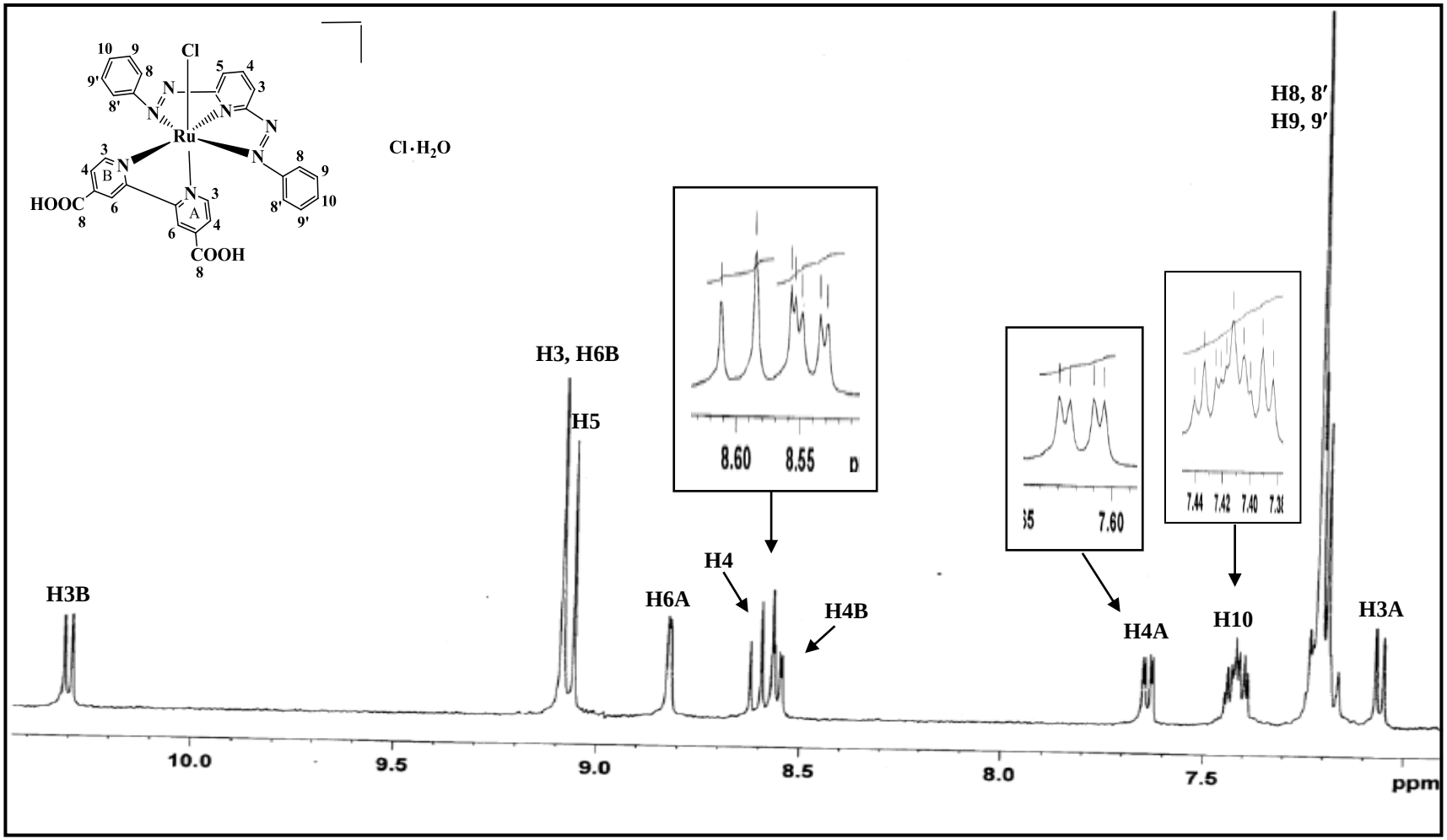

Figure 16 ^{1}H NMR spectrum of [Ru(diazpy)(H_2dcbpy)Cl]Cl·H_2O in methanol-d_4 (300 MHz).

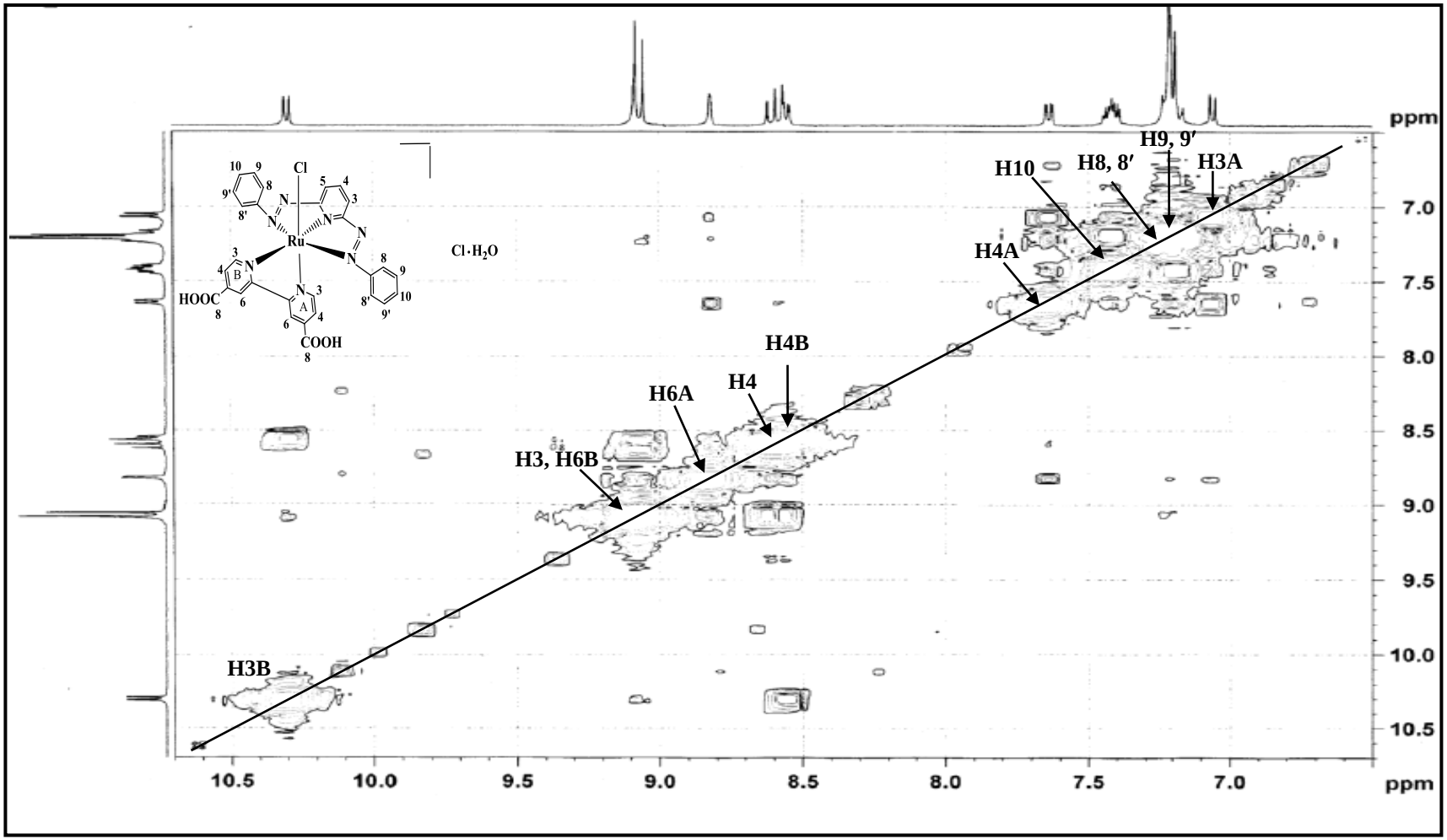

Figure 17 ^{1}H-^{1}H COSY NMR spectrum of [Ru(diazpy)(H_2dcbpy)Cl]Cl·H_2O in methanol-d_4 (300 MHz).

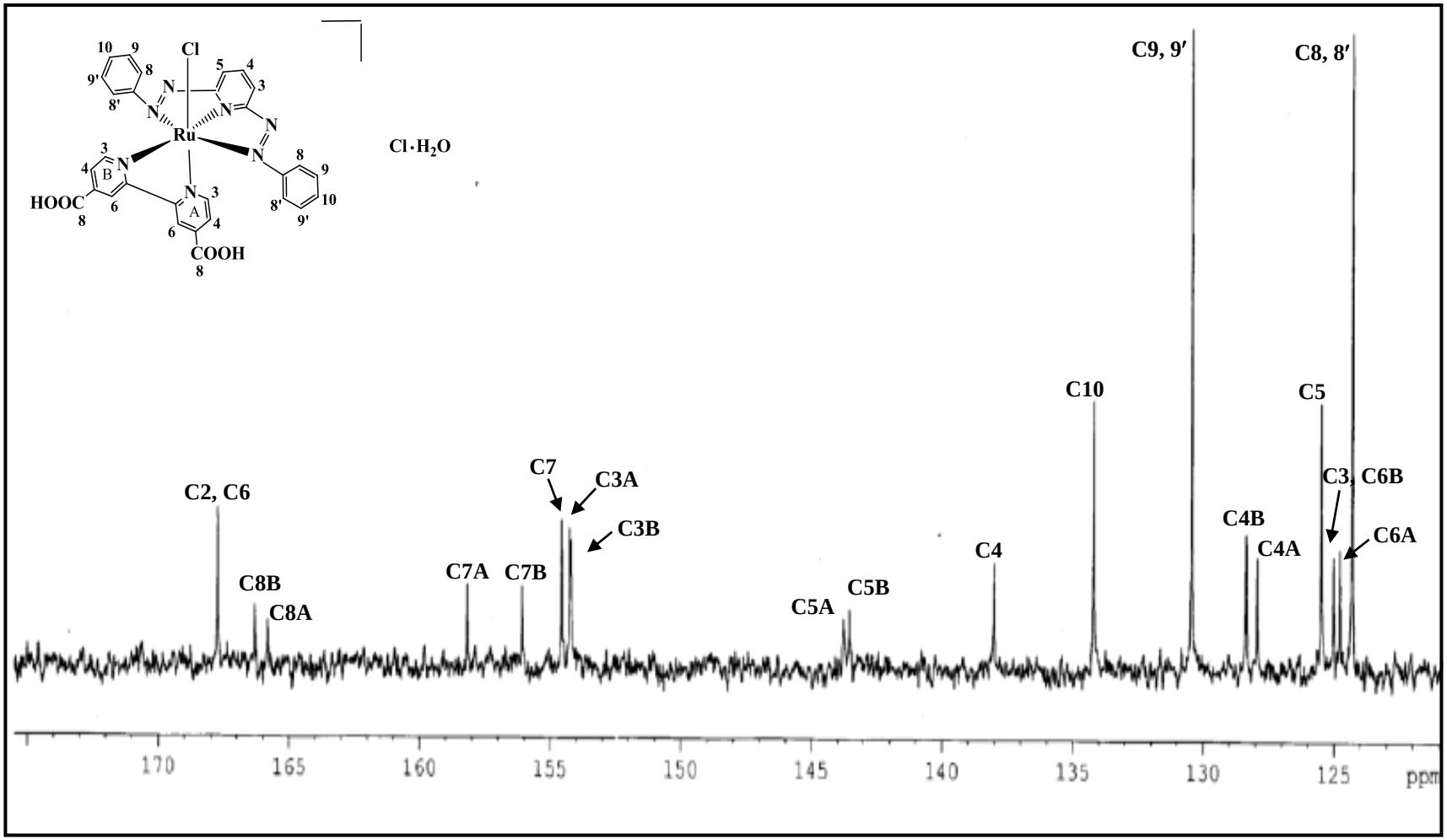

Figure 18 ^{13}C NMR spectrum of [Ru(diazpy)(H_2dcbpy)Cl]Cl·H_2O in methanol-d_4 (300 MHz).

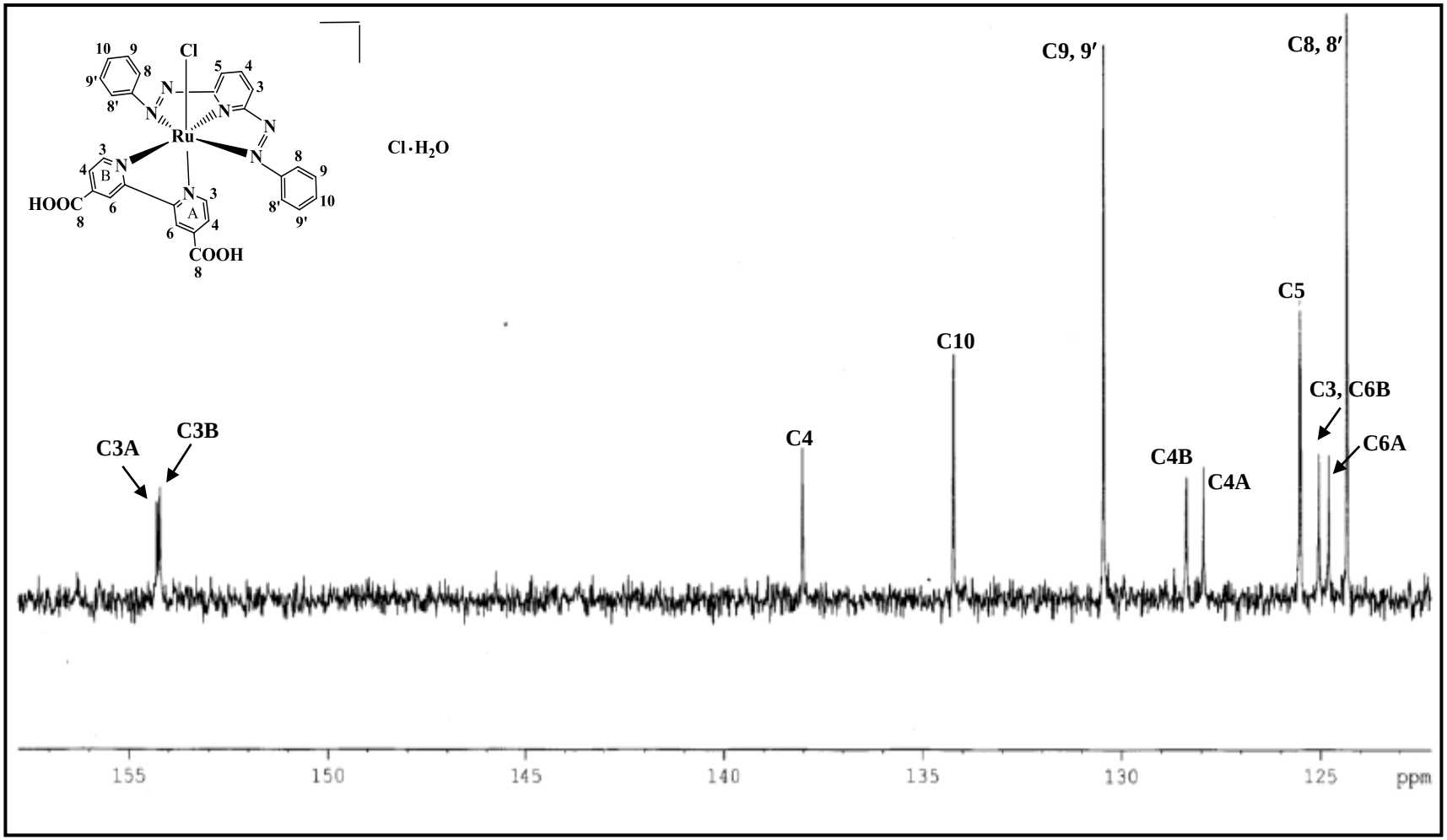

Figure 19 DEPT-90 NMR spectrum of [Ru(diazpy)(H_2dcbpy)Cl]Cl·H_2O in methanol-d_4 (300 MHz).

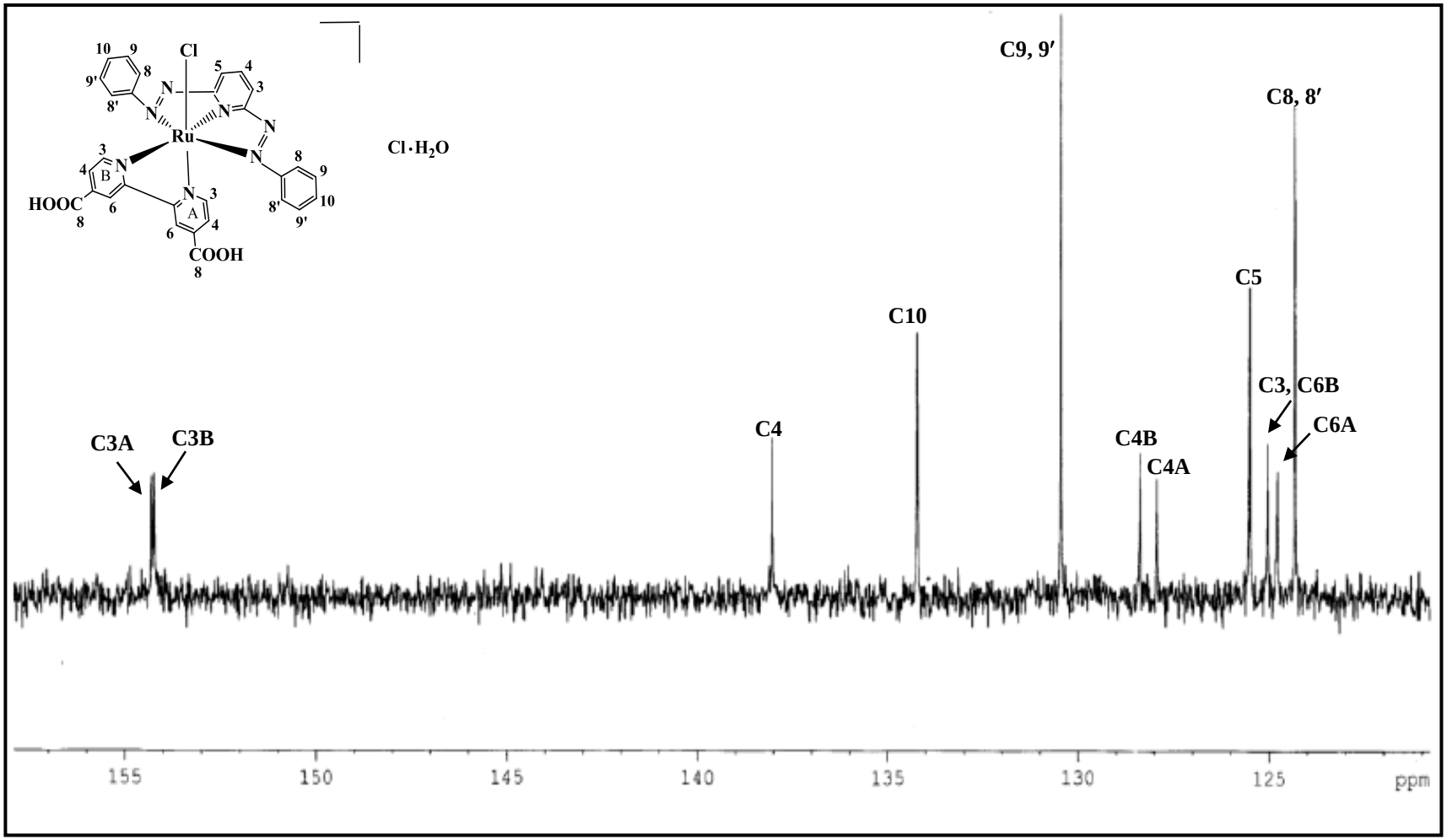

Figure 20 DEPT-135 NMR spectrum of [Ru(diazpy)(H_2dcbpy)Cl]Cl·H_2O in methanol-d_4 (300 MHz).

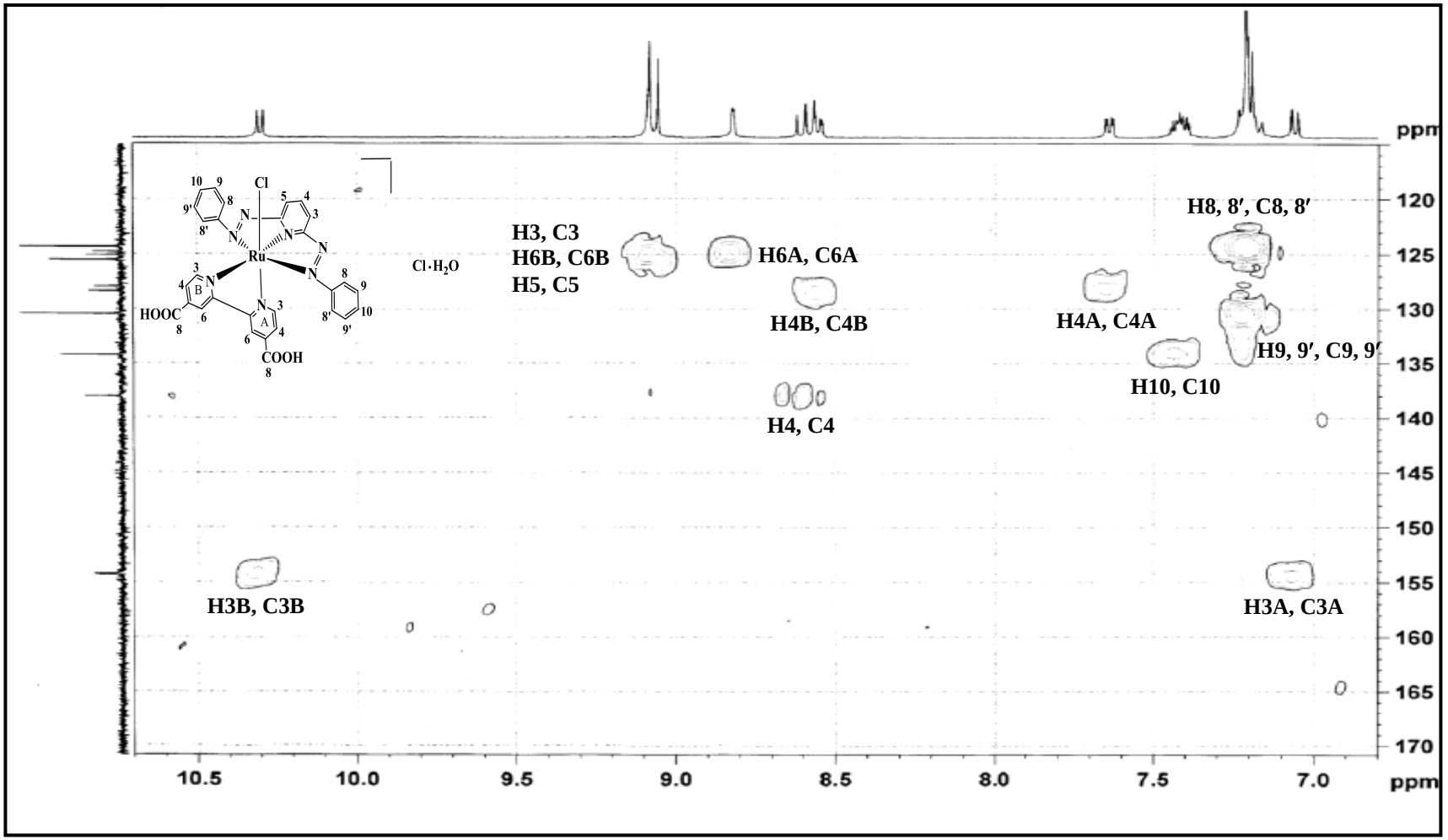

Figure 21 ^{1}H-^{13}C HMQC NMR spectrum of [Ru(diazpy)(H_2dcbpy)Cl]Cl·H_2O in methanol-d_4 (300 MHz).

Nuclear Magnetic Resonance spectroscopy of the
$[Ru(H_2dcbpy)_2(diazpy)]Cl_2 \cdot 6H_2O$ complex

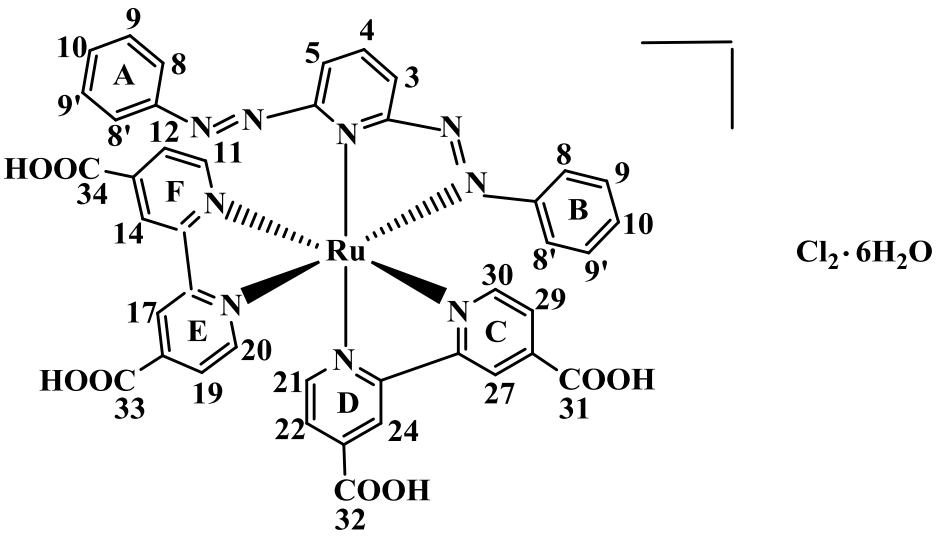

The chemical shift and *J*-coupling constant data of the $[Ru(H_2dcbpy)_2(diazpy)]Cl_2 \cdot 6H_2O$ complex are summarized in Table 12 and NMR spectra are shown in Figure 22 to Figure 27.

The ^1H NMR spectrum of the $[Ru(H_2dcbpy)_2(diazpy)]Cl_2 \cdot 6H_2O$ complex recorded in methanol-d_4 (Figure 22). The NMR spectroscopic data of $[Ru(H_2dcbpy)_2(diazpy)]Cl_2 \cdot 6H_2O$ are summarized in Table 12. Twenty-one resonances are expected for twenty-five hydrogens in the $[Ru(H_2dcbpy)_2(diazpy)]Cl_2 \cdot 6H_2O$ complex, nine signals for thirteen hydrogens of diazpy ligand and twelve signals for twelve hydrogens of H_2dcbpy ligands. Integration of the signals corresponds to twenty-five hydrogens present in complex. The spectrum displayed distinct chemical shift of each H_2dcbpy ligand. This result indicated that both H_2dcbpy ligands in this complex were not equivalent. The ^1H signals of the H_2dcbpy ligand which was *trans* to coordinated N=N azo of diazpy occurred at lower field than another that was *trans* to N-pyridine of diazpy. This is due to a strong withdrawing group of azo (N=N). A chemical shift of proton on

pyridine ring in diazpy ligand exhibited at lower field than phenyl rings because of inductive effect of N atom in pyridine ring. The H3 on pyridine ring of diazpy ligand appeared at lowest field (9.01 ppm). Moreover, the ^{1}H signals of phenyl ring (that bonded with free N=N) appeared at higher field than the free diazpy ligand. This may be due to difficult electron delocalization in asymmetric diazpy molecule. In addition, the peak assignments were confirmed using ^{1}H-^{1}H COSY NMR spectrum, which showed the correlation of ^{1}H-^{1}H coupling and the spectrum is shown in Figure 23.

The ^{13}C NMR of $[Ru(H_2dcbpy)_2(diazpy)]Cl_2 \cdot 6H_2O$ is shown in Figure 24. The result of spectrum corresponded to the DEPT-90 and DEPT-135 NMR spectrum (Figure 25, 26). The ^{13}C NMR spectrum of $[Ru(H_2dcbpy)_2(diazpy)]Cl_2 \cdot 6H_2O$ showed thirty-six signals of forty-one carbons, twenty-one signals from twenty-five methine carbons, eleven signals from twelve quaternary carbons and four signals from four carbons on the carboxylate group. The quaternary carbons of 2C(C2, C6), C7A, C7B, C5C, C7C, C5D, C7D, C5E, C7E, C5F and C7F were assigned to the signals at 167.2, 156.2, 153.4, 151.1, 158.4, 149.9, 157.4, 150.5, 158.1, 148.9 and 155.2 ppm, respectively. The signals of carbon C2, C6 occurred at a lowest field because it located between the nitrogen atoms on pyridine ring. The ^{13}C NMR signal assignments were based on the ^{1}H-^{13}C HMQC spectrum (Figure 27).

Table 12 ^{1}H and ^{13}C NMR spectroscopic data of the $[Ru(H_2dcbpy)_2(diazpy)]Cl_2 \cdot 6H_2O$ complex

Position (complex)	δ_H (ppm), (Multiplicity, *J* in Hz), (Number of H)	δ_C (ppm), (C-type)
2, 6(diazpy)	-	167.2 (C)
3(diazpy)	9.01, (*d*, 7.5), (1H)	129.4 (CH)
4(diazpy)	8.51, (*t*, 7.8), (1H)	143.8 (CH)
5(diazpy)	7.63, (*m*), (1H)	117.6 (CH)
7A(diazpy)	-	156.2 (C)
8, 8′A(diazpy)	6.94, (*d*, 7.8), (2H)	122.5(CH)
9, 9′A(diazpy)	7.15, (*t*, 7.5), (2H)	130.6 (CH)
10A(diazpy)	7.29, (*m*), (1H)	131.8 (CH)
7B(diazpy)	-	153.4 (C)
8, 8′B(diazpy)	7.11, (*d*, 7.2), (2H)	124.1 (CH)
9, 9′B(diazpy)	7.38 (*m*), (2H)	130.2 (CH)
10B(diazpy)	7.48, (*m*), (1H)	135.5 (CH)
3C	7.93, (*m*), (1H)	154.4 (CH)
4C	8.02, (*dd*, 5.7, 1.2), (1H)	128.8 (CH)
5C	-	151.1(C)
6C	8.81, (*brs*), (1H)	124.4 (CH)
7C	-	158.4 (C)
8C	-	169.3 (C=O)

brs = broad singlet, *d* = doublet, *dd* = doublet of doublet, *t* = triplet, *m* = multiplet

Table 12 ^{1}H and ^{13}C NMR spectroscopic data of the $[Ru(H_2dcbpy)_2(diazpy)]Cl_2 \cdot 6H_2O$ complex (Continued)

Position (complex)	δ_H (ppm), (Multiplicity, *J* in Hz), (Number of H)	δ_C (ppm), (C-type)
3D	7.64, (*m*), (1H)	152.4 (CH)
4D	7.63, (*m*), (1H)	128.2 (CH)
5D	-	149.9 (C)
6D	8.56, (*brs*), (1H)	124.4(CH)
7D	-	157.4 (C)
8D	-	169.1(C=O)
3E	8.12, (*d*, 5.7), (1H)	153.4 (CH)
4E	7.94, (*m*), (1H)	128.3 (CH)
5E	-	150.5 (C)
6E	8.92, (*brs*), (1H)	124.8 (CH)
7E	-	158.1 (C)
8E	-	169.5 (C=O)
3F	7.47, (*d*, 5.7), (1H)	150.6 (CH)
4F	7.39, (*m*), (1H)	130.2 (CH)
5F	-	148.9(C)
6F	8.68, (*brs*), (1H)	124.7 (CH)
7F	-	155.2 (C)
8F	-	168.7 (C=O)

brs = broad singlet, *d* = doublet, *dd* = doublet of doublet, *t* = triplet, *m* = multiplet

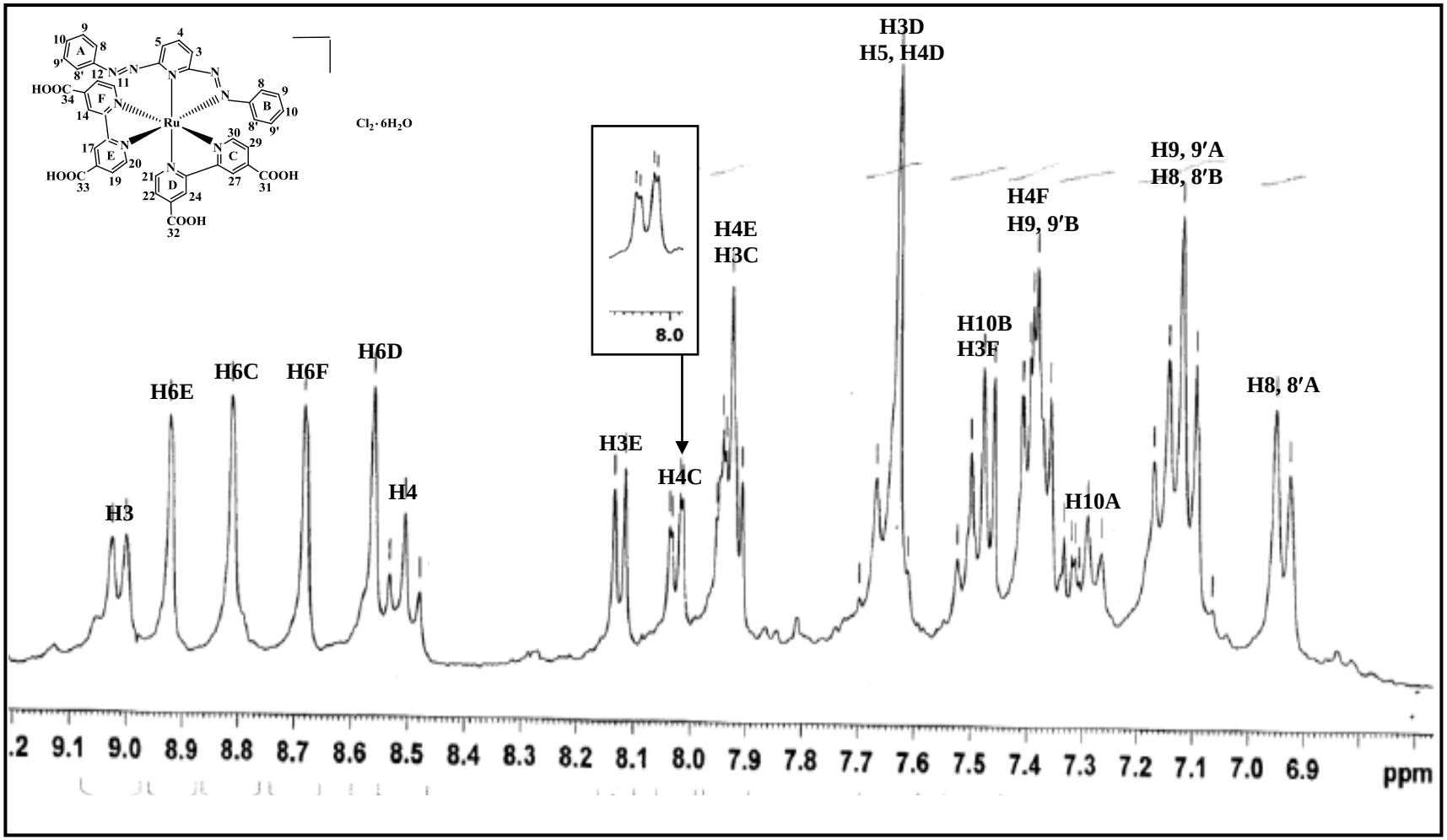

Figure 22 ^{1}H NMR spectrum of $[Ru(H_2dcbpy)_2(diazpy)]Cl_2{\cdot}6H_2O$ in methanol-d_4 (300 MHz).

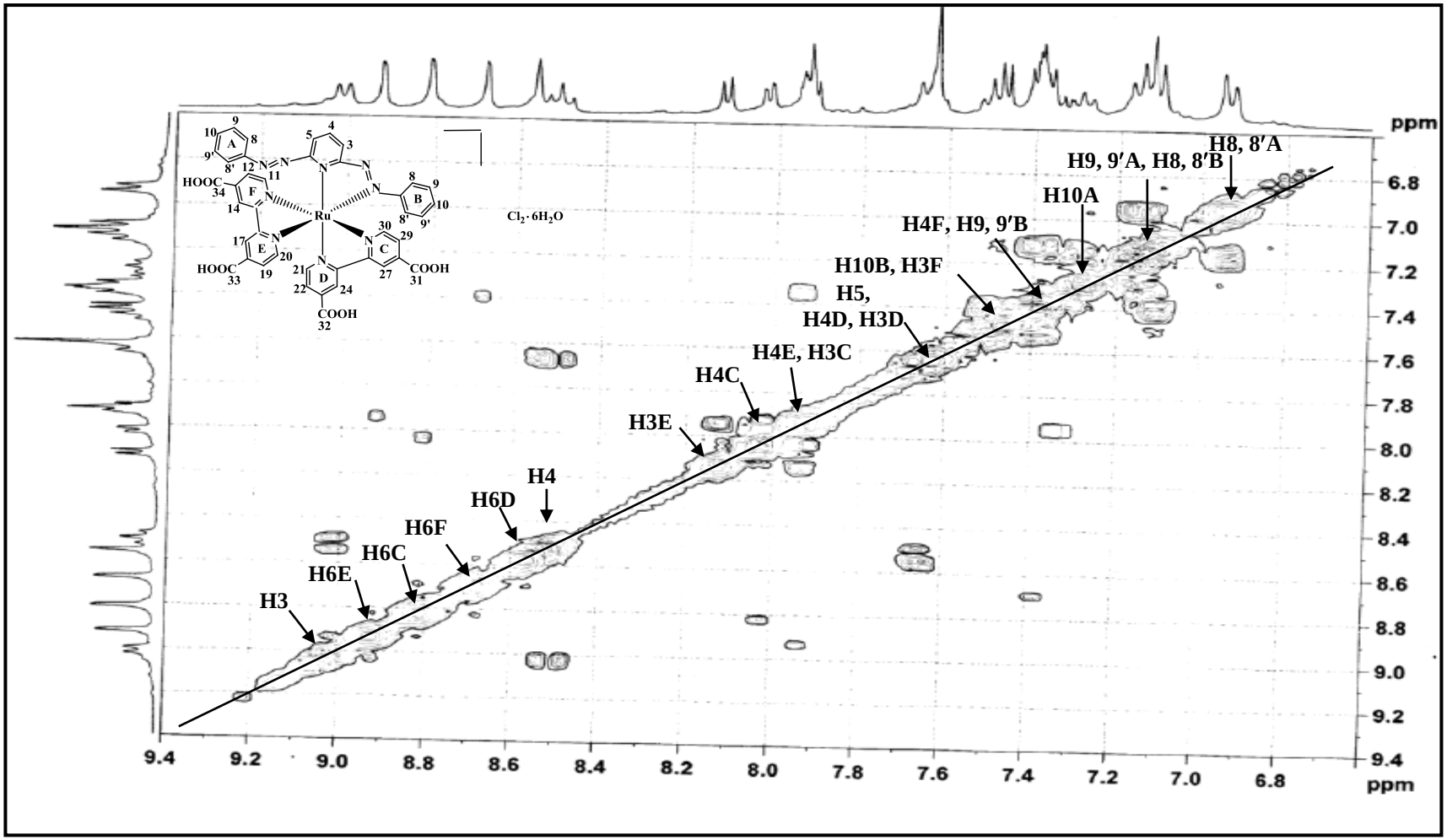

Figure 23 ^{1}H-^{1}H COSY NMR spectrum of $[Ru(H_2dcbpy)_2(diazpy)]Cl_2 \cdot 6H_2O$ in methanol-d_4 (300 MHz).

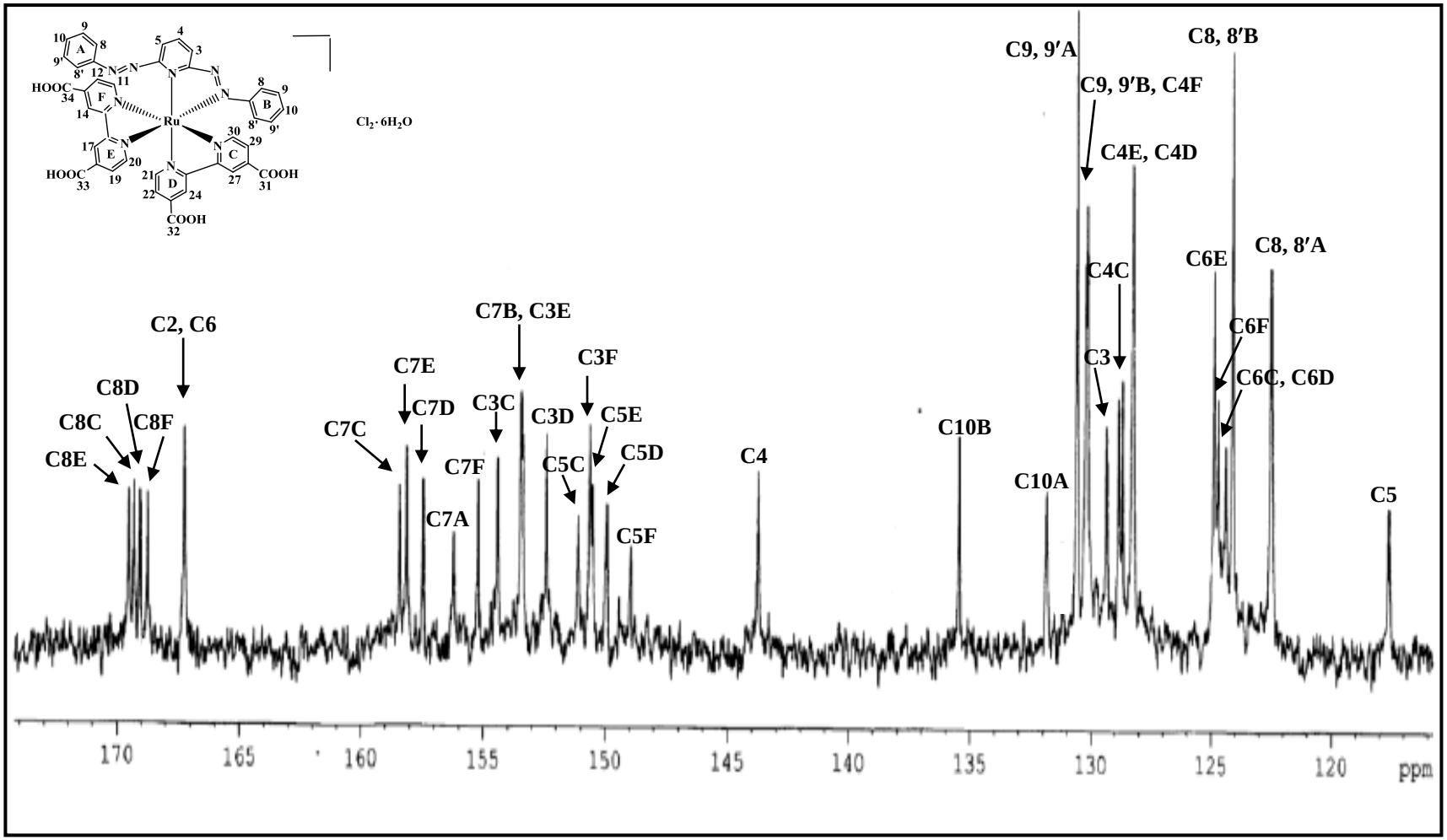

Figure 24 ^{13}C NMR spectrum of $[Ru(H_2dcbpy)_2(diazpy)]Cl_2 \cdot 6H_2O$ in methanol-d_4 (300 MHz).

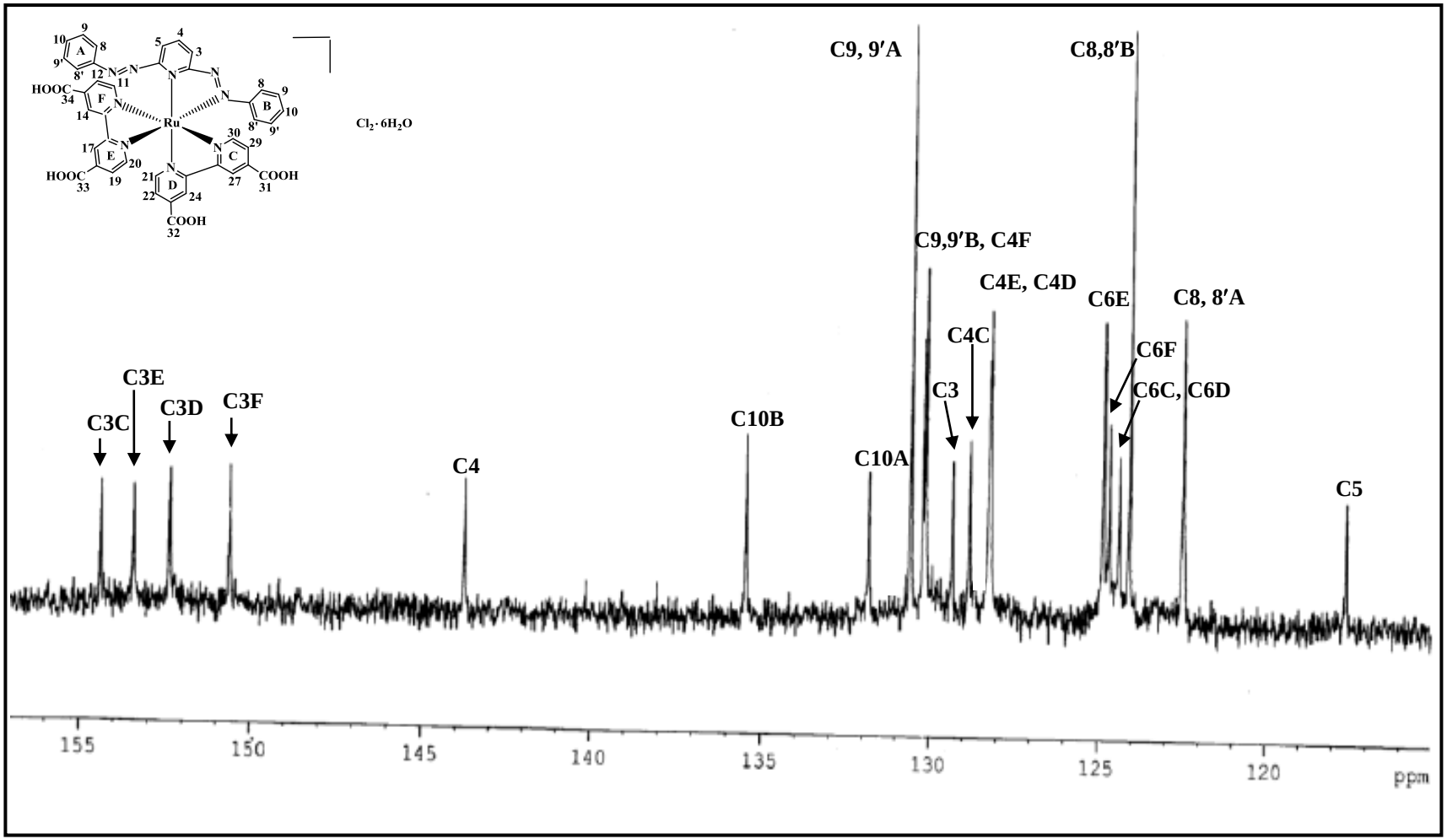

Figure 25 DEPT-90 NMR spectrum of $[Ru(H_2dcbpy)_2(diazpy)]Cl_2 \cdot 6H_2O$ in methanol-d_4 (300 MHz).

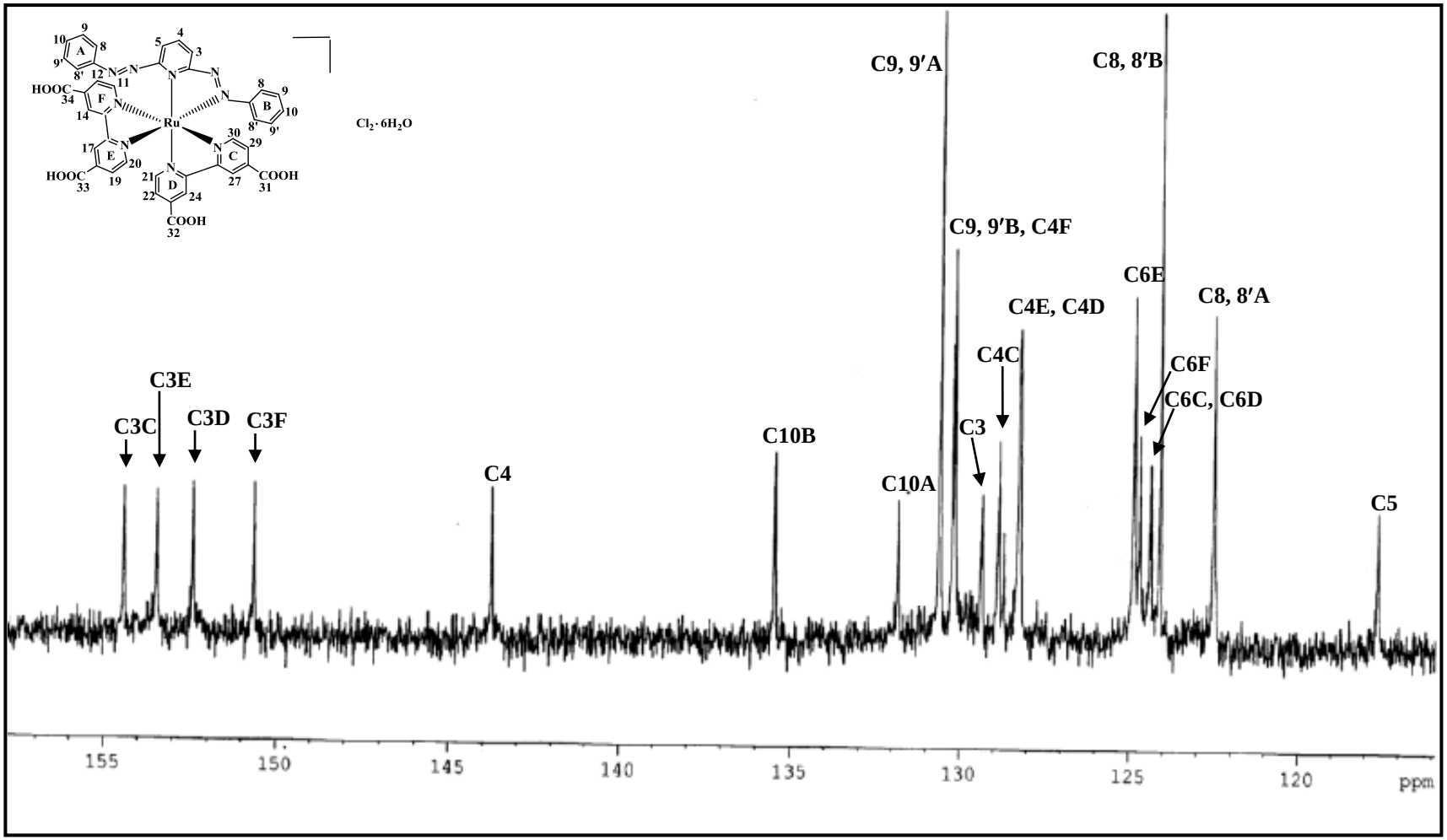

Figure 26 DEPT-135 NMR spectrum of $[Ru(H_2dcbpy)_2(diazpy)]Cl_2 \cdot 6H_2O$ in methanol-d_4 (300 MHz).

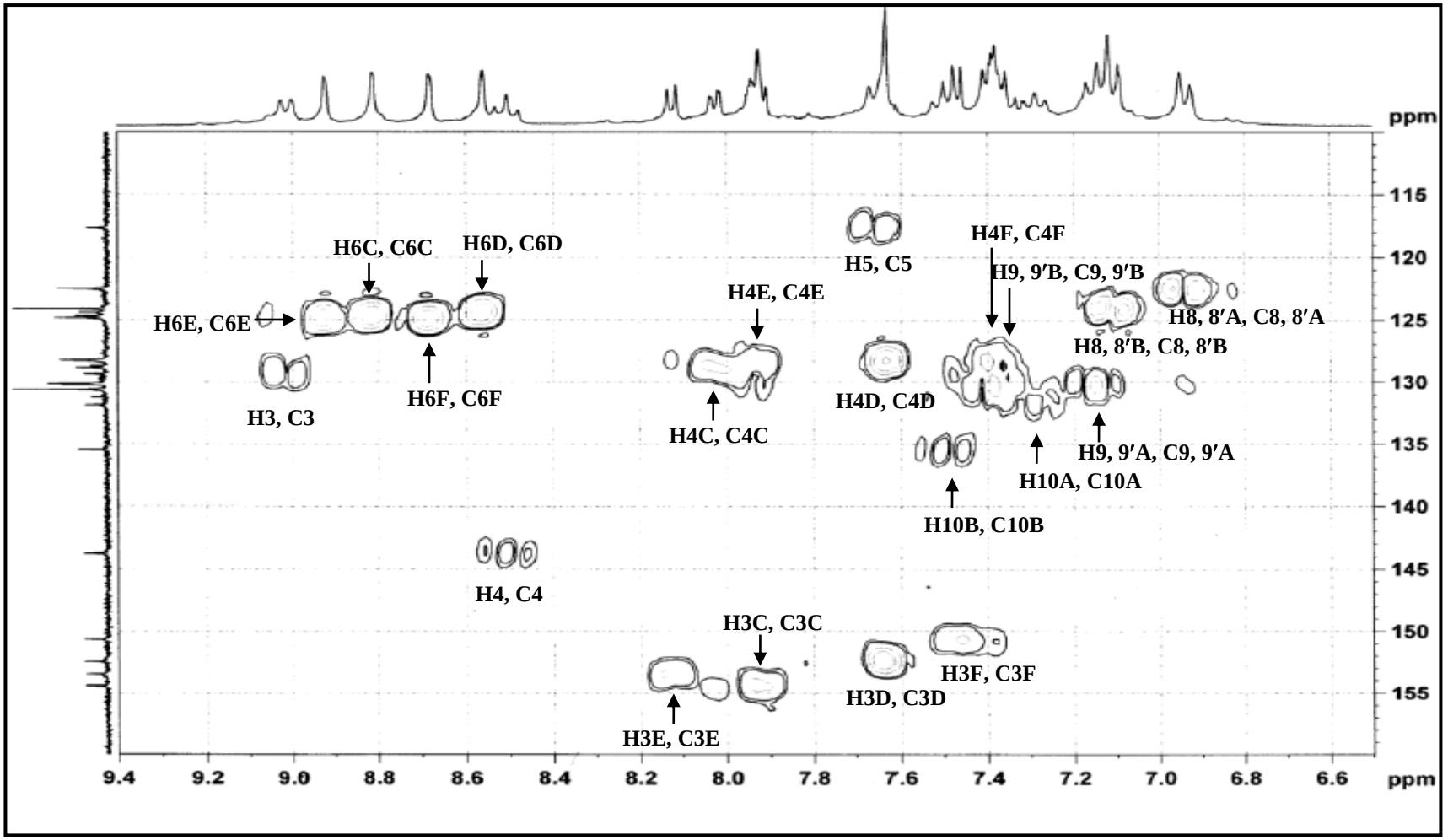

Figure 27 ^{1}H-^{13}C HMQC NMR spectrum of $[Ru(H_2dcbpy)_2(diazpy)]Cl_2 \cdot 6H_2O$ in methanol-d_4 (300 MHz).

3.2.2.5 Cyclic Voltammetry

Electrochemical properties of the [Ru(diazpy)(H_2dcbpy)Cl]Cl·H_2O and [Ru(H_2dcbpy)$_2$(diazpy)]Cl_2·6H_2O complexes were examined in acetonitrile and dimethylformamide solution, respectively. The reported potential data was compared with the values for the ferrocenium-ferrocence couple, under our experimental conditions. When $E_{1/2}$ value are calculated from the average of the anodic and cathodic peak potential ($E_{1/2} = (E_{pa}+E_{pc})/2$) at the scan rate of 50 mV/s and ΔE value is calculated from the difference of the both of peak. The cyclic voltammetric data are given in Table 13 and selected voltammograms are shown in Figure 28 and 29.

Table 13 Cyclic voltammetric data for [Ru(diazpy)(H_2dcbpy)Cl]Cl·H_2O complex in 0.1 M TBAH CH_3CN and [Ru(H_2dcbpy)$_2$(diazpy)]Cl_2·6H_2O complex in 0.1 M TBAH DMF at scan rate 50 mV/s (ferrocence as an internal standard)

Compounds	[a] $E_{1/2}$ (V) (ΔE_p (mV))			
	Oxidation	Reduction		
		I	II	III
[Ru(diazpy)(H_2dcbpy)Cl]Cl·H_2O	[b] 1.03	-0.49 (250)	-1.02 (70)	-1.46 (100)
[Ru(H_2dcbpy)$_2$(diazpy)]Cl_2·6H_2O	n	-0.96 (60)	-1.52 (160)	-1.78 (80)

[a] $E_{1/2} = (Ep_a + Ep_c)/2$, where Ep_a and Ep_c are anodic and cathodic peak potentials, respectively; ΔEp = Epa-Epc

n = cannot be observed

[b] observed only an anodic peak potential, E_{pa}

Oxidation range

The cyclic voltammograms of the $[Ru(diazpy)(H_2dcbpy)Cl]Cl\cdot H_2O$ and $[Ru(H_2dcbpy)_2(diazpy)]Cl_2\cdot 6H_2O$ complexes were measured in the potential range 0.00 V to +1.5 V at scan rate of 50 mV/s (Figure 28 and 29, respectively).

The $[Ru(diazpy)(H_2dcbpy)Cl]Cl\cdot H_2O$ complex exhibits an irreversible oxidation peak for the Ru(II)/Ru(III) couple, giving at E_{pa} = 1.03 V. The redox potential of Ru(II)/Ru(III) in $[Ru(H_2dcbpy)_2(diazpy)]Cl_2\cdot 6H_2O$ complex was not observed. It is possible that the Ru(II)/Ru(III) couple of this complex lied beyond the accessible potential range.

Reduction range

The cyclic voltammogram in negative range of the complexes showed reduction of all coordinate ligands within this solvent window. Polypyridyl ligands were also capable of accepting electrons. However, it was well documented in literature that the azopyridine ligands were better π-acceptors and underwent easier reductions than those of the polypyridyl ligands (Krause and Krause, 1980).

The electrochemistry of $[Ru(diazpy)(H_2dcbpy)Cl]Cl\cdot H_2O$ complex was measured in the potential range 0.00 V to - 1.70 V at scan rate of 50 mV/s (Figure 28). The scan rates were varied from 50 mV/s up to 500 mV/s (Figure 31 - 33). The cyclic voltammogram of $[Ru(diazpy)(H_2dcbpy)Cl]Cl\cdot H_2O$ complex shows three quasi-reversible couple at $E_{1/2}$ = -0.49 V (ΔE = 250 mV), $E_{1/2}$ = -1.02 V (ΔE = 70 mV) and $E_{1/2}$ = -1.46 V (ΔE = 100 mV). The cyclic voltammogram of $[Ru(diazpy)(H_2dcbpy)Cl]Cl\cdot H_2O$ complex displayed three electron reductions. The data from Table 13, the first and the second of these reductions occurred at more positive potentials (-0.49 V and -1.02 V) relative to the reduction of azo function of diazpy while the one quasi-reversible couple at -1.46 V was related to the reduction of H_2dcbpy ligand (Zakeeruddin, 1998) with one electron transfer in each equation (4-6).

$[Ru^{II}(diazpy)(H_2dcbpy)Cl]^{+} + e^{-} \rightleftharpoons [Ru^{II}(diazpy^{-1})(H_2dcbpy)Cl]^{0}$ (4)

$[Ru^{II}(diazpy^{-1})(H_2dcbpy)Cl]^{0} + e^{-} \rightleftharpoons [Ru^{II}(diazpy^{-2})(H_2dcbpy)Cl]^{-1}$ (5)

$[Ru^{II}(diazpy^{-2})(H_2dcbpy)Cl]^{-1} + e^{-} \rightleftharpoons [Ru^{II}(diazpy^{-2})(H_2dcbpy^{-1})Cl]^{-2}$ (6)

In the $[Ru(H_2dcbpy)_2(diazpy)]Cl_2 \cdot 6H_2O$ complex was measured in the potential range -0.60 V to -2.10 V at scan rate of 50 mV/s (Figure 29). The scan rates were varied from 50 mV/s up to 500 mV/s (Figure 35 - 37). The electrochemistry of $[Ru(H_2dcbpy)_2(diazpy)]Cl_2 \cdot 6H_2O$ complex shows one reversible couple at $E_{1/2}$ = -0.96 V (ΔE = 60 mV) and two quasi-reversible couple at $E_{1/2}$ = -1.52 V (ΔE = 160 mV) and $E_{1/2}$ = -1.78 V (ΔE = 80 mV). The cyclic voltammogram of $[Ru(H_2dcbpy)_2(diazpy)]Cl_2 \cdot 6H_2O$ complex displayed three electron reductions. The data from Table 13, the first of these reduction occurred at more positive potentials (-0.96 V) relative to the reduction of azo function of diazpy while the two quasi-reversible couple at -1.52 V and -1.78 V were related to the reduction of H_2dcbpy ligand (Lagref, 2008) with one electron transfer in each equation (7-9).

$[Ru^{II}(H_2dcbpy)_2(diazpy)]^{2+} + e^{-} \rightleftharpoons [Ru^{II}(H_2dcbpy)_2(diazpy^{-1})]^{+}$ (7)

$[Ru^{II}(H_2dcbpy)_2(diazpy^{-1})]^{+} + e^{-} \rightleftharpoons [Ru^{II}(H_2dcbpy^{-1})_2(diazpy^{-1})]^{0}$ (8)

$[Ru^{II}(H_2dcbpy^{-1})_2(diazpy^{-1})]^{0} + e^{-} \rightleftharpoons [Ru^{II}(H_2dcbpy^{-2})_2(diazpy^{-1})]^{-1}$ (9)

The first reduction couple of the $[Ru(diazpy)(H_2dcbpy)Cl]Cl \cdot H_2O$ complex ($E_{1/2}$ = -0.49 V) occurred at more potential than that in the $[Ru(H_2dcbpy)_2(diazpy)]Cl_2 \cdot 6H_2O$ complex ($E_{1/2}$ = -0.96 V). These results showed that the $[Ru(diazpy)(H_2dcbpy)Cl]Cl \cdot H_2O$ complex accepted electron better than the $[Ru(H_2dcbpy)_2(diazpy)]Cl_2 \cdot 6H_2O$ complex. It could be concluded that the diazpy ligand was a good π-acceptor, where diazpy acting as a tridentate ligand.

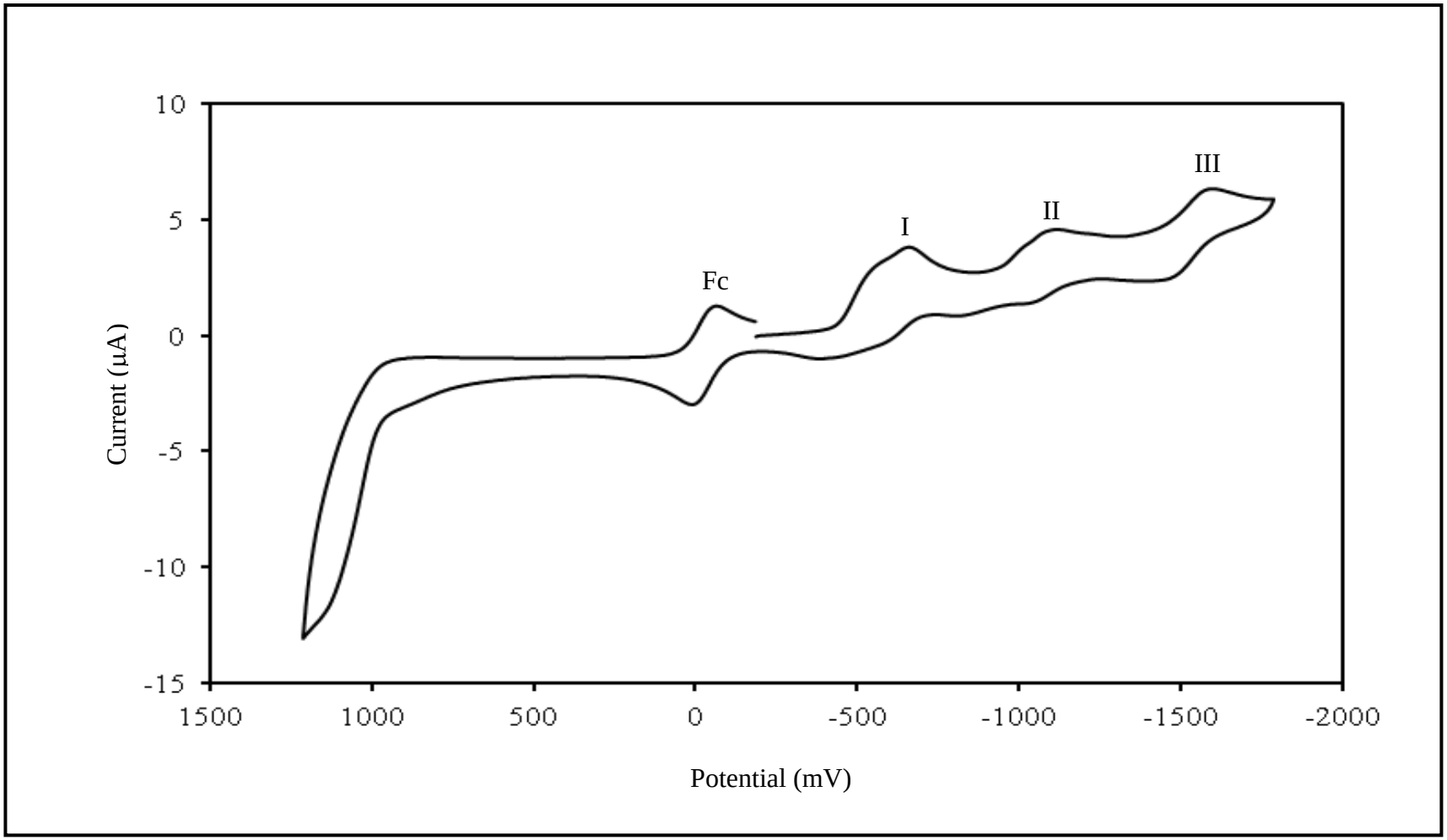

Figure 28 Cyclic voltammogram of [Ru(diazpy)(H_2dcbpy)Cl]Cl·H_2O in 0.1 M TBAH CH_3CN at scan rate 50 mV/s.

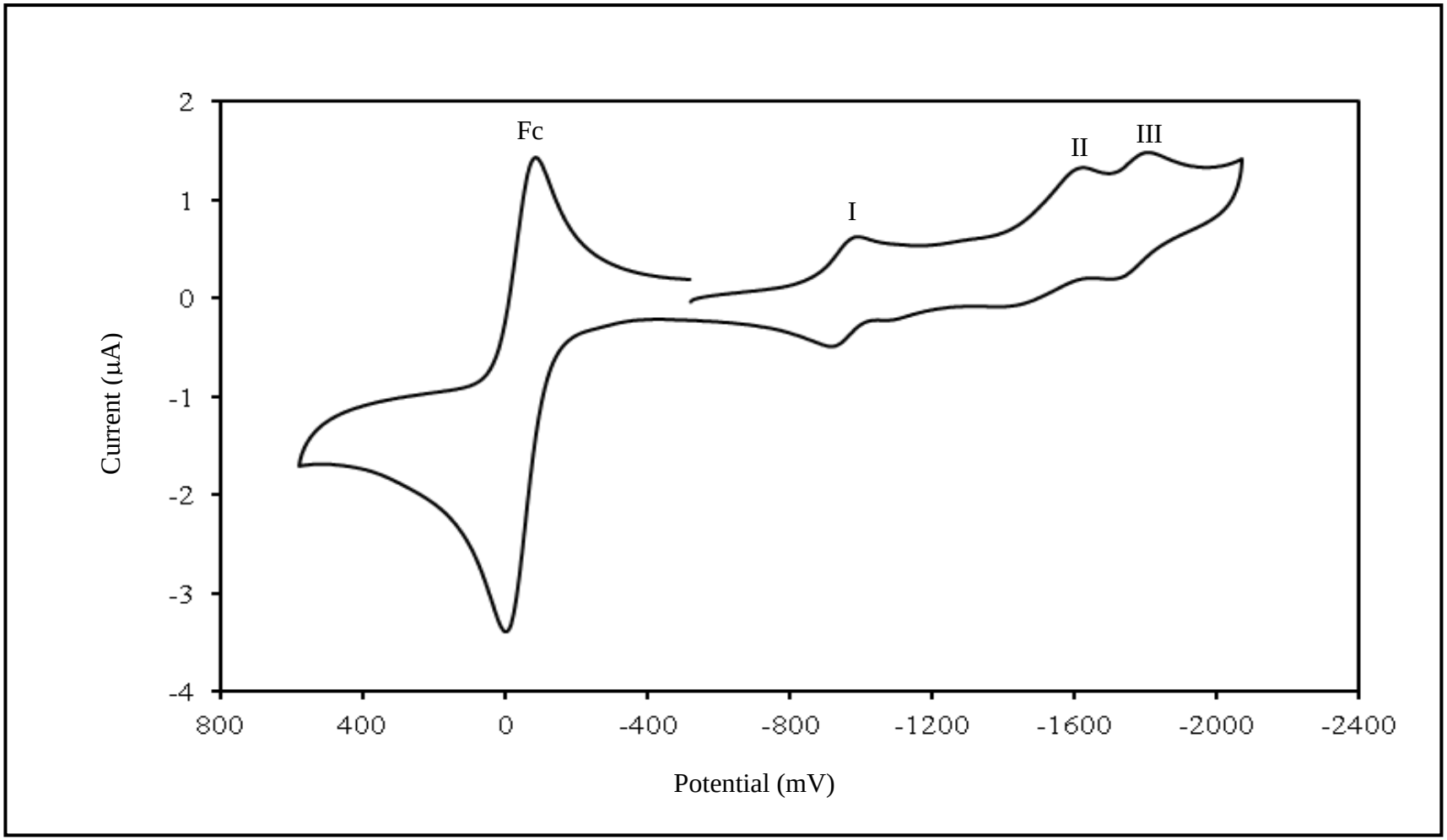

Figure 29 Cyclic voltammogram of $[Ru(H_2dcbpy)_2diazpy]Cl_2 \cdot 6H_2O$ in 0.1 M TBAH DMF at scan rate 50 mV/s.

CHAPTER 4
CONCLUSION

The 2,6-(diphenylazo) pyridine (diazpy) which is an azo compound, -N=N-C=N-, like azpy but there are two azo functions. The ligand was synthesized and characterized. Then the $[Ru(diazpy)(H_2dcbpy)Cl]Cl\cdot H_2O$ complex, where diazpy is acts as a tridentate ligand and $[Ru(H_2dcbpy)_2(diazpy)]Cl_2\cdot 6H_2O$ complex, where diazpy is acts as a bidentate ligand were also synthesized. They were characterized by using elemental analysis, infrared spectroscopy, UV-Visible absorption spectroscopy, 1D and 2D NMR spectroscopy and their electrochemical properties were studied by cyclic voltammetry.

Results from the elemental analysis, the analytical data of the complexes correspond to the calculated values. The infrared spectroscopic data shows remarkable different N=N (azo) stretching frequencies of free ligand and complexes. In the $[Ru(diazpy)(H_2dcbpy)Cl]Cl\cdot H_2O$ complex, the N=N (azo) vibrational frequency is red shifted from free diazpy ligand about 188 and 187 cm^{-1} and the $[Ru(H_2dcbpy)_2(diazpy)]Cl_2\cdot 6H_2O$ complex, the N=N (azo) vibrational frequency is red shifted from free diazpy ligand about 45 and 44 cm^{-1}, which is a good indication of N-azo coordination. It is because of the π-back bonding between diazpy ligand and ruthenium (II) result. Moreover, characteristic of the C=O bond stretching on the carboxylate group due to the presence of H_2dcbpy ligand in both complexes appeare at 1723 cm^{-1}.

Electronic spectra of the complexes exhibit highly intense MLCT transitions. The energy of the MLCT transition is an allowed transition. The ^1H NMR, ^{13}C NMR and DEPT NMR spectra between the ligand and complexes were compared in order to study the structures and the stereochemistry of the compounds. Results of 2D NMR experiments, ^1H-^1H COSY and ^1H-^{13}C HMQC, corresponded to the 1D NMR data.

The cyclic voltammogram shows that the [Ru(diazpy)(H_2dcbpy)Cl]Cl·H_2O complex is able to accept electrons better than the [Ru(H_2dcbpy)$_2$(diazpy)]Cl_2·6H_2O complex. It can be concluded that the diazpy ligand is a good π-acceptor, where diazpy acts as a tridentate ligand.

BIBLIOGRAPHY

Albon, J. M., Edwards, D. A. and Moore, P. J. 1989. Metal Carbonyl Complexes Involving 2,6-Bis[1-(phenylimino)ethyl] pyridine; Bidentate Coordination of Potentially Tridentate. *Inorg. Chim. Acta.* **159**: 19-22.

Anandan, S., Latha, S., Murugesan, S., Madhavan, J., Muthuraaman, B. and Maruthamuthu, P. 2005. Synthesis, characterization and fabrication of solar cells making use of [Ru(dcbpy)(tptz)X]X(where X = Cl^-, SCN^-, CN^-) complexes. *Sol. Energy*. **79**: 440–448.

Anandan, S., Madhavana, J., Maruthamuthua, P., Raghukumarb, V. and Ramakrishnan, V. T. 2004. Synthesis and characterization of naphthyridine and acridinedione ligands coordinated ruthenium (II) complexes and their applications in dye-sensitized solar cells. *Sol. Energy Mater. Sol. Cells*. **81**: 419-428.

Barf, G. A and Sheldon, R. A. 1995. Ruthenium(II) 2-(phenylazo) pyridine complexes as epoxidation catalysts. *J. Mol. Catal. Chem.* **98**: 143-146.

Barton, J. K., Goldberg, J. M., Kumar, C. V. and Turro, N. J. 1986. Binding Modes and Base Specificity of Tris(phenanthroline)ruthenium(II) Enantiomers with Nucleic Acids: Tuning the Stereoselectivity. *J. Am. Chem. Soc.* **108**: 2081-2088.

Cetinkaya, B., Citinkaya, E., Brookhart, M. and White, P. S. 1999. Ruthenium(II) Complexes with 2,6-pyridyl-diimine Ligands: Synthesis, Characterization and Catalytic Activity in Epoxidation Reactions. *J. Mol. Catal. A: Chemical.* **142**: 101-112.

Chatzivasiloglou, E., Stergiopoulos, T., Spyrellis, N. and Falaras, P. 2005. Solid-state sensitized solar cells, using $[Ru(dcbpyH_2)_2Cl_2]\cdot 2H_2O$ as the dye and PEO/titania/I^-/I_3^- as the redox electrolyte. *J. Mat. Pro. Tech*. **161**: 234–240.

Chryssou, K., Catalano, V. J., Kurtaran, R. and Falaras, P. 2002. Synthesis and characterization of bdmpp-dcbpy-Ru (II) complex for dye-sensitized solar cells [where bdmpp is 2,6-bis(3,5-dimethyl-*N*-pyrazoyl)pyridine and dcbpy is 2,2′ bipyridine-4,4′-dicarboxylic acid]. *Inorg. Chim. Acta*. **328**: 204–209.

Chryssou, K., Stergiopoulos, T., and Falaras, P. 2002. Synthesis and spectroscopic properties of a new bipyridine-bipyrazoyl(pyridine)-thiocyanato-ruthenium(II) complex. *Polyhedron*. **21**: 2773–2781.

Corral, E., Hotze, A. C. G., Dulk, H. d., Leczkowska, A., Rodger, A., Hannon, M. J. and Reedijk, J. 2009. Ruthenium polypyridyl complexes and their modes of interaction with DNA: Is there a correlation between these interactions and the antitumor activity of the compounds?. *J. Biol. Inorg. Chem.* **14**: 439–448.

Corral, E., Hotze, A. C. G., Tooke, D. M., Spek, A. L. and Reedijk, J. 2006. Ruthenium polypyridyl complexes containing the bischelating ligand 2,2′ azobispyridine. Synthesis, characterization and crystal structures. *Inorg. Chim. Acta*. **359**: 830–838.

Falaras, P. 1998. Synergetic effect of carboxylic acid functional groups and fractal surface characteristics for efficient dye sensitization of titanium oxide. *Sol. Energy Mater. Sol. Cells*. **53**: 163-175.

Goswami, S., Chakravarty, A. R. and Chakravorty, A. 1981. Chemistry of Ruthenium 21. Synthesis, Structure, and Redox Properties of 2-(Arylazo)pyridine Complexes. *Inorg. Chem.* **20**: 2246-2250.

Hamaguchi, T., Inoue, Y., Ujimoto, K. and Ando, I. 2008. Synthesis, crystal structure and electrochemistry of a ruthenium complex coordinated with an ambidentate 2-mercaptopyridinato *N*-oxide ligand. *Polyhedron*. **27**: 2031–2034.

Hansongnern, K., Saeteaw, U., Mostafa, G., Jiang, Y-C., and Lu, T-H. 2001. Crystal Structure of Chloro(2,2′,6′,2″-terpyridine)(2-phenylazopyridine)ruthenium(II) Chloride. *Anal Sci.* **17**: 683-684.

Hansongnern, K., Saeteaw, U., Mostafa, G., Liao, F-L., and Lu, T-H. 2003. Crystal Structure of Bromo(2,2′,6′,2″-terpyridine)(2-phenylazopyridine)ruthenium(II) Tetrafluoroborate. *Anal Sci.* **19**: 971-972.

Hotze, A. C. G., Velders, A. H., Ugozzoli, F., Biagini-Cingi, M., Manotti-Lanfredi, A. M., Haasnoot, J. G. and Reedijk, J. 2000. Synthesis, Characterization, and Crystal Structure of α-$[Ru(azpy)_2(NO_3)_2]$ (azpy = 2-(Phenylazo) pyridine) and the Products of Its Reactions with Guanine Derivatives. *Inorg. Chem.* **39**: 3838-3844.

Konno, H., Ishii, Y., Sakamoto, K. and Ishitani, O. 2002. Synthesis, spectroscopic characterization, electrochemical and photochemical properties of ruthenium(II) polypyridyl complexes with a tertiary amine ligand. *Polyhedron*. **21** : 61–68.

Krause, R. A. and Krause, K. 1980. Chemistry of Bipyridyl-like Ligands. Isomeric Complexes of Ruthenium(II) with 2-(phenylazo)pyridine. *Inorg. Chem.* **19**: 2600-2603.

Krause, R. A. and Krause, K. 1982. Chemistry of Bipyridyl-like Ligands. 2 Mixed Complexes of Ruthenium(II), with 2-(phenylazo)pyridine; A new π-Bonding Probe[1]. *Inorg. Chem.* **21**: 1714-1720.

Krause, R. A. and Krause, K. 1984. Chemistry of Bipyridyl-like Ligands. 3. Complexes of Ruthenium(II) with 2-((4-Nitrophenyl)azo)pyridine. *Inorg. Chem*. **23**: 2195-2198.

Lagref, J.-J., Nazeeruddin, Md. K. and Grätzel, M. 2008. Artificial photosynthesis based on dye-sensitized nanocrystalline TiO_2 Solar cells. *Inorg. Chim. Acta*. **361**: 735–745.

Leesakul, N., Yoopensuk, S., Pakawatchai, C., Saithong, S. and Hansongnern K. 2010. *N*,*N*-Dimethyl-4-[(2-pyridyl)diazenyl]-aniline. *Acta Cryst*. **E66**: o1923.

Liska, P., Vlachopoulos, N., Nazeeruddin, M.K., Comte, P. and Grätzel, M. 1988. *Cis*-Diaquabis(2,2′-bipyridyl-4,4′-dicarboxylate)-ruthenium(II) Sensitizes Wide Band Gap Oxide Semiconductors Very Efficiently over a Broad Spectral Range in the Visible. *J. Am. Chem. Soc*. **110**: 3686-3687.

Maruthamuthu, P. and Anandan, S. 1999. Synthesis, characterization and photo-conversion study of [Ru(II)(dcbpy (terpy)Cl Cl.$3H_2O$, [Ru(II) (dcbpy(terpy)SCN]- SCN.$3H_2O$ and [Ru(II)(dcbpy)(terpy)CN]CN.$3H_2O$ systems. *Sol. Energy Mater. Sol. Cells*. **59**: 199-209.

Meyer, G. J. 1997. Efficient Light-to-Electrical Energy Conversion : Nanocrystalline TiO_2 Films Modified with Inorganic Sensitizers. *J. Chem. Ed*. **74**: 652-656.

Mondal, B., Walawalkar, M. G. and Lahiri, G. K. 2000. Ruthenium terpyridine complexes incorporating azo-imine based ancillary ligands. Synthesis, crystal structure, spectroelectrochemical properties and solution reactivities. *J. Chem. Soc*. *Dalton Trans*. 4209–4217.

Nazeeruddin, M. K., Kay, A., Rodicio, I,. Humpbry-Baker, R., Miiller, E., Liska, P., Vlachopoulos, N. and Grätzel, M. 1993. Conversion of Light to Electricity by *cis*-X_2Bis(2,2′-bipyridyl-4,4′-dicarboxylate)ruthenium(II) Charge-Transfer

Sensitizers (X = $C1^-$, Br^-, I^-, CN^-, and SCN^-) on Nanocrystalline TiO_2 Electrodes. *J. Am. Chem. Soc.* **115** : 6382-6390.

Nazeeruddin, M. K., Zakeeruddin, S. M., Humphry-Baker, R., Jirousek, M., Liska, P., Vlachopoulos, N., Shklover, V., Fischer, C-H. and Grätzel, M. 1999. Acid-Base Equilibria of (2,2′-Bipyridyl-4,4′-dicarboxylic acid)ruthenium(II) Complexes and the Effect of Protonation on Charge-Transfer Sensitization of Nanocrystalline Titania. *Inorg. Chem*. **38**: 6298-6305.

Nookong, P. 2003. Synthesis and Characterization of Ruthenium(II) Complexes with 2,6-(diphenylazo)pyridine Ligand. M. Sc. Inorganic Chemistry, Prince of Songkla University. (Unpublished)

Onozawa-Komatsuzaki, N., Yanagida, M., Funaki, T., Kasuga, K., Sayama, K. and Sugihara, H. 2009. Near-IR sensitization of nanocrystalline TiO_2 with a new ruthenium complex having a 2,6-bis(4-carboxyquinolin-2-yl)pyridine ligand. *Inorg. Chem. Comm.* **12**: 1212–1215.

Onozawa-Komatsuzaki, N., Yanagida, M., Funaki, T., Kasuga, K, Sayama, K. and Sugihara, H. 2011. Near-IR dye-sensitized solar cells using a new type of ruthenium complexes having 2,6-bis(quinolin-2-yl)pyridine derivatives. *Sol. Energy Mater. Sol. Cells*. **95**: 310-314.

Panneerselvam, K., Hansongnem, K., Rattanawit, N., Liao, F-l. and Lu, T-H. 2000. Crystal Structure of the [Protonated 2-(phenylazo)pyridine and Protonated 2-(4-hydroxyphenylazo)pyridine (3:l)]tetrafluoroborate. *Anal Sci.* **16**: 1107-1108.

Philippopoulos, A. I., Terzis, A., Raptopoulou, C. P., Catalano, V. J. and Falaras, P. 2007. Synthesis, Characterization, and Sensitizing Properties of Heteroleptic Ru^{II} Complexes Based on 2,6-Bis(1-pyrazolyl)pyridine and 2,2′-Bipyridine-4,4′-dicarboxylic Acid Ligands. *Eur. J. Inorg. Chem.* 5633–5644.

Pramanik, N. C., Pramanik, K., Ghosh, P. and Bhattacharya, S. 1998. Chemistry of $[Ru(tpy)(pap)(L')]^{n+}$ (tpy = 2,2′,6′,2″-terpyridine; pap = 2-(phenylazo)pyridine; L′ = Cl^-, H_2O, CH_3CN, 4-picoline, N_3^-; n = 1,2). X-ray crystal structure of $[Ru(tpy)(pap)(CH_3CN)](ClO_4)_2$ and catalytic oxidation of water to dioxygen by $[Ru(tpy)(pap)(H_2O)]^{2+}$. *Polyhedron.* **17**: 1525-1534.

Sahavisit, L., and Hansongnern, K. 2005. Synthesis, spectral studies and electrochemical properties of ruthenium(II) complex with the new bidentate ligand 5-Chloro-2-(phenylazo)pyridine. *Songklanakarin J. Sci. Technol.* **27**: 751-759.

Santra, P. K., Misra, T. K., Das, D., Sinha, C., Slawin, A. M. Z. and Woollins, J. D. 1999. Chemistry of azopyrimidine. Part II. Synthesis, spectra, electrochemistry and X-ray crystal structures of isomeric dichloro bis[2-(arylazo)pyrimidine] complexes of ruthenium(II). *Polyhedron.* **18**: 2869-2878.

Seok, W. K., Gupta, A. K., Roh, S-J., Lee, W. and Han, S-H. 2007. Synthesis and Application of New Ru(II) Complexes for Dye-Sensitized Nanocrystalline TiO_2 Solar Cells. *Bull. Korean Chem. Soc*. **28**: 1311-1316.

Song, H-K., Park, Y. H., Han, C-H. and Jee, J-G. 2009. Synthesis of ruthenium complex and its application in dye-sensitized solar cells. *J. Ind. Eng. Chem.* **15**: 62–65.

Stergiopoulos, T., Karakostas, S.and Falaras, P. 2004. Comparative studies of substituted ruthenium(II)–pyrazoyl–pyridine complexes with classical N3 photosensitizer: the influence of –NCS dye ligands on the efficiency of solid state nanocrystalline solar cells. *J. Photochem. Photobiol. A: Chem.* **163**: 331-340.

Swarnalatha, K., Rajkumar, E., Rajagopal, S., Ramaraj, R., Lu, Y-L., Lu, K-L. and Ramamurthy, P. 2005. Photoinduced electron transfer reactions of ruthenium(II) complexes containing 2,2′-bipyridine-4,4′-dicarboxylic acid with phenols Steric and charge effects. *J. Photochem. Photobiol. A: Chem.* **171**: 83–90.

Velders, A. H., Kooijman, H., Spek, A. L., Haasnoot, J. G., Vos, D. d. and Reedijk, J. 2000. Strong Differences in the in Vitro Cytotoxicity of Three Isomeric Dichlorobis(2-phenylazopyridine)ruthenium(II) Complexes. *Inorg. Chem.* **39**: 2966-2967.

Vogler, L. M., Jones, S.W., Jensen, G. E., Brewer, R.G. and Brewer, K. J. 1996. Comparing the spectroscopic and electrochemical properties of ruthenium and osmium complexes of the tridentate polyazine ligands 2,2′:6′,2′′-terpyridine and 2,3,5,6-tetrakis(2-pyridyl) pyrazine. *Inorg. Chim. Acta*. **250**: 155–162.

Wang, P., Yuan, Y. and Zhu, G. Y. 1999. Synthesis, Electrochemistry, Fluorescence and ECL of Ru $(phen)_2$ (dcbpy) $(PF_6)_2$ *Chinese Chem. Lett*. **10**: 255–256.

Zakeeruddin, S. M., Nazeeruddin, Md. K., Humphry-Baker, R. and Grätzel, M. 1998. Stepwise Assembly of Tris-Heteroleptic Polypyridyl complexes of Ruthenium(II). *Inorg. Chem*. **37**: 5251-5259.

APPENDIX

A. Cut off solvents

Table 14 The solvents for UV-Visible spectrum and the minimum values for measurement

Solvents	λ(nm)
CH_3CN	195
MeOH	205
EtOH	205
CH_2Cl_2	230
DMSO	265

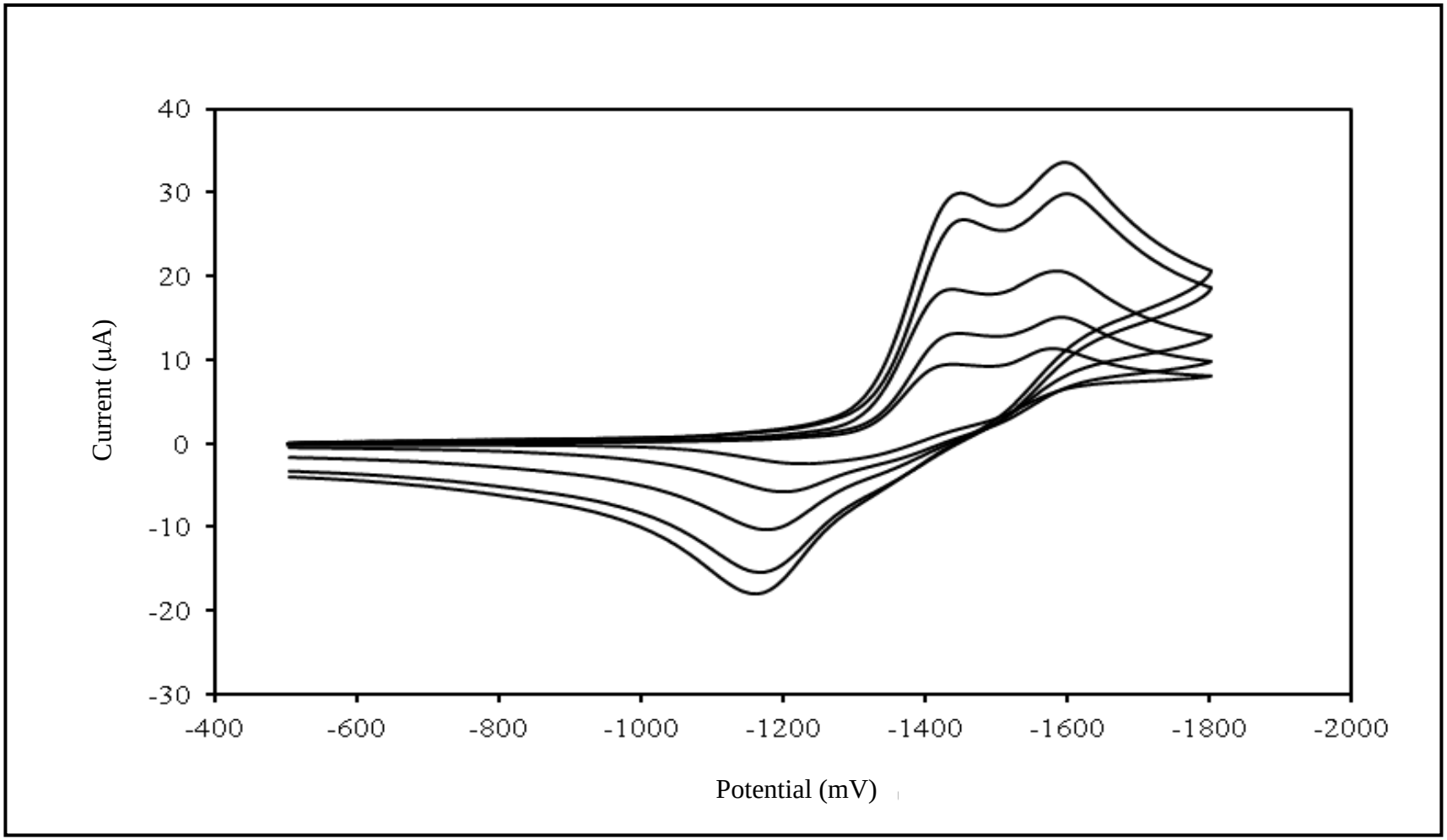

Figure 30 Cyclic voltammogram of diazpy in the reduction ranges with various scan rate 50-500 mV/s.

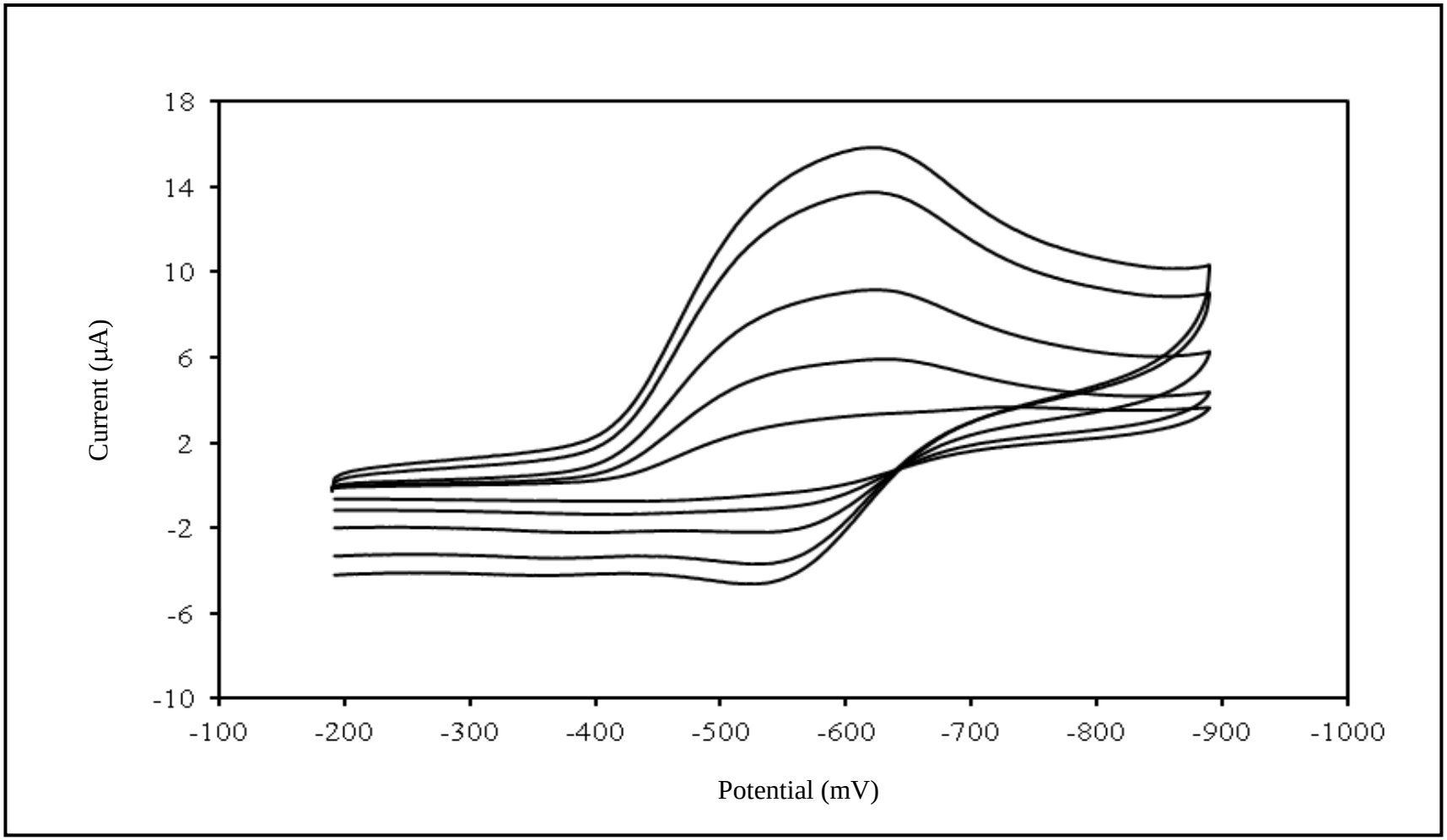

Figure 31 Cyclic voltammogram of [Ru(diazpy)(H_2dcbpy)Cl]Cl·H_2O-couple I in the reduction ranges with various scan rate 50-500 mV/s

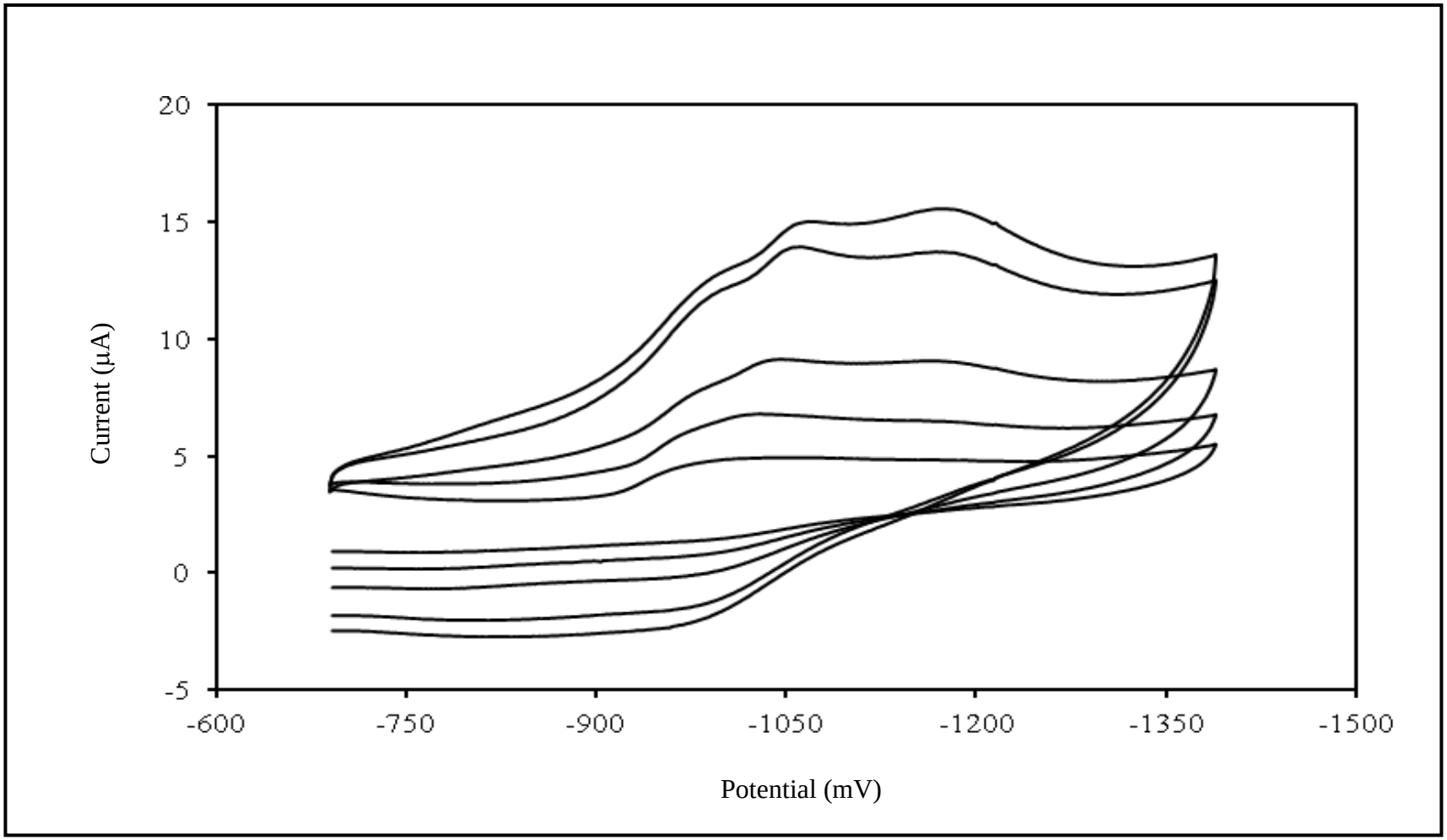

Figure 32 Cyclic voltammogram of [Ru(diazpy)(H_2dcbpy)Cl]Cl·H_2O-couple II in the reduction ranges with various scan rate 50-500 mV/s

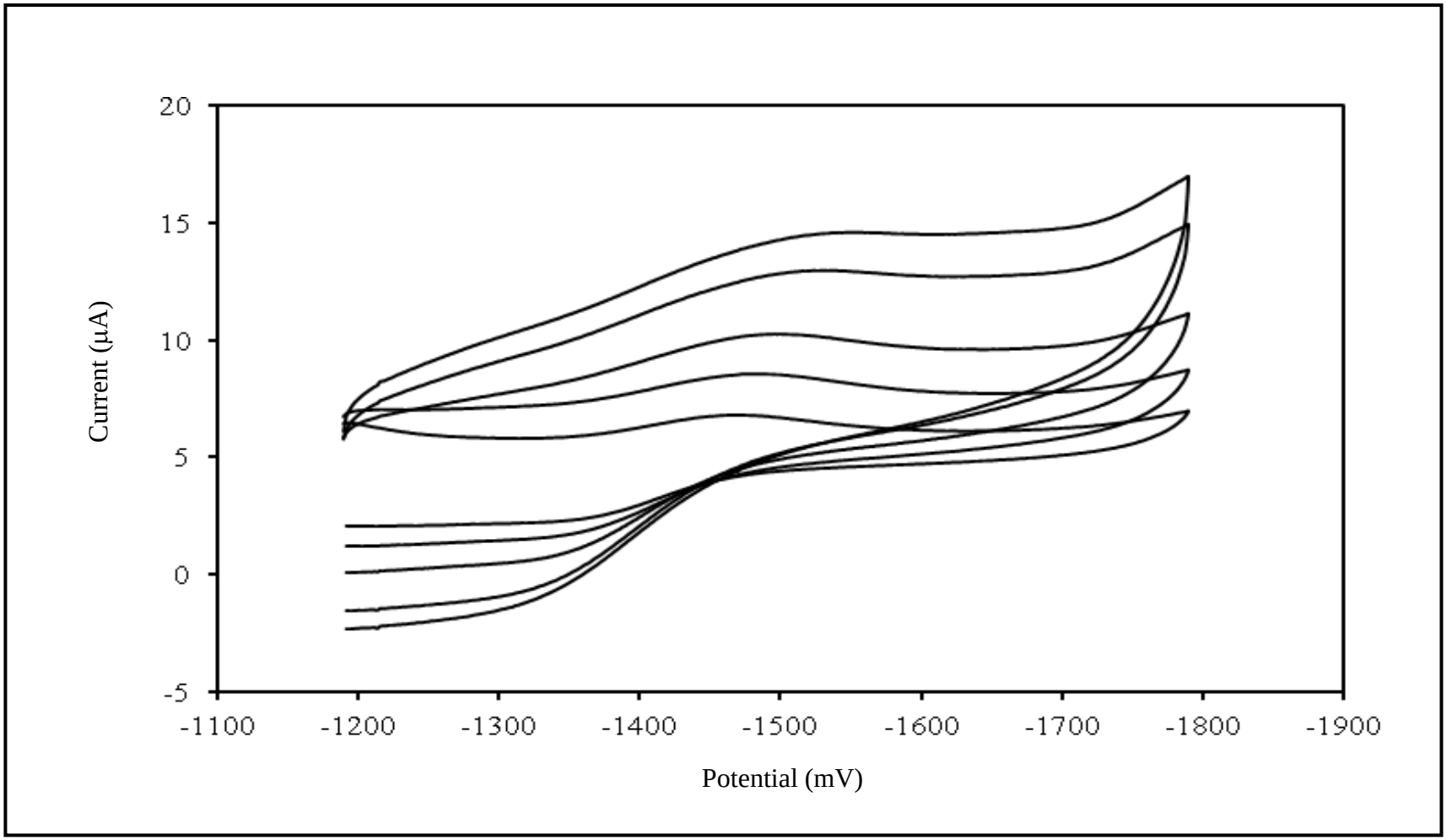

Figure 33 Cyclic voltammogram of [Ru(diazpy)(H_2dcbpy)Cl]Cl·H_2O-couple III in the reduction ranges with various scan rate 50-500 mV/s

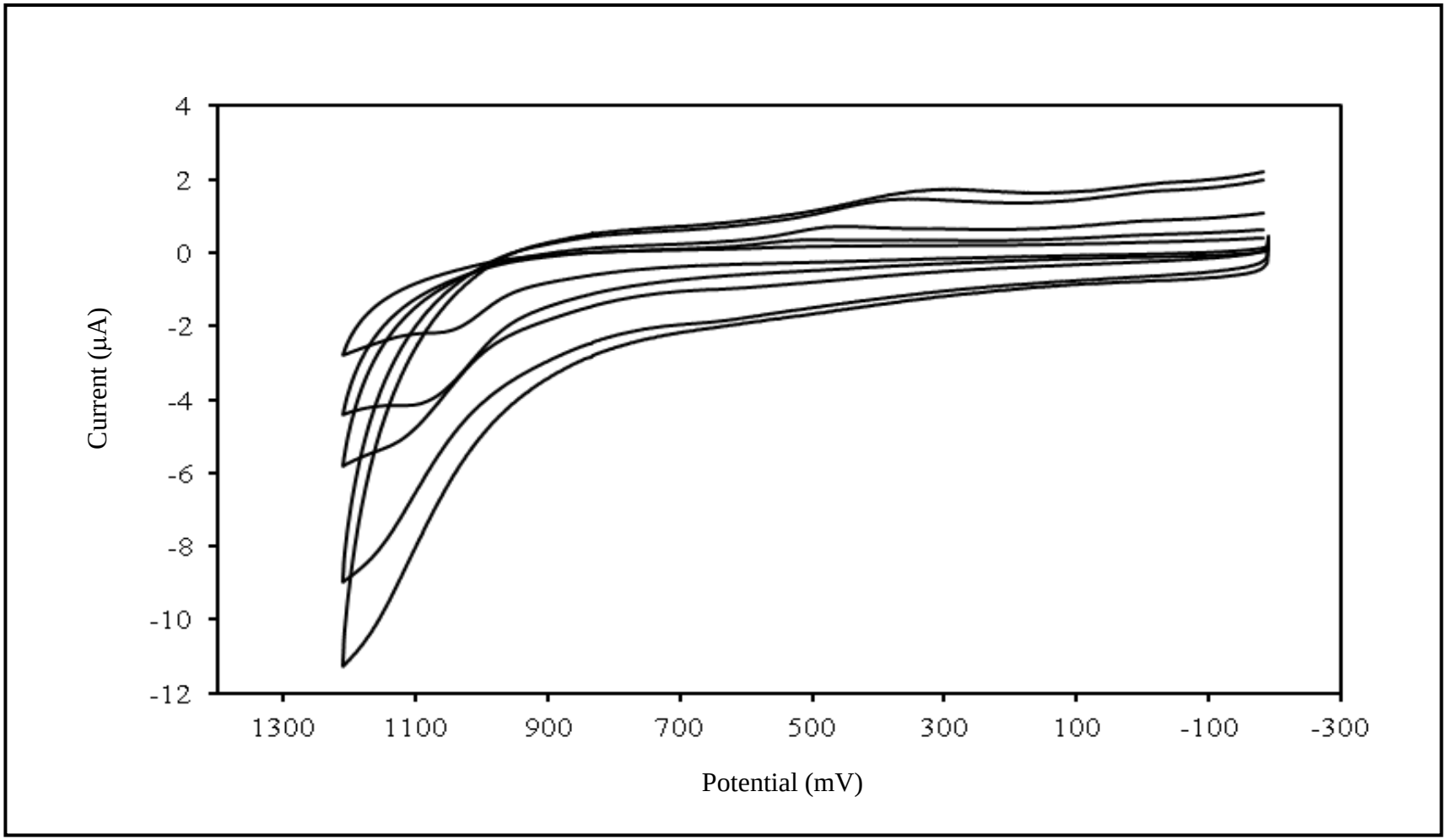

Figure 34 Cyclic voltammogram of [Ru(diazpy)(H_2dcbpy)Cl]Cl·H_2O in the oxidation ranges with various scan rate 50-500 mV/s

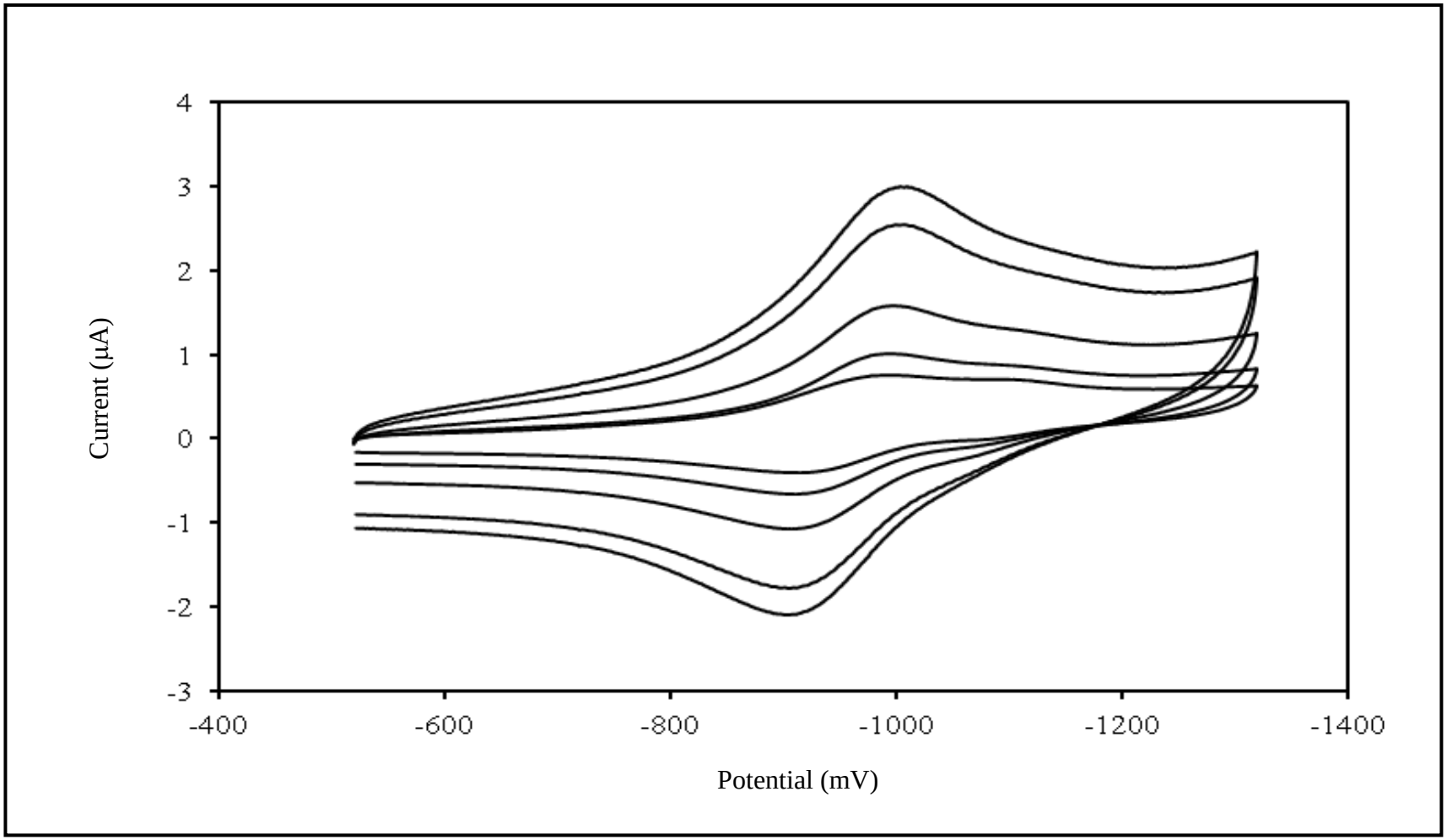

Figure 35 Cyclic voltammogram of $[Ru(H_2dcbpy)_2diazpy]Cl_2 \cdot 6H_2O$ -couple I in the reduction ranges with various scan rate 50-500 mV/s

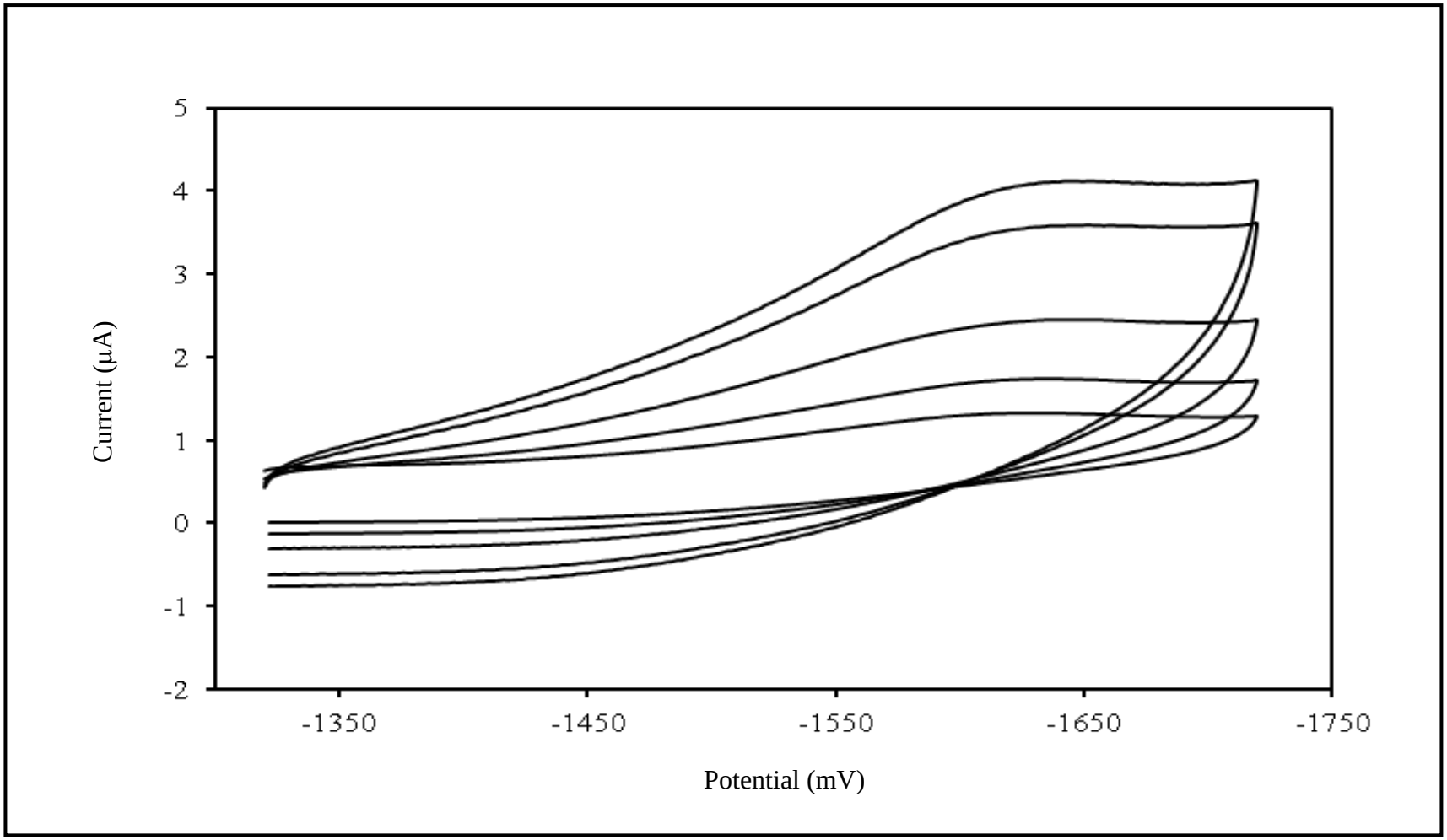

Figure 36 Cyclic voltammogram of $[Ru(H_2dcbpy)_2diazpy]Cl_2 \cdot 6H_2O$ -couple II in the reduction ranges with various scan rate 50-500 mV/s

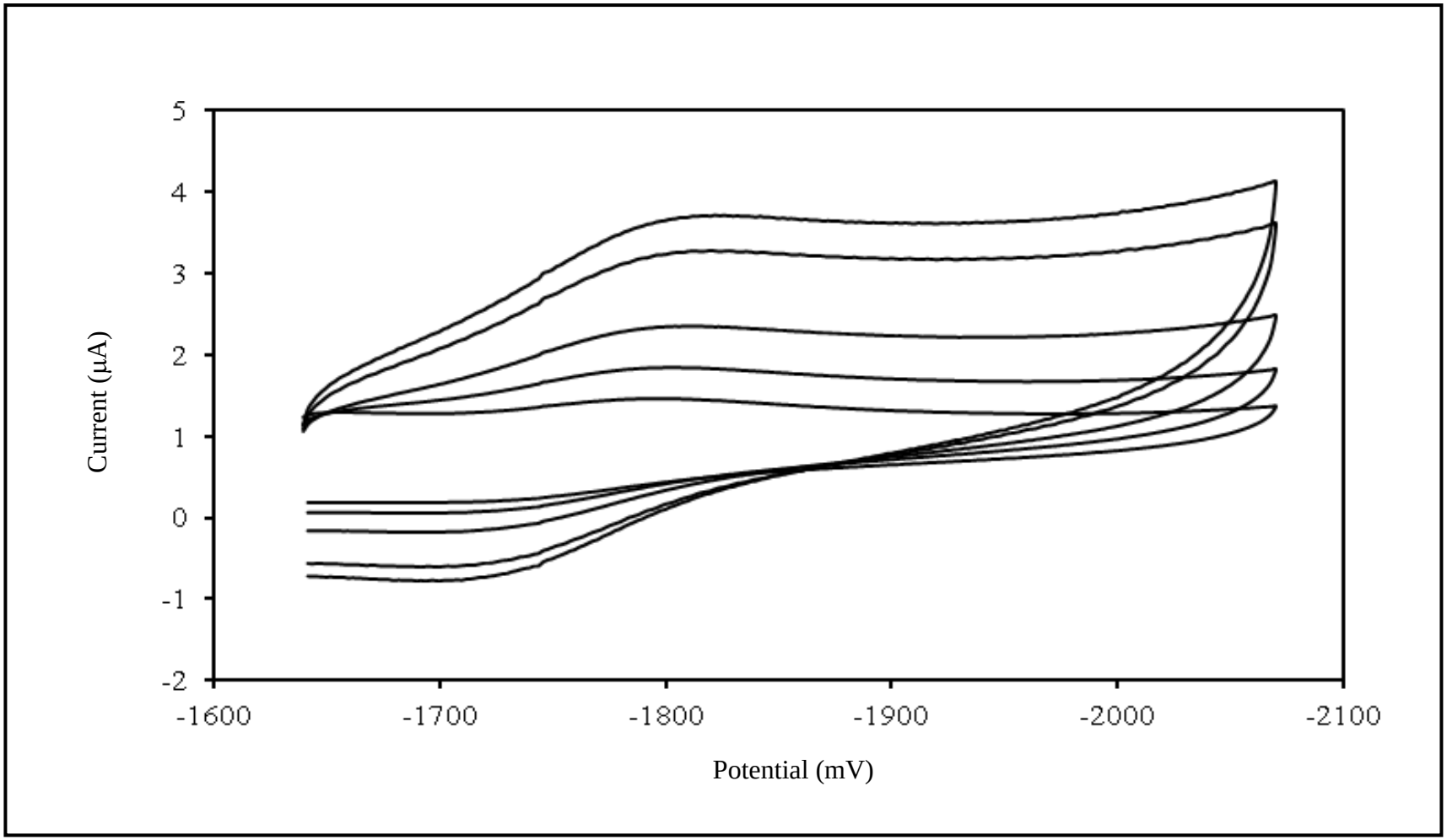

Figure 37 Cyclic voltammogram of $[Ru(H_2dcbpy)_2diazpy]Cl_2 \cdot 6H_2O$ -couple III in the reduction ranges with various scan rate 50-500 mV/s

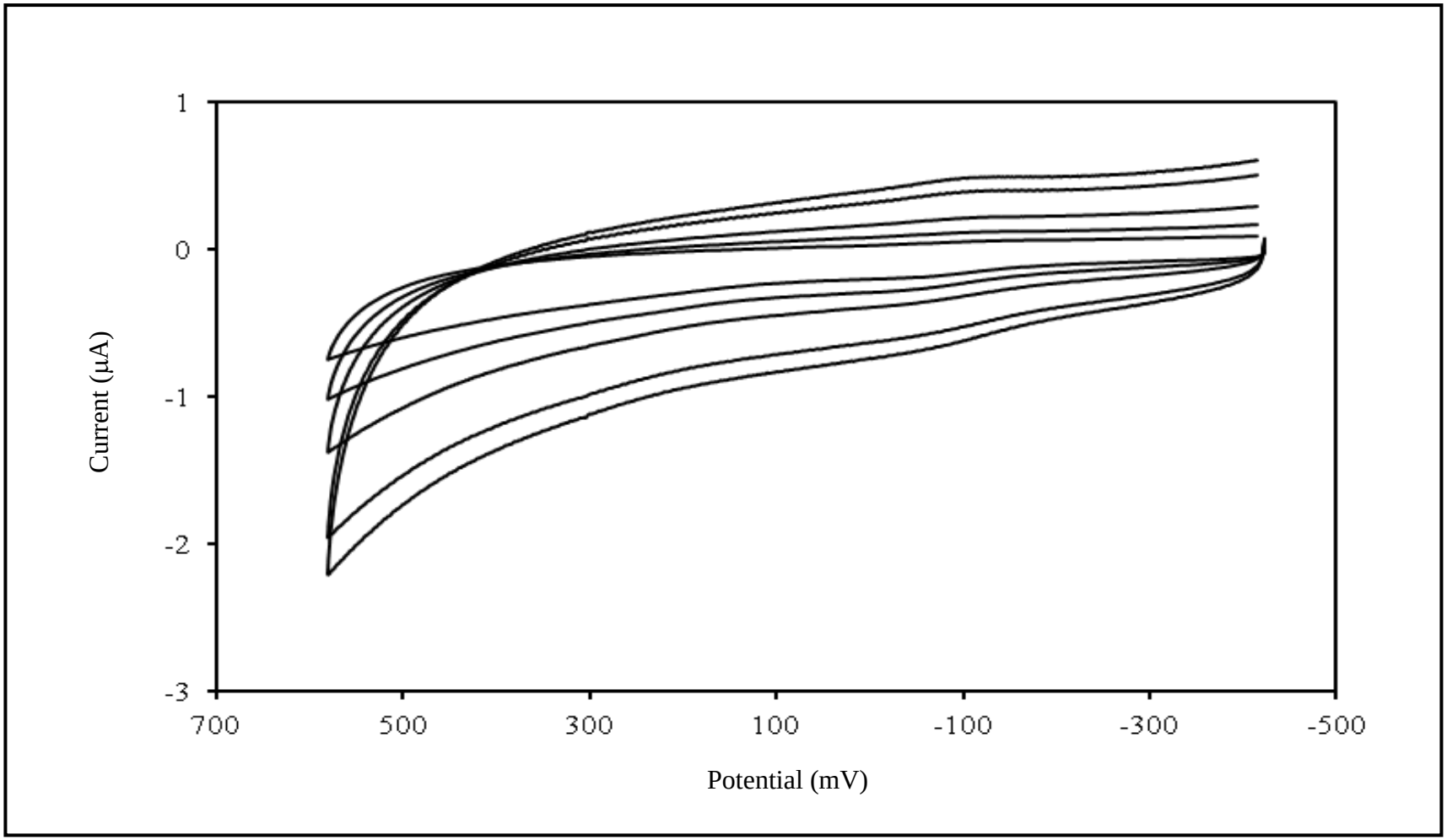

Figure 38 Cyclic voltammogram of $[Ru(H_2dcbpy)_2diazpy]Cl_2 \cdot 6H_2O$ in the oxidation ranges with various scan rate 50-500 mV/s.

VITAE

Name Miss. Sukanpirom Siritam

StudentID 5210220124

Educational Attainment

Degree Graduation	Name of Institution	Year of
Bachelor of Science (Chemistry)	Prince of Songkla University	2009

Scholarship Awards during Enrolment

1. Center of Excellence for Innovation in Chemistry (PERCH-CIC): Commision on Higher Education, Ministry of Education
2. Teaching Assistant, Department of Chemistry, Prince of Songkla University

List of Publication and Proceedings

Poster presentation

Siritam S., Hansongnern K., Puetpaiboon W., and Leesakul N. "Synthesis and characterization of $[Ru(dcbpy)_2(diazpy)]Cl_2$ (dcbpy = 4,4′-dicarboxy 2,2′-bipyridine, diazpy = 2,6-(diphenylazo)pyridine)", Pure and Applied Chemistry International Conference 2011 (PACCON 2011), Miracle Grand Convetntion Hotel Bangkok, Thailand, January 5–7, 20011.

Poster presentation

Siritam S., Hansongnern K., Puetpaiboon W., and Leesakul N. "Synthesis and Characterization of The Ruthenium(II) Complex Containing 4,4′-Dicarboxy-2,2′-bipyridine and 2,6-(Diphenylazo)pyridine", The International Congress for Innovation in Chemistry (PERCH-CIC Congress VII), Jomtien Palm Beach Hotel & Resort Pattaya Chonburi, Thailand, May 4–7, 2011.